Fast Oscillations and Synchronization of Neuronal Activity in Human, Monkey, and Simulation

Dissertation
zur Erlangung des Doktorgrades der
Naturwissenschaften
(Dr. rer. nat.)

dem Fachbereich Physik
der Philipps-Universität Marburg
vorgelegt von

Egbert Jürgens

aus Unna

Marburg/Lahn 1997

Vom Fachbereich Physik der Philipps-Universität als Dissertation angenommen am 14.11.1997

Erstgutachter: Prof. Dr. R. Eckhorn
Zweitgutachter: Prof. Dr. F. Rösler

Tag der mündlichen Prüfung: 19.01.1998

Contents

Zusammenfassung

Es wurde bisher gezeigt, daß Amplitude und Synchronisation von Gamma-Oszillationen (30-100 Hz) in kortikalen und subkortikalen Gebieten des Gehirns stimulus-spezifisch sind. Basierend auf diesen und anderen Ergebnissen wurde vorgeschlagen, daß Synchronisation oszillatorischer und nicht-oszillatorischer Aktivität eine wichtige Rolle bei verschiedenen Gehirnfunktionen spielt, einschließlich sensorischer Merkmalsintegration, Aufmerksamkeit, Gedächtnis und Bewußtsein. Untersuchungen des menschlichen Elektro- und Magnetoenzephalograms (EEG, MEG) versprachen eine geeignete Methode zur Untersuchung dieser Hypothesen zu sein. Tatsächlich wurde in neueren Publikationen die Entdeckung solcher Oszillationen im EEG und MEG des Menschen dargelegt. Allerdings gibt es in solchen Untersuchungen schwierige methodische Probleme, so daß über die Bedeutung dieser Ergebnisse disputiert wurde. In dieser Dissertation wurden Gamma-Oszillationen im menschliche EEG daher unter besonderer Berücksichtigung möglicher Artefakte untersucht. In der ersten Untersuchung war keine stimulusbezogene Modulation von Gamma-Aktivität im menschlichen EEG während einer Lern- und Abrufaufgabe vorhanden, abgesehen von Harmonischen von Alpha-Aktivität, die als Epiphänomen angesehen werden können. In einer zweiten Untersuchung wurde wiederum keine Modulation von Gamma-Aktivität im menschlichen EEG während der Präsentation von Gitterreizen gefunden. Es wird argumentiert, daß Fehlinterpretationen von Analyseergebnissen, wie von Harmonischen von Alpha-Aktivität, oder andere Artefakte, für zumindest einige der für das menschliche EEG berichteten Gamma-Band-Effekte verantwortlich sein können. Im Gegensatz zu diesen Ergebnissen verursachte identische Stimulation Gamma-Oszillationen im Skalp-EEG des Affen, die dem Zeitverlauf lokaler Feldpotentiale (LFP), abgeleitet im primären visuellen Kortex, entsprachen. Ähnliche positive Ergebnisse wurden mit anderen visuellen Stimuli in EEG-Ableitungen von Dura, Ableitkammer und Skalp eines Affen erhalten. Die allgemeine Annahme, daß das EEG hauptsächlich synchronisierte Komponenten neuronaler Aktivität widerspiegelt, wurde für visuell induzierte Gamma-Oszillationen bestätigt: Die maximalen EEG-Amplituden wurden bei maximaler Kohärenz zwischen Signalen verschiedener intrakortikaler Elektroden, nicht bei maximalen LFP-Amplituden gemessen. Übereinstimmend mit neueren Ergebnissen in der Literatur waren die Gamma-Oszillationen während des langsamen Kontrastanstiegs visueller Reize nicht phasenstarr an den Stimulus gekoppelt. Es konnte allerdings gezeigt werden, daß sie phasenstarr an das abrupte Einsetzen visueller Reize gekoppelt waren. Eine neuere Publikation beanspruchte phasenstarr an den Reiz gekoppelte Gamma-Oszillationen in menschlichen Reaktionszeitverteilungen während auditorischer und visueller Diskriminationsaufgaben gezeigt zu haben. Unsere exakte Replikation des auditorischen Paradigmas und der Datenauswertemethoden zeigte allerdings nicht die berichteten Effekte, was zu Zweifeln hinsichtlich der Reliabilität dieses Phänomens führt. Um elementare Mechanismen relevanter Prozesse in neuronalen Netzwerken zu demonstrieren, wurde die Entstehung von Oszillationen mit einem Computermodell lateral gekoppelter "integrate-and-fire" Neuronen untersucht. Bei Eingangssignalen mit hohem Mittelwert und geringer zeitlicher Variation erzeugte das Netzwerk, mit zunehmender Stärke lateraler Kopplung, korrelierte Aktivität oszillatorischen, stochastischen und rhythmisch burstenden Typs. Die Verarbeitung zweier Gruppen stochastischer Signale mit unterschiedlichem Korrelationsgrad ("Korrelationskontrast") wurde in Zuständen geringerer genereller Aktivierung untersucht. Ohne laterale Kopplung war die Korrelation der Ausgangssignale reduziert. Laterale Kopplung erhöhte jedoch den Korrelationskontrast, ein wesentliches Ergebnis für Korrelationstheorien der Hirnfunktion.

Summary

The amplitude and synchronization of gamma oscillations (30-100 Hz) were previously shown to be stimulus-specific in cortical and subcortical brain areas of higher mammals. Based on these and other results, synchronization of oscillatory and non-oscillatory neuronal activity was suggested to play an important role in different brain functions, including sensory feature integration, attention, memory, and consciousness. Investigations of the human electro- and magneto-encephalograms (EEG, MEG) promised to be a suitable method of investigating these hypotheses. In fact, recent publications stated findings of such oscillations in human EEG and MEG. However, such studies have to cope with difficult methodological problems, so that the significance of these results has been disputed. In this thesis, gamma oscillations in the human EEG were therefore investigated with special regard to possible artifacts. In the first study, no stimulus related modulation of gamma activity was present in the human EEG during a memory and retrieval task, except for harmonics of alpha activity, which could be regarded as an epiphenomenon. In a second study, again no modulation of gamma activity was found in the human EEG during the presentation of grating stimuli. It is argued, that misinterpretations of analysis results, e.g., of harmonics of gamma activity, or other artifacts, might be responsible for at least some of the gamma band effects reported for the human EEG. In contrast to these results, identical visual stimulation yielded gamma oscillations in the scalp EEG of monkey, reflecting the time course of local field potentials (LFP) recorded in the primary visual cortex. Similar positive results were obtained with other visual stimuli in EEG recordings from a monkey's dura, recording chamber, and scalp. The common assumption, that the EEG mainly reflects synchronized components of neuronal activity, was confirmed for visually induced gamma oscillations: The maximal EEG amplitudes were reached at maximal coherence between signals from different intracortical electrodes, rather than at maximal LFP amplitudes. In accordance with results in the recent literature, gamma oscillations were not phase-locked to the slow contrast increase of visual stimuli. It could be demonstrated, however, that they were phase-locked to the sharp onsets of visual stimuli. A recent publication claimed to have demonstrated stimulus-locked gamma oscillations in human reaction time distributions during auditory and visual discrimination tasks. However, our exact replication of the auditory paradigm and data analysis procedures did not show the reported effects, leading to doubts concerning the reliability of this phenomenon. In order to show basic mechanisms of relevant processes in neuronal networks, the generation of gamma oscillations was analyzed with a computer model of laterally coupled integrate-and-fire neurons. With input signals of high mean and low temporal variation the network generated, with increasing strength of lateral coupling, correlated activity of oscillatory, stochastic, and rhythmic bursting type. The processing of two groups of stochastic signals with different degrees of correlation ("correlation contrast") was analyzed in states of lower general activation. Without lateral coupling the correlation of the output signals was reduced. However, lateral coupling did enhance the correlation contrast, a result which is crucial for correlation theories of brain function.

1 General Introduction

1.1 Introduction to the topic

The cooperation of many neurons is necessary even for simple brain functions. Such cooperation involves the convergence of different processing streams. Convergence is very pronounced in the nervous system: Each cortical neuron receives signals from about 10,000 other neurons. Synchronized[1] signals, given that they converge on a neuron, produce much higher maximal membrane potentials than statistically independent spike patterns do. If the membrane potential exceeds a certain threshold, there is a steep increase in the probability of firing. Therefore, synchronization of incoming neuronal activity strongly affects the output of each neuron and, if present, should play an essential role in neuronal information processing. Experimental evidence shows that there actually is abundance of synchronized neuronal activity in the brain. In this thesis, synchronized neuronal signals with a certain time structure, namely oscillatory[2] gamma band activity (30-100 Hz), was a focus of interest. The following paragraphs provide an overview of relevant experimental methods and comment on the role of synchronization in the measurement process. In addition, a classification of different types of synchronization is given, followed by a summary of basic experimental results. Finally, functional aspects of neural synchronization are introduced.

1.1.1 Methods

Different methods are used for the investigation of different aspects of neuronal activity and synchronization, especially for the study of different spatial scales. The techniques which are described in the following allow the investigation of synchronization on the time scale of some milliseconds, which is a prerequisite for the analysis of gamma band activity. Intracortical microelectrode recordings are used for the analysis of single or multiple cell spike activity, as well as for the analysis of local field potentials (LFP), representing the average activity of larger cell groups. Magnetoencephalogram (MEG) and electroencephalogram (EEG)

[1] "Synchronized" in this context does not mean the exact synchronization of two signals, but rather a certain degree of correlation, here defined by a non zero normalized cross-correlation or coherence function.

[2] "Oscillatory" means a repetitive time structure, which is defined here as a distinct peak in the power spectrum.

recordings from the dura or scull reveal the average activity of areas which are again orders of magnitude larger. Not only electrophysiological recordings but also behavioral responses provide information about neuronal processes. The analysis of reaction time distributions yields such information, which is rather indirect compared to electrophysiological recordings. This is due to the fact that complex neuronal systems are involved in the generation of behavioral responses. On the other hand, mathematical models and computer simulations allow the analysis of certain aspects of neuronal activity in simplified and controllable systems. Such models might in turn influence further experimental work. Methods used in this dissertation were intracortical recordings of local field potentials, the electroencephalogram, reaction time distributions, and computer models.

1.1.2 Synchronization and the measurement process

Synchronization plays an important role in the measurement process of mass signals as the EEG and MEG, which reflect the activity of many neurons. While synchronized activity superimposes constructively, statistically independent activity mainly cancels out. Thus, mass signals essentially reflect synchronized components of the constituting signals. Consequently, the amplitude as well as the synchronization of the underlying brain activity has to be considered for an understanding of mass signal generation.

1.1.3 Classification

Experimental results on neuronal synchronization can be classified according to the spatial scale, temporal structure, and stimulus coupling of the signals involved. Spatial ranges of synchronization (see also "Methods") include the levels of (i) single neurons, (ii) local groups of neurons, (iii) larger groups of neurons with similar function and (iv) cortical areas. Concerning temporal structure, oscillatory signals can be opposed to aperiodic signals. When considering stimulus coupling, simultaneous activation of neurons by sensory stimuli ("stimulus-locked synchronization") is distinguished from synchronization by neuronal connections, which does not necessarily have a constant temporal delay to the stimulus ("stimulus-induced synchronization"). This dissertation thesis considers all the spatial levels and temporal structures mentioned, as well as different types of stimulus-response coupling.

1.1.3 Basic experimental results

Synchronized neuronal activity has been observed in many species and brain regions, often with an oscillatory time course. In some investigations the correlated firing of neuron pairs was analyzed (Perkel et al. 1967; review in Aertsen and Arndt 1993). Synchronization of

oscillatory activity in the gamma range (30-100 Hz) was a focus of research in the last years. After studies of Freeman an coworkers in the olfactory system of rabbit (1975) and visual cortex of monkey (1987), investigations in the visual cortex of cat (Eckhorn et al. 1988; Gray et al. 1989) and monkey (Kreiter et al. 1992; Eckhorn et al. 1993) showed that amplitude and synchronization of gamma oscillations were highly stimulus-specific (reviews in Eckhorn 1994; Singer and Gray 1995). Gamma oscillations were also observed in other cortical and subcortical areas of higher mammals, for example in the motor (Murthy and Fetz 1992) and somatosensory (Sanes and Donoghue 1993) cortex, as well as in thalamic nuclei (Steriade et al. 1996). In the human EEG and MEG gamma oscillations were reported after visual (Tallon-Baudry et al. 1996), auditory (Joliot et al. 1994), and tactile (Desmendt and Tomberg 1994) stimulation. Although gamma oscillations were described as stimulus-induced in most previously cited reports (i.e. without a certain phase relation to the stimulus), in some investigations an early stimulus-locked component was observed during visual (Cracco and Cracco 1978; Tallon-Baudry et al. 1996) and auditory (Pantev et al. 1991) stimulation. Periodicities in human reaction time distributions during visual and auditory tasks, reported by Dehaene (1993), were interpreted as reflecting such stimulus-locked gamma band activity.

1.1.4 Proposed functions of synchronized neuronal activity

The widespread incidence, stimulus specificity, and particularly the known effects of synchronization on neuronal activation led to hypotheses relating it to different aspects of brain function. It was suggested that feature binding and scene segmentation (Milner 1974; Reitböck 1983; v.d. Malsburg 1983) might be supported by the synchronization of the representing neurons. In addition, other important brain functions such as attention (Sheer 1889) and consciousness (Crick and Koch 1990) have been attributed to synchronized activity. Another variant of these theories is the assembly coding concept (Gerstein et al. 1989) which uses synchronization as one of several possible features to define and demarcate groups of neurons participating in a certain function. It might be noted, that synchronization, and not the time structure (oscillatory versus nonoscillatory) of the signals was judged as critical prerequisites for the proposed functions in all these ideas. It is not quite clear in most theories (however poses an interesting question) whether synchronization is only a necessary precondition or already the equivalent for the considered phenomena. Or, according to Mountcastle (1992), aimed at theories about gamma band oscillations:

> The general proposition driving the field is that the stimulus-induced slow wave oscillations are related to / are signs of / generate or are generated by / are representations of / those higher order neuronal operations intercalated between initial central sensory processing and such complex brain functions as perception, or the willing and execution of movement patterns, or storage in memory - in short, those functions whose study makes up a large part of what is now called by the inclusive term of Cognitive Neuroscience.

1.2 Introduction to the thesis

At the present time, it is difficult to decide whether the "correlation theories" of brain function introduced above are correct. Main reasons for this uncertainty are experimental difficulties in attributing synchronization to behavior and lacking insight into the generation and processing of synchronized neuronal activity. Some questions in this scope were clarified in this thesis but also new conceptual and methodological problems were brought into view. Synchronized activity was analyzed on different scales of spatial resolution. The scope of investigations spanned the range of small local networks, hypercolumns, cortical areas, interareal networks, and behavior. The applied methods were computer modeling, analysis of microelectrode and EEG recordings, and reaction time analysis. Experimental procedures comprised presentation of visual stimuli during fixation, a match to sample task, memory storage and retrieval, and choice reactions to auditory stimuli.

1.2.1 Overview

In the following section, the investigations presented in the different chapters will be summarized briefly. A more comprehensive abstract is given at the beginning of each chapter.

Chapter 2: "Parallel processing by a homogeneous group of coupled model neurons can enhance, reduce and generate signal correlations"

Computer simulations were used to analyze the generation and transmission of synchronized oscillatory and nonoscillatory signals in laterally coupled neuronal networks. In states of high discharge rates (high average input level), the emergence of qualitatively different network activity at different noise amplitudes and lateral coupling strengths was investigated. Especially the generation of stimulus-induced oscillations and the transition to periodic burst activity at stronger lateral coupling was examined. In states of low activation (low average input level), the processing of a group of partially synchronized nonoscillatory input signals was analyzed. Differences in correlation were reduced without lateral coupling but were enhanced with increasing lateral coupling. This enhancement was more pronounced with multiplicative than with additive interactions commonly used. In all simulations, the correlations between input and output signals were analyzed to quantify the information transmission of the network under different conditions.

Chapter 3: "Identical visual stimulation elicited fast oscillations in EEG and LFP of monkey but not in human EEG"

While it is well known that oscillatory activity is present in intracortical recordings from monkey during visual stimulation, it has not been investigated whether the monkey scalp EEG reveals such oscillatory components, as well. Nevertheless, this point is of basic impor-

tance for a comparison between oscillatory phenomena in humans and monkeys, since only extracortical recordings are available from humans. In the present investigation, synchronization was revealed by simultaneous microelectrode and EEG recordings from monkey visual cortex and by EEG recordings from human subjects during similar stimulation. The analysis of intracortical LFP amplitude and coherence, together with extracortically measured EEG, allowed the investigation of EEG generation in monkey. A repetition of one of the experiments with EEG recordings from human subjects provided further information about the relation between findings in monkey and human. The results showed that stimulus-induced and stimulus-locked oscillations, present in microelectrode and EEG recordings of monkey, were not visible in the human EEG. Harmonics of alpha activity, possibly playing a role in previous investigations on human gamma band activity, are examined in the following chapter.

Chapter 4: "Stimulus-induced gamma oscillations: harmonics of alpha activity?"

The human EEG was analyzed during the storage and retrieval of spatial and semantic information. A Fourier analysis showed the presence of harmonics of alpha activity in the upper frequency bands, pointing towards possible misinterpretations of previously analyzed gamma band activity in the human EEG.

Chapter 5: "No oscillations in human reaction time distributions?"

Behavioral reactions can be used to reveal stimulus-locked oscillatory brain processes, as well. A recent publication (Dehaene 1993) reported on oscillatory reaction time distributions in human subjects during auditory and visual discrimination tasks. The auditory tasks of this experiment were repeated to replicate the results. Nevertheless, the reported effects could not be verified despite identical stimulation and signal analysis procedures.

1.2.2 Hints for reading

The thesis was written for readers with an elementary background in neuroscience. The different main chapters are self-contained: Each contains a separate introduction and discussion of the respective topic. Readers interested in the generation of gamma oscillations, which are the main topic of the following chapters, might first read Chapter 2. It presents a simplified computer model and an overview of other model approaches. Chapters 3 and 5 are related: They both deal with stimulus-locked oscillations, in the visual or auditory modalities, respectively. Chapter 4 makes a critical contribution to the discussion about reports on gamma oscillations in human subjects, which are a main topic of Chapter 3. Interrelations between results from the different chapters are discussed in the concluding Chapter 6.

Parts of this thesis have already been published (Chapter 2: Jürgens and Eckhorn, 1997; Chapter 4 Jürgens and Rösler, 1995).

2 Parallel Processing by a Homogenous Group of Coupled Model Neurons can Enhance, Reduce and Generate Signal Correlations

2.0 Abstract

Correlated activities have been proposed as correlates of flexible association and assembly coding. We addressed the basic question of how signal correlations on parallel pathways are enhanced, reduced and generated by homogeneous groups of coupled neurons, and how this depends on the input activities and their interactions with internal coupling processes. For this we simulated a fully connected group of identical impulse-coded neurons with dynamic input- and threshold-processes and additive or multiplicative lateral coupling. Input signals were Gaussian white noise (GWN), completely independent or partially correlated on a subgroup of the parallel inputs. We show that in states of high average spike rates input-output correlations were weak while the network could generate correlated activities of stochastic, oscillatory and rhythmic bursting types depending exclusively on lateral coupling strength. In states of low average spike rates input-output correlations were high and the network could effectively enhance or reduce differences in spatial correlation applied to its parallel inputs. The correlation differences were more pronounced with multiplicative lateral coupling than with the additive interactions commonly used. As the different modes of correlation processing emerged already by global changes in the average spike rate and lateral coupling strength we assume that in real cortical circuits changes in correlational processing may also be induced by unspecific modulations of activation and lateral coupling.

2.1 Introduction

Correlations among neural signals are present in all structures of the brain. They have always been assumed to be functionally important because correlated spike trains can, if they converge, cause considerably stronger activations than uncorrelated patterns and therefore provide distributed signalling at high signal-to-noise ratios (review in Abeles 1991). It has been possible to study correlations in detail only in the last 10-20 years with the invention of practicable multiple-site recording (review in Krüger 1983) and signal analysis (review in

Gerstein et al. 1986). Signal correlations have been most intensively investigated in the cortex (reviews in Steriade et al. 1990; Abeles 1991). The interest in correlations increased considerably when processes of stimulus-specific synchronization were found in the visual cortex and attractive functional interpretations were proposed, including mechanisms of flexible association (Eckhorn et al. 1988; Gray et al. 1989; reviews in Aertsen and Arndt 1993, Gray 1994), assembly coding (Aertsen et al. 1989, Gerstein et al. 1989), directed attention (Sheer 1989) and consciousness (Crick and Koch 1990).

Despite these challenging hypotheses little is known about the cortical circuits that generate and process the observed correlations. It was expected that at least some basic neural structures would be discovered on the basis of multiple-site recordings and cross-correlation analyses because the signal correlations contain information about the structure they were recorded from. However, the numerous investigations utilizing correlation methods allowed only vague "glimpses" of the neural networks that influence and generate cortical correlations (Aertsen et al. 1989; Gerstein et al. 1986, 1989), because practicable analysis methods were developed mainly for pairs or small groups of neurons and these could seldom provide unique insight into the circuitry (Gerstein and Perkel 1969; Melssen and Epping 1987). Problems of cross-correlation analysis are the distinction between "common input" and "mutual connections", between mono- and polysynaptic connections, and the visualization of data from many pairs of recordings. However, monosynaptic excitation and inhibition can be assessed when strong coupling of short latency is present, particularly if one recording is made intracellularly.

Modelling approaches provide another possibility for understanding neural structures with respect to their ability in generating and modifying correlations. In most biologically inspired models impulse-coded neurons have been used (e.g., French and Stein 1970) and often collectively synchronized modes of oscillatory activations were investigated (e.g., Eckhorn et al. 1990; Gerstner et al. 1993; Deppisch et al. 1993; Usher et al. 1993; Nischwitz and Glünder 1995; Hansel et al. 1995; Bibbig et al. 1995; Wennekers et al. 1995). These models generated states of synchronized oscillations if the input signals either remained constant or changed slowly so that the oscillations were not disturbed by dynamic input signals. Dynamically changing signals, on the other hand, play an important role in neural processing. Models that aim at explanations for generating and modifying correlations in the brain should, therefore, include transiently changing (dynamic) and sustained (static) input signals in order to gain insight into network processing during input-dominated and network-dominated (often rhythmic) modes. It seems particularly interesting to analyze the parallel processing of partially correlated signals by a coupled group of neurons, in which different subgroups receive differently correlated external input signals. Such processing of input "correlation contrast" plays a central role in theories of association and assembly coding but has barely been analyzed. In these theories it is important that local groups of neurons (assemblies) can segregate into subassemblies under the influence of different configurations of correlations among their inputs. This is relevant, for example, for the feature-linking hypothesis of visual scene segmentation,

which requires that the neural representation of a visual object is represented by synchronized signals while that of the background (or another object) is uncorrelated with the object's activity (Reitböck 1983; von der Malsburg and Schneider 1986; Eckhorn et al. 1988; Gray et al. 1989; reviews in Aertsen and Arndt 1993; Gray 1994). For such coding it is essential that the spatial "input correlation contrast" among object and background can be amplified or at least be preserved by passing a processing network to its outputs. The processing of partially correlated input signals by elements with sigmoidal transfer characteristics was treated analytically by Bedenbaugh and Gerstein (1994), but the influence of lateral connections was not investigated. To our knowledge no neural network simulation exists that investigated this aspect explicitly - only in a single work was one aspect of correlation enhancement investigated (Koch and Schuster 1992).

In our simulations we therefore addressed the basic question of whether and how differences in spatial correlation, defined by different degrees of correlation in subgroups of parallel input signals, can be enhanced, reduced and generated by small groups of coupled neurons. In addition, we asked how the input-output coupling across the group (its "information transmission") is changed by the average activation level and the states of more stochastic or rhythmic correlated activities that are generated as a consequence of the groups' lateral connections. For this we simulated a fully connected group of impulse-coded neurons with dynamic input- and threshold-processes and systematically changed the parameters in discrete steps to the same values for all neurons. We were particularly interested whether, and under what circumstances, this group can segregate into temporary assemblies exclusively due to the current correlation structure at its parallel inputs and the type and strength of lateral coupling among the neurons. In the present investigation two basically different states of activation were modelled which closely resemble activation states of sensory cortices during stimulation. In the "low" state the external input produced a subthreshold mean membrane potential causing low average discharge rates of typically 5-10/s, due to random variations in these driving inputs. This state is typical in the cortex for the many neurons being suboptimally stimulated. In contrast, in the "high" state the mean membrane potential was higher than the resting threshold which caused discharge at relative high rates (40-150/s) while the external inputs and lateral coupling modulated the spatio-temporal spike patterns. The latter state resembles more "optimal" sustained stimulus activations where weak oscillatory coupling is typical in the cortex (e.g., Kruse and Eckhorn 1996). Direct comparability with experimental results was achieved by quantifying all signal correlations in our simulations by conventional cross-correlation methods. (An abstract version of this work has been published: Jürgens and Eckhorn 1993).

2.2 Methods

2.2.1 Network model

The network model simulates a local group of 20 neurons with complete lateral connections of equal strength which corresponds to a small local subassembly in the cortex (Palm 1993). We chose a model neuron with spike output since this type of model resembles the dynamic properties of real neurons quite closely and is therefore especially suited to the simulation of correlation phenomena (more details are given below and in Eckhorn et al. 1990). The model neuron can be divided into a dendritic/somatic part and a spike encoder.

The *dendritic part* processes two different kinds of input signals: external *feeding signals* (E, see sect. 2.2) and lateral *coupling signals* (S). The feeding signals are lowpass filtered (the "synapse" is a first-order lowpass filter with time constant τ_F = 10, gain V_F = 1) constituting the *feeding potentials* (see Fig. 2.4):

$$F_k(t) = E_k(t) * h(V_F, \tau_F, t), \tag{1}$$

where t denotes time (in steps of Δt = 1), k is the index of the model neuron, $E_k(t)$ is the external input, the asterisk denotes the convolution operator and $h(V_F, \tau_F, t)$ is the impulse response of the leaky-integrators at the feeding inputs

$$h(V, \tau, t) = \begin{cases} V \cdot \exp(-t/\tau), & \text{if } t \geq 0 \\ 0 & \text{, else} \end{cases}; \tag{2}$$

where V denotes the gain and τ the time constant of the leaky-integrator.

Due to the complete connectivity of the lateral network, weighted sums of all output signals of the network constitute the *coupling signals*

$$S_k(t) = \sum_{i=1}^{N} \omega_{ki} Y_i(t), \tag{3}$$

where N is the number of model neurons, ω_{ki} the synaptic weight of coupling input from the i th to the k th neuron and $Y_i(t)$ is the spike output from the i th neuron. The ω_{ki} have identical values ω_c for all k, i ($i \neq k$), while $\omega_{ii} = 0$. The coupling signals reach the coupling synapses with one timestep delay, are lowpass filtered (first order, $\tau_L = \tau_F$, $V_L = V_F$) and constitute the *coupling potentials*:

$$L_k(t) = S_k(t) * h(V_L, \tau_L, t). \tag{4}$$

For the cortex, in which we are especially interested, there is experimental evidence that lateral connections among excitatory neurons are often acting in a facilitatory (modulatory) manner on the afferent feeding inputs (e.g., Hirsch and Gilbert 1991). Therefore the *membrane potential* was calculated as $M = F \cdot (1 + L)$ (Eckhorn et al. 1990). In order to demonstrate the specific effect of this multiplicative type of lateral coupling further simulations were performed with additive lateral interactions: $M = F + L$ (as has conventionally been implemented). Since the exact functional dependencies of the membrane potentials on feeding and linking signals are not known, these two models present extremes in a continuum of possible synaptic couplings.

In the dynamic spike encoder, the membrane potential M is compared with a threshold potential θ. If M exceeds θ, the model neuron produces an output spike, i.e., the output signal Y is assigned a value of 1. The threshold potential is the sum of a constant offset value θ_0 and the output signal of the model neuron which was filtered by two parallel first order lowpass filters:

$$\theta_k(t) = \theta_0 + Y_k(t) * \left[h(V_{\theta 1}, \tau_{\theta 1}, t) + h(V_{\theta 2}, \tau_{\theta 2}, t) \right] \tag{5}$$

One lowpass filter simulated the fast ($\tau_{\theta 1}$ = 2, $V_{\theta 1}$ = 5; "refractory") and the second the slow ($\tau_{\theta 2}$ = 20, $V_{\theta 2}$ = 2; "adaptation") properties of the threshold (Lankheet et al. 1989), i.e. the latter reduced the excitability of the model neuron during a period of some 10 bins after a spike. A physiologically realistic time scale in our simulations corresponds to 1 ms per time step.

2.2.2 Input signals

The continuous signals at the feeding inputs resembled the probability density of action potentials from many neurons providing input to the network. A good estimate is Gaussian white noise (GWN), if we assume a high number of statistically independent spike trains of sufficient rate at the input. This seems appropriate because cortical neurons receive about 10^4 synaptic inputs from different neurons (Braitenberg and Schüz 1991).

In the *first series* of simulations (sect. 3.1) all input signals were GWN, independent at all feeding inputs,

$$E_i = G_i + E_0 . \tag{6}$$

The common mean value ("DC-bias") was set to E_0 = 0.15 to generate sufficiently high firing rates that favored the internal generation of collective correlations. Standard deviations of the GWN ("AC-amplitude") were chosen as 0.2, 0.1 and 0.05 in three different simulation runs.

In a *second series* of simulations (sect. 3.2) half the neuron group received partly correlated GWN input signals (G1 neurons) while the other half received GWN that was completely independent among the inputs (G2 neurons). Input signals were computed as

$$E_i = \begin{cases} (G_c + G_i)/\sqrt{2}, & 1 \le i \le N/2 \\ G_i, & N/2 < i \le N \end{cases} \tag{7}$$

where G_c was a common input to subpopulation G1. G_c and G_i ($1 \le i \le N$) were statistically independent GWN (zero mean, s.d. = 0.2). Thus all E_i had identical mean values and standard deviations. Since the feeding input to a neuron *i* in G2 was independent of any other input signal, cross-correlations among feeding inputs of neurons in G2 vanished. On the other hand, each G1-pair had a cross-correlation coefficient of 0.5 among their feeding input signals.

In real networks the strength of lateral connections as well as other parameters such as time constants of synapses and spike encoders will underlie random variations. As we used identical values, it is important that the strong stochastic input components in all our simulations prevented effects that are merely due to exact symmetries of the network. For example, coupling efficacies are modulated by the current state of activation in single neurons (Aertsen et al. 1994).

2.2.3 Correlation analysis

In order to quantify correlations among network activities, we calculated cross-correlations of all possible combinations of input and output signals (each over 100.000 time steps). Cross-coincidence histograms (CCH) among output spikes were normalized to the respective average spike rates of the neurons (n_i and n_j)

$$CCF^N_{YiYj}(\tau) = CCF_{YiYj}(\tau) / \sqrt{n_i \cdot n_j}\,. \tag{8}$$

In the simulations with low spike rates correlations were quantified by the central peak in the range of $|\tau| \le$ 10-20 bins. Outside this range only small variations around a mean value *m* were present (except with very strong lateral coupling where sustained bursts occurred). As a correlation index (CI) we therefore defined the peak area above expectation level m

$$CI_{ij} = \sum_{\tau \in P} (CCF^N_{YiYj}(\tau) - m)\,. \tag{9}$$

All positively deviating bins *P* in the central area of the CCF_N were used for the calculation of the peak area. *P* is the set of τ satisfying

$$CCF^{N}_{YiYj}(\tau) > m + 2 \cdot sd \tag{10}$$

where m is the average value and sd is the standard deviation of the normalized $CCF^{N}_{YiYj}(\tau)$ outside the central peak area, i.e. for $30 \le |\tau| \le 128$ bins. This measure can exceed the value 1.0. When, for example, correlated short bursts occur in two neurons, the peak area increases quadratically with the number of spikes in these bursts. The above-defined measure was used because the physiological significance (the impact on other neurons which receive convergent input from both neurons) of correlated bursts is stronger than that of correlated single spikes. For comparison we also calculated a correlation index CI^{N}_{ij} which was normalized by the peak area of the auto-coincidence histogram (ACH) and therefore could have values only in the range $-1 \le CI^{N}_{ij} \le 1$:

$$CI^{N}_{ij} = CI_{ij} \,/\, \sqrt{CI_{ii} \cdot CI_{jj}}\,. \tag{11}$$

The correlation indices defined above could not be used in simulations with oscillatory activities since there were no restricted central peaks in these cases. Therefore we defined alternative measures to describe results in oscillatory states: (1) the average spike rate; (2) the oscillation frequency, determined as $1/T$ for periodic auto-coincidence histograms, where T is the time interval between consecutive side peaks of the ACH; (3) a synchronization index, determined as the difference between the CCH for $\Delta t = 0$ and the background correlation expected by chance for independent signals and (4) ACH and CCH modulation indices, calculated as the difference between the first side maximum of the auto- and cross-coincidence histogram and the next minimum normalized by the arithmetic mean of these two values.

Cross-correlations between analog feeding input and spike output signals were calculated as spike triggered averages (STA)

$$STA_{ij}(\tau) = CCF_{EiYj}(\tau) \,/\, n_j\,. \tag{12}$$

where $CCF_{EiYj}(\tau)$ denotes the cross-correlation histogram of the feeding input signal of model neuron i and the output spikes of model neuron j (n_j is the number of spikes of neuron j). Again, the peak area above the background level was used for calculating the correlation index.

2.3 Results

2.3.1 States of high discharge rates

High average rates of activation (r > 40/s) were evoked by setting the "DC level" of the parallel inputs to a fixed value of 0.15. The standard deviation of the GWN at the feeding inputs was set to values of 0.2, 0.1 and 0.05 and multiplicative coupling-feeding interactions were used. The lateral coupling strength was varied from 0.0 to 0.105 in discrete steps of 0.015.

2.3.1.1 Different modes of network activity

With an input DC level of 0.15 the mean value of the membrane potential $\langle M(t)\rangle = V_F \cdot \tau_F \cdot E_0 = 1.5$ (value without lateral coupling) exceeded the threshold offset θ_0 = 1.0 and high average rates were generated. In this situation spike initiation was determined primarily by the dynamics of the spike encoder and the type and strength of recurrent coupling connections. It was less influenced by the current amplitude values of the external inputs.

With random GWN input of high amplitude (σ = 0.2) rhythmic activity of single neurons was absent at zero lateral coupling; collective rhythms even did not occur at weak and medium values of coupling. However, with stronger lateral coupling ($\omega_c \geq 0.09$) collective bursts of spikes were initiated, interrupted by phases of low or no spike activity. Reduction of the GWN input's standard deviation by 50% (σ = 0.1) produced a richer dynamical behavior of the network at increasing coupling strengths: 1. regular spike trains; 2. high-frequency "oscillation spindles"; 3. aperiodic synchronized bursts; 4. periodic synchronized bursts. Figure 2 shows a parametrization of the resulting network states by spike rate, oscillation frequency, synchronization index and modulation indices of auto- and cross-coincidence histograms

State 1: Without lateral coupling rhythmic activity of single neurons, independent among different outputs, was visible in the auto- and cross-coincidence histograms.

State 2: Lateral coupling enabled the emergence of rhythmic activity (40-80 Hz) which was partially synchronized among the neurons' output spike trains (Fig. 2.1A, ω_c = 0.045). The collective oscillations were not stable but alternated with periods of more asynchronous activity. No bursting behavior was visible in the auto-coincidence histograms in this state.

State 3: With stronger lateral coupling (Fig. 2.1B, ω_c = 0.06) the regularity of the oscillation periods decreased, while correlations with short latency ($|\Delta t| \leq 3$ ms) remained strong on average. Correspondingly, the auto- and cross-coincidence histograms showed no rhythmical modulation, although the spike patterns had short periods of rather regular spike intervals.

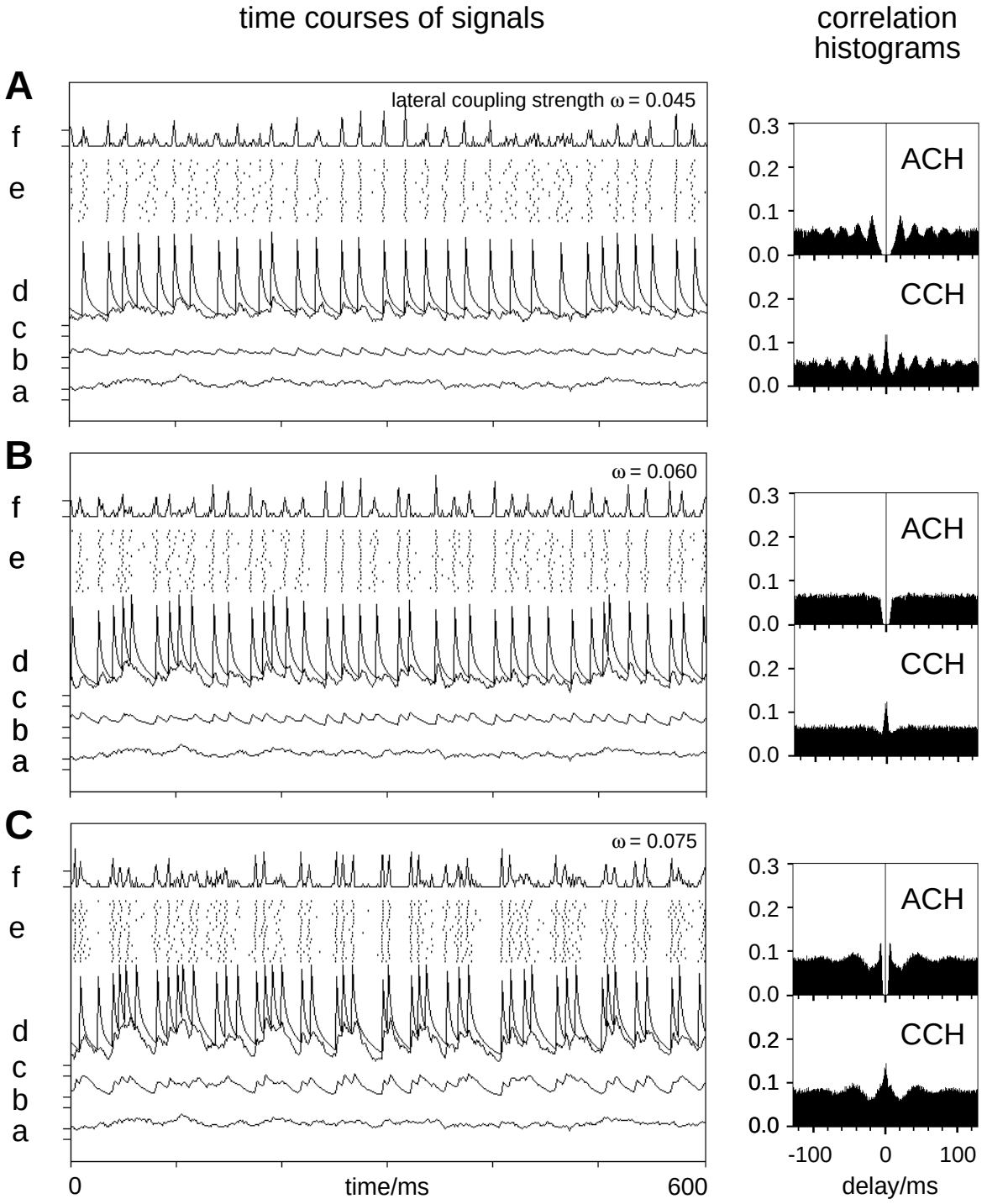

Fig. 2.1A-C. Three different modes of network dynamics produced by changing the lateral coupling strength when the random amplitudes of the Gaussian white noise (GWN) inputs were low ($\sigma = 0.1$) and their high mean value caused high average discharge rates. **A** Alternating stochastic and oscillatory activity (weak lateral coupling $\omega_c = 0.045$). **B** Synchronized short oscillations with random frequencies in successive events (medium coupling $\omega_c = 0.06$). **C** Rhythmical bursts (stronger coupling $\omega_c = 0.075$). *a*, Feeding potential; *b*, linking potential; *c*, membrane potential; *d*, threshold potential; *e*, spike output patterns; *f*, multiple unit activity. ACH, auto-coincidence histogram of output spikes; CCH, cross-coincidence histogram of output spikes from two different model neurons (averaged over 100 000 time steps).

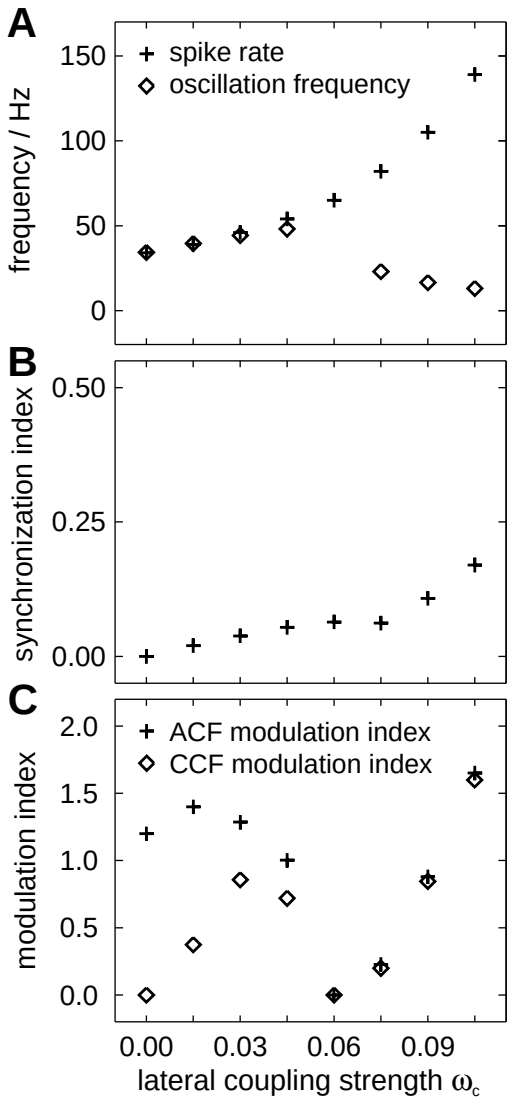

Fig. 2.2A-C. Transitions of network activity from oscillatory single spike to rhythmic burst activity due to changes in lateral coupling strength (σ = 0.1). **A** The spike rate increased continuously with lateral coupling strength ω_c while the oscillation frequency corresponded to the spike rate only for $\omega_c < 0.045$. For $\omega_c = 0.06$ no rhythmic activity was present at all. With stronger lateral coupling the oscillation frequency decreased (burst mode). **B** The synchronization index of network activities increased with lateral coupling strength. **C** Modulation of auto-coincidence (ACH) and cross-coincidence histograms (CCH) first increased with lateral coupling, dropped at ω_c = 0.06 (synchronized non-rhythmic activity) and then increased again

However, the variability was so high that the histograms showed no satellite peaks. The trough in the CCH for 3 ms < $|\Delta t|$ < 20 ms was caused by the refractory phases of the neurons. No correlation exceeding the chance level was visible in either the auto- or cross-coincidence histograms for $|\Delta t|$ > 20 ms.

State 4: With even stronger lateral coupling (ω_c = 0.075) collective spike bursts occurred rhythmically at low frequencies (10-30 Hz, Figs. 1C, 2A). The intervals between spikes within bursts were mainly determined by the fast lowpass filter in the threshold feedback ("refractory period"), whereas the interval between bursts was determined by the time constant of the slow threshold component ("adaptation"). With further strengthened lateral coupling, the modulation of the auto- and cross-coincidence histograms and the time between bursts increased (Fig. 2.2A, C).

When the GWN standard deviation was reduced to 0.05 (while the external input "DC bias" remained at 0.15) the spike intervals became more regular. Under these conditions, considerably weaker lateral coupling was sufficient to synchronize the network's outputs (ω_c = 0.015: synchronization index = 0.147). In addition the coupling strength necessary for evoking strong bursts was diminished (bursts with a modulation index of 1.12 were evoked with ω_c = 0.075, compare with Figs. 1C and 2C).

2.3.1.2 Input-output correlation during high activity states

Generally, the correlation between the output spike train of a neuron and its feeding input was low with the positive ("DC") offset at the feeding inputs (which caused high average discharge rates at the outputs). Input-output correlation was as low as CI = 0.23 (see Sect. 3.2.5: CI = 2.0) without lateral coupling and with a standard deviation of the GWN of σ = 0.2. Input-output correlations increased more than proportionally with the standard deviation of GWN at the feeding inputs. Increasing the lateral coupling strength, however, reduced the input-output correlations continuously (Fig. 2.3). This was rather unexpected, because different modes of strongly correlated network activities (oscillatory, stochastic, and rhythmic bursting) were found in the same range of lateral coupling strengths (Fig. 2.1). In short, the input-output correlations were barely dependent on the transitions of the network to different states of correlated activations.

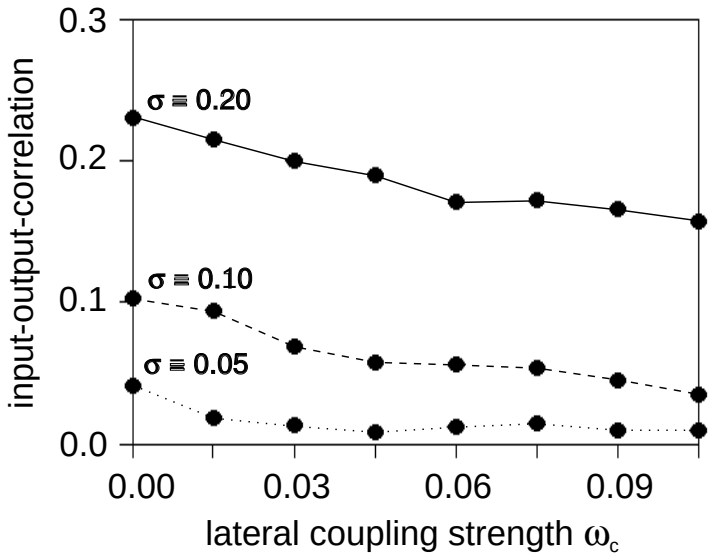

Fig. 2.3. Input-output synchronization index versus strength of lateral coupling for three different amplitudes σ of the random input signals. *Continuous line*: σ = 0.2; *dashed line*, σ = 0.1; *dotted line*, σ = 0.05

2.3.2 States of low discharge rates

2.3.2.1 Network dynamics

The dynamics of the network changed completely when the constant input bias ("DC-offset") at the feeding inputs was set to zero. The mean spike rates of the neurons decreased from more than 40/s (45-150/s; see Sect. 3.1) to less than 20/s (typically 5-10/s). This state of low rate was correlated with changes of some basic properties of the network's dynamics (Fig. 2.4 is a typical example). Here rhythmic activity was completely absent and the neurons were primarily coupled to their random GWN inputs. In this state of low activity the network could effectively process differences in input correlation strength defined by the feeding signals. Neurons 1-10 (G1) received partially correlated GWN inputs while neurons 11-20 (G2) had uncorrelated GWN input. Consequently, the G1 output spike trains displayed stronger mutual correlations than those of G2 neurons. There are two obvious reasons for this. First, the correlated input signals to G1 neurons led to correlated output signals in this group. Second, the lateral coupling connections among all neurons particularly supported synchronization between G1 outputs. A more detailed and quantitative characterization of these network dynamics follows in the next section.

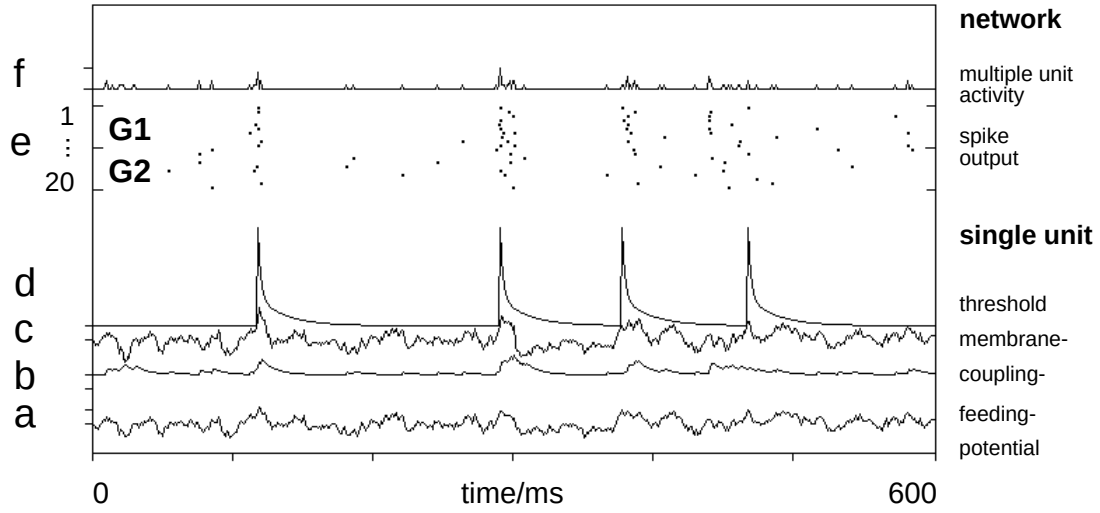

Fig. 2.4. Processing of partially correlated random input signals. The feeding input signals of one half of the model neurons (G1, 1-10) were 50% correlated GWN, while the other half (G2, 11-20) received uncorrelated GWN input. *a* to *d*, Time courses of variables of a single G1 neuron; *a*, feeding potential $F(t)$; *b*, coupling potential $L(t)$; *c*, membrane potential $M(t) = F(t) \cdot (1 + L(t))$; *d*, dynamic threshold $\theta(t)$; *e*, spike patterns of all model neurons (*dots* denote spike instances). Note, that synchronized spikes are visible as *vertical lines* in the spike pattern; *f*, multiple unit activity (MUA), calculated as the superposition of all output spikes. Lateral coupling strength ω_c = 0.15, threshold offset θ_0 = 1.0

2.3.2.2 Effect of multiplicative lateral coupling on output correlations

We were particularly interested in the ability of the network to amplify or reduce correlations among the parallel input signals - the modulation of "spatial correlation contrast". Correlations among spike trains of neurons with uncorrelated input signals (G2) had to remain weak if the differences between internal G1 and internal G2 correlations should be preserved or even enhanced.

Figure 5 shows how the correlation indices (CI) among output spike trains depended on the strength of the multiplicative lateral connections. Without lateral coupling CI was only 0.13 among pairs of G1 neurons. This value was considerably smaller than the mutual correlation among their feeding inputs signals (0.5), which means that the single neuron properties caused "decorrelation" under this condition. Increasing strength of lateral connections enhanced the influence of input correlations on the output. For example, a lateral coupling of ω_c = 0.15 increased the correlations at the outputs of G1-pairs to about CI = 0.5 while the correlation among G2-pairs remained very low (CI = 0.06). Stronger lateral coupling amplified the correlations within both the G1- and G2-groups. As expected, correlations between G1- and G2-neurons were always stronger than those between G2-pairs.

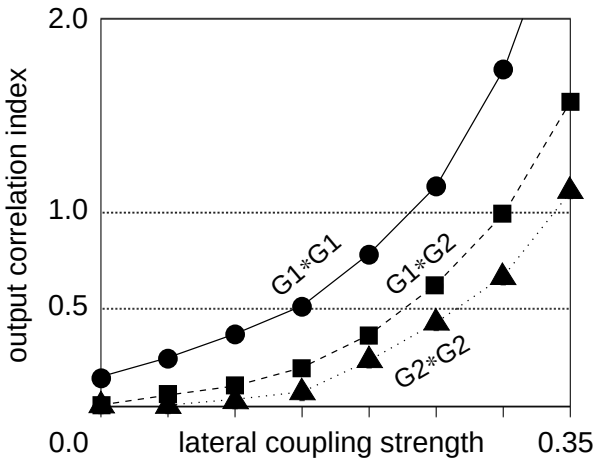

Fig. 2.5. Correlation among output spike trains as a function of lateral coupling strength (multiplicative coupling). *Solid line*: Pairs of G1-neurons (receiving partially correlated random inputs). *Dotted line*: Pairs of G2-neurons (with independent random inputs). *Dashed line*: Pairs of G1-G2 neurons. Without lateral coupling the output correlation among G1-pairs is much smaller (CI = 0.16) than the input correlation of 0.5. Increasing coupling strength enhanced the correlation among G1-neurons more steeply than among G2-neurons so that the difference between both groups was actively enhanced by the network.

2.3.2.3 Comparison of multiplicative and additive coupling

We compared multiplicative with additive interactions among feeding and coupling connections. As the threshold offset θ_0 is an important global variable influencing the network's correlational properties, we varied θ_0 in steps (θ_0 = 0.7, 1.0, 1.3) which caused lower average spike rates at higher thresholds. Figure 6A shows the correlation among G2 spike trains versus those in G1 with multiplicative lateral coupling, in Fig. 2.6B the same is plotted for additive coupling. This kind of diagram allows a comparison of different coupling types and threshold levels.

In the case of multiplicative lateral coupling the G1 output correlations could be increased to values of 0.5 (the correlation value among the input signals) by increasing the lateral coupling strength while correlations among G2 outputs remained at very low values. Hence, the difference in correlation between G1 and G2 subassemblies was enhanced in this range compared with signal processing without lateral coupling. Further increase in lateral coupling strength caused the correlation among G2-outputs to rise about half as steeply as that among G1-outputs.

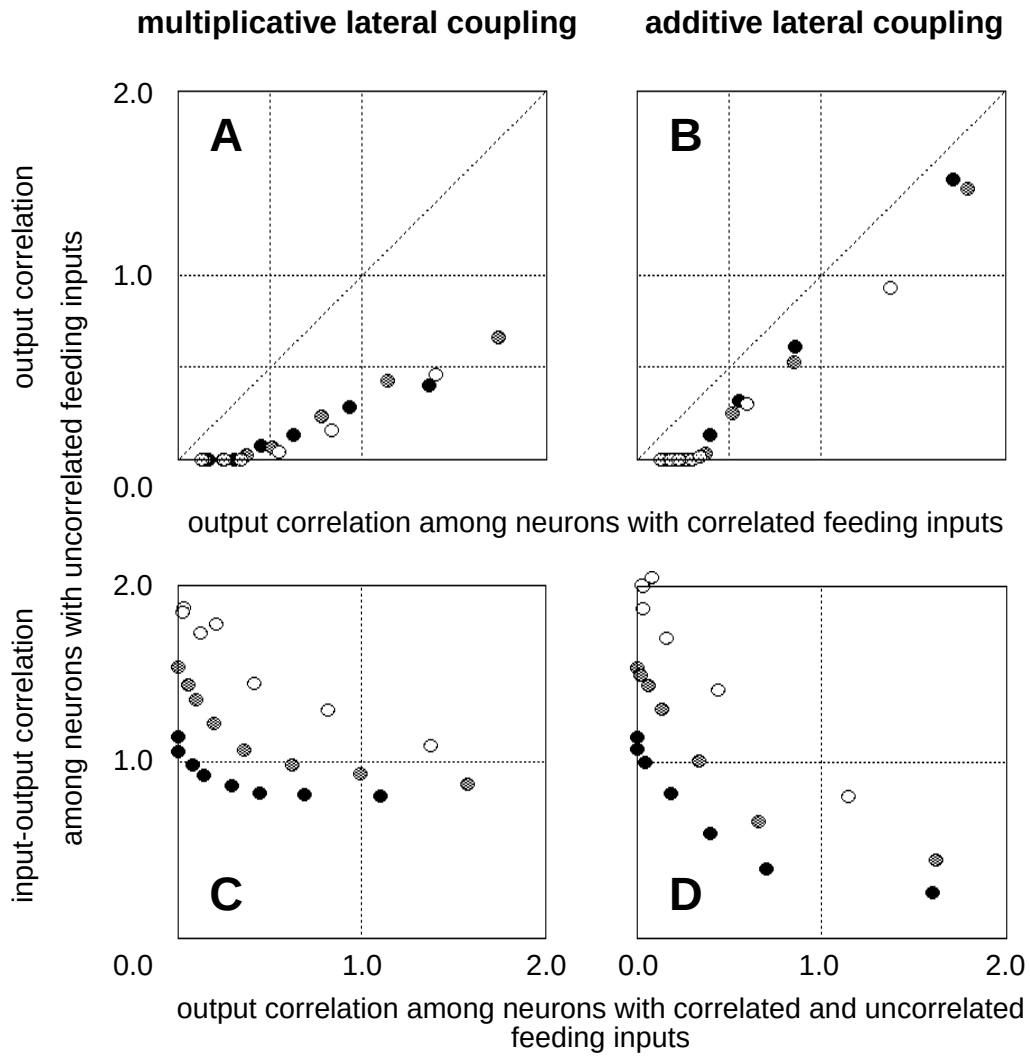

Fig. 2.6A-D. Scatter plots of correlations allowing comparisons among different lateral coupling strengths, coupling types and thresholds θ_0. **A**, **B**: Correlations among G1-neurons plotted against those among G2-neurons. Note, that lateral connections can selectively enhance the correlation of G1 selectively without increasing G2 correlation significantly. Multiplicative connections yielded a better separation between both groups while the threshold level had minor influence. **C**, **D**: Ordinate: Input-output correlations of G2-neurons. Abscissa: Correlation of G2-outputs with those from G1-neurons. *Filled circles*: θ_0 = 0.7, *grey circles*: θ_0 = 1.0, *open circles*: θ_0 = 1.3. **A**, **C**: multiplicative, **B**, **D**: additive lateral coupling.

Additive lateral coupling (Fig. 2.6 B), in contrast, was less suitable for processing differences in correlation among G1- and G2-subassemblies. Here we found a steep rise in correlation among G2-outputs if the correlation among G1-outputs exceeded CI = 0.4. Stronger coupling caused strong correlations both among G1- and G2-pairs, resulting in small differences in correlation between the two groups. The results concerning the differences in correlation were confirmed by the use of the normalized correlation index CI^N, which yielded smaller absolute correlation indices both among G1- and G2-outputs for strong lateral coupling (CI_{G1} > 0.7).

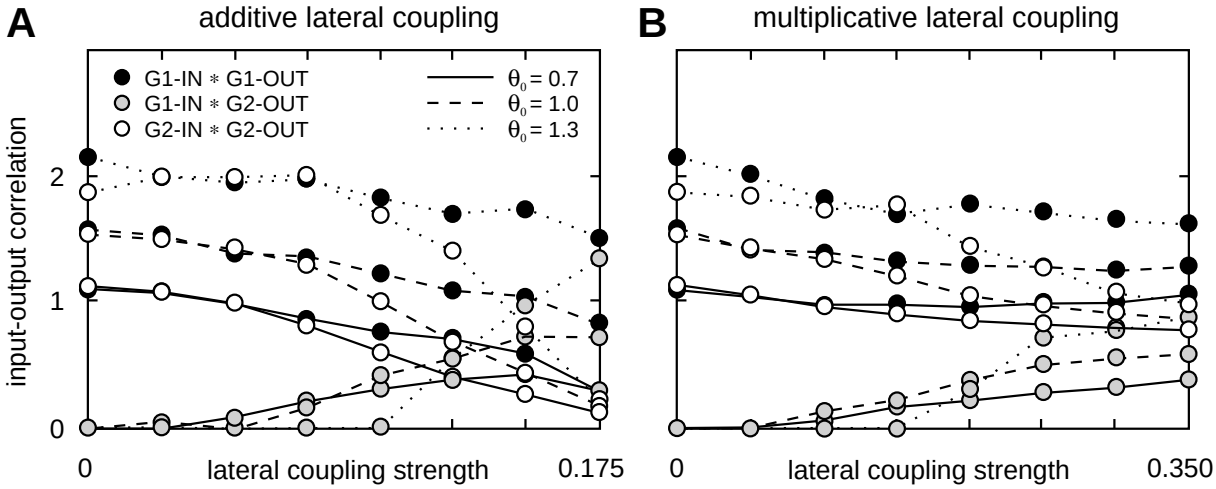

Fig. 2.7A, B. Input-output correlation as a function of lateral coupling strength. **A**: Additive, **B**: multiplicative coupling. The level of threshold offset θ_0 is indicated by *solid, dashed* and *dotted lines*. *Filled dots*: G1-neurons (partially correlated inputs). *Circles*: G2-neurons (uncorrelated inputs). *Gray dots*: Correlation of G1-input with G2-output.

The level of the average firing rates (induced by threshold offset θ_0) influenced the correlation indices of the output signals. Without lateral coupling lower threshold offsets yielded higher correlation indices than higher thresholds (θ_0 = 0.7: CI = 0.11, θ_0= 1.3: CI = 0.16). When lateral coupling was present, the influence of threshold offset on the relation between G1- and G2-correlations was small, but a lower threshold caused higher spike rates and stronger correlations among all outputs at any strength of lateral coupling. This means that the effective strength of the lateral connections was reduced by a higher threshold level (resembling the lower excitability of the neurons).

2.3.2.4 Dependence of spike rates on type and strength of lateral coupling

Spike rates without lateral coupling depended on threshold offset (8.6/s, 3.8/s, 0.9/s for threshold offsets of 0.7, 1.0, 1.3, respectively). The increase in firing rates with lateral coupling strength depended also on the type of coupling. As the strengths of additive and multiplicative coupling cannot be compared directly we compared their effects, i.e. the correlation among output signals. At coupling strengths yielding correlations between the outputs of G1 neurons of 0.5, average firing rates were 22.0/s, 7.7/s and 1.3/s for additive and 15.4/s, 7.8/s and 2.2/s for multiplicative coupling (threshold offsets of 0.7, 1.0, 1.3, respectively). Interestingly, a difference between G1 and G2 firing rates was observed only for multiplicative but not for additive lateral coupling: for a lateral coupling yielding an internal G1 correlation of 0.5 the firing rates were higher in G1 than in G2 (θ_0 = 0.7: 15.9/s vs. 15.0/s; θ_0 = 1.0: 8.2/s vs. 7.3/s; θ_0 = 1.3: 2.5/s vs. 1.9/s) .

2.3.2.5 Input-output correlations during low activity states

Generally, the correlation among the output spike train of a neuron and its GWN feeding input (Fig. 2.7) was high with the zero ("DC") offset at the feeding inputs (which caused low average discharge rates at the outputs). Input-output correlation was as high as CI = 2.0 without lateral coupling and a standard deviation of σ = 0.2 of the input GWN. It declined when the spike rates were increased, either by lowering the threshold offset, or by adding a constant value to the feeding inputs (see 3.1.2). Lateral coupling also reduced the input-output correlations across single neurons in which neurons with partially correlated inputs declined slightly less than neurons that received independent inputs. However, multiplicative lateral coupling caused weaker reductions of input-output correlations than additive lateral coupling.

Of additional interest are correlations among the input of one subgroup and the output of the other subgroup which resulted from the complete lateral connectivity of the network. For example, the GWN signals at the feeding inputs of G1-neurons (50% input correlation) were nearly uncorrelated with the spike patterns at the output of G2-neurons (uncorrelated inputs) as long as the lateral coupling strengths were low or medium. However, stronger lateral coupling increased the strength of these input-output correlations.

A more complex aspect of network correlations is illustrated in Fig. 2.5C and D. It shows the correlation of the output of a G2-neuron with its own input signal (ordinate) and with the output of a G1-neuron (abscissa). In general, input-output correlations decreased with increasing correlations among outputs. This result corresponds to the increase in output correlations and the concurrent decrease in input-output correlations due to strengthened lateral coupling. The relative decrease in input-output correlation was weaker with multiplicative compared with additive lateral coupling. For example, the input-output correlation was reduced by 29% with multiplicative coupling compared with 65% with additive coupling when the correlation among pairs of G1-G2 output spike trains was increased from CI = 0.0 to 0.5 (threshold offset θ_0 = 0.7).

2.4 Discussion

We addressed the basic question of whether and how signal correlations on parallel pathways can be enhanced, reduced and generated by parallel processing in a homogeneous group of completely coupled neurons. In addition, we asked how different types and degrees of lateral correlation influence the input-output coupling of single neurons, which is indicative of their ability to transmit information. Two main input situations causing high and low average discharge rates were investigated. GWN of identical standard deviation was present at each input driving the neurons dynamically.

In the situation of high average discharge rates (high mean value of external input) the network generated different partially synchronized types of activity that could already be controlled by global changes in lateral coupling strength: oscillatory, stochastic, and rhythmically bursting activity. In these states, input-output correlations were relatively weak (compared with the low discharge regime) because the activity of the neurons was dominated by the dynamics of the spike encoder and the lateral coupling. Domination of the network by rhythmic activities could partially be overcome by increasing the standard deviation of the GWN input signals.

In contrast, when spike rates were on average low (low mean value of external input), input-output correlations were strong. Here the network was dominated by the random GWN inputs (no rhythmic components were generated). A key result of our model is that the difference in correlation strengths among spike trains at the outputs of neurons in the two subgroups (G1 and G2), which was exclusively induced by the correlational structure among their stochastic inputs, was reduced compared with the difference in correlation among the inputs (if lateral coupling connections were weak or absent and average discharge rates were low).

Another key result is that in this low activity state partial correlation in the inputs to a subgroup of neurons (G1) could effectively be reduced or enhanced, exclusively under the control of the coupling strength of lateral connections. This is important because the coupling was identical for each neuron while a correlation contrast at the inputs was exclusively defined by their signal correlations (and not by different amplitudes). It is important, therefore, that this reduction in correlation difference could be counteracted by making the lateral coupling connections stronger. This capability of modulation was considerably better with multiplicative interactions than with the additive interactions commonly used in other neural network models.

2.4.1 Generation of different correlation modes during high sustained input activations

We studied the generation of correlated activities by a group of coupled neurons with completely independent GWN of identical mean and standard deviation at each input. This ensured that all correlations among outputs were generated within the network. A high "DC level" was applied to the inputs in order to generate high spike rates. Four well-defined states of different output correlations emerged reliably when the strength of the internal coupling connections was increased from zero to larger values: 1. regular spike trains, independent among different outputs; 2. high-frequency "oscillation spindles" (40-80 Hz) of different duration, synchronized among the outputs; 3. aperiodic synchronized bursts of spikes; 4. periodic bursts synchronized at medium frequencies (10-30 Hz). The occurrence of partially synchronized rhythms depended, in these simulations, on the supply of sustained suprathreshold input which was mimicked by an increased mean "DC level" at the feeding inputs.

Modes of continuous synchronized oscillations have been investigated in many network simulations, including those with impulse-coded neurons and excitatory (e.g., Eckhorn et al. 1990; Gerstner et al. 1993; Hansel et al. 1995; Bibbig et al. 1995) or inhibitory (Nischwitz and Glünder 1995) lateral connections. The emergence of oscillation "spindles" (state 2), as metastable states of synchronized rhythmic activity, was caused by the competition between synchronizing coupling processes and desynchronizing noise at the external inputs. Deppisch et al. (1993), Usher et al. (1993), and Bauer and Pawelzik (1993) also found such metastable states of synchronized rhythmic activity in fully connected networks of spiking model neurons when the strength of lateral coupling and the external input amplitude were in an appropriate range. Oscillation spindles have been observed in various cortical and subcortical structures of mammals under conditions of enhanced average activation (reviews in Aertsen and Arndt 1993; Gray 1994).

2.4.1.1 Transition from single spike oscillations to rhythmic bursts

The transition from single spike synchronized oscillations to a mode of synchronized, rhythmically occurring bursts (state 3; Fig. 2.1C) has not been observed in neural network models, as far as we know. However, the existence of fast spiking (state 2) and slower bursting (state 4) oscillations is a common observation in cortical group activities although it has attracted no special attention in the literature. Gradual transitions among these modes have been analyzed in some detail in the visual cortex of awake monkeys (Eckhorn and Frien 1995). There, an increase in the "strength" of sustained visual stimuli (e.g., by increasing their contrast or size) gradually lowered the frequency of collective oscillations while the probability of rhythmic bursting modes increased. In our model, such transitions occurred in the range of stronger lateral coupling (modelled explicitly). However, strengthening of the effective coupling can already be caused by an overall increase in activation. Such changes in coupling efficacy without explicit changes in coupling weights at synapses have been analyzed recently (Aertsen et al. 1994; see below). An alternative explanation for the occurrence of bursting modes in real networks is the action of a common inhibitory interneuron that "chops" the sustained activation supplied by the group's inputs (Douglas and Martin 1991; Kruse and Eckhorn 1996): Stronger inputs would activate the inhibitory neurons to longer bursts which thereby interrupted the activities of excitatory neurons.

Our results are compatible with the findings of Bringuier et al. (1992), who observed rhythmic spike bursts in the visual cortex of kittens mostly in the range of 7-20 Hz. In their recordings the amplitude but not the frequency depended on the resting membrane potential, so that the rhythms were assumed to be a network property (as in our simulations) rather than intrinsic to single neurons.

2.4.1.2 Intermediate state of synchronized non-rhythmic activity

The state of partially synchronized non-rhythmic activity (Fig. 2.1B) occurred at medium strength of lateral coupling in the transitory regime between fast spindle oscillations and slower burst rhythms. Such precisely correlated activity has been observed for pairs of neurons in the cortex, especially in neurons with overlapping receptive fields (e.g. Krüger 1983, Nelson et al. 1992, König et al. 1995). In our model it was caused by a nearly constant excitability of the model neurons during the adaptation period after each spike due to a parallel decline in membrane potential and threshold time courses (being correlated by feedback via coupling synapses). When nearly synchronous spikes were discharged by many neurons the threshold levels as well as the lateral coupling signals rose steeply and then fell again to their respective resting levels. In this state, the resulting differences between membrane potentials and threshold levels were nearly constant. Thereby the initiation of spikes depended strongly on stochastic fluctuations of the membrane potentials. This explains why spike intervals were more variable for medium than for weak lateral coupling. We expect that this state of synchronized non-rhythmic activities also emerges in real networks at medium levels of coupling strength. Nevertheless, it will be difficult to change lateral coupling strengths in cortical circuits systematically in order to investigate the role of lateral coupling in the generation of such modes of correlation.

2.4.2 Parallel processing of signal correlations

2.4.2.1 Reduction of correlation

Reduction of correlation occurred - among parallel outputs with respect to correlations among inputs - in a network state with low firing rates where one half of the neurons had correlated inputs while the inputs of the others were uncorrelated. Here we found the previously unnoticed effect (by correlation theories of brain function) that the correlation strength among output spike patterns of different neurons was reduced relative to the correlation of their input signals. Such reduction was, however, only observed with weak or no lateral connections. A supposed reason is that the membrane potential's average level was subthreshold, so that only high-amplitude excursions of the membrane potential triggered spikes. Hence, noise strongly influenced their occurrence and, therefore, reduced correlations among output spike trains. A similar explanation was derived theoretically for a simpler system where two "model neurons" with sigmoidal transfer characteristics had no coupling connections at all (Bedenbaugh and Gerstein 1994). Here the output correlation was reduced when the two neurons received partially correlated GWN inputs (of the same mean and standard deviation), using similar input parameters as in our simulations. Hence, reduction of correlation may be a

general property of parallel processing by networks with weak or no lateral connections at low firing rates. We can conclude, therefore, that the signal transmission properties of a single neuron, and especially the nonlinearity of the spike encoder, caused the reduction of output correlations. For this reason it seems extremely important that this reduction in correlation can be counteracted by strengthening of the lateral coupling connections, as found in the present investigation.

2.4.2.2 Enhancement of input correlations

Enhancement of input correlations by the network could be achieved by lateral coupling connections. It increased particularly the correlation of output spikes of neurons with correlated external input signals while the correlation of output spikes of neurons with uncorrelated inputs remained low. This means that the difference in correlation was preserved at appropriate lateral coupling strength - a result that was robust under variation of threshold offset. This can be explained as follows. Each output spike caused identical (perfectly correlated) postsynaptic signals at every neuron's coupling input. The interactions of these synchronized components and the correlated components of the feeding inputs resulted in contributions to the membrane potentials that were strongly correlated among different neurons. Interactions with uncorrelated components of the feeding inputs led, correspondingly, to components of weaker correlation. Hence, increasing lateral coupling strength increased the effective amplitude of correlated components in the membrane potential and, therefore, the probability of generating correlated spikes at the output in only those neurons that received partially correlated GWN input.

Larger networks should support the separation between correlated and uncorrelated components because the uncorrelated signals will average out more completely. In addition, topologically organized lateral connections would favor the separation between subgroups of neurons with correlated input signals were, on average, stronger connected.

2.4.2.3 Multiplicative versus additive coupling

Multiplicative lateral coupling improved the difference in output correlation (G1 vs. G2 neurons) considerably better than additive coupling (Fig. 2.5A, B). This can be understood by extending our explanation for the general mechanism of correlation improvement (in the preceding paragraph) to the special conditions of multiplicative versus additive interactions among feeding potentials F and coupling potentials L. If the lateral coupling is additive, each spike at a coupling input leads to a fixed increase in the feeding potential, regardless of the feeding potential's current amplitude. In contrast, with multiplicative coupling, the average increase depends on the temporal correlation of the linking with the feeding input. This correlation was higher in G1 neurons because they received, via coupling input, signal components

that were partially correlated with their feeding input, so that the effective coupling (and the correlation of the output signals) was stronger among these neurons. It also explains the higher firing rates in this group.

2.4.2.4 Changing effective coupling without changing coupling factors

There are many indications from neural recordings (review in Gerstein et al. 1989) and models (Aertsen et al. 1994) that coupling efficacies can be changed by dynamic variations in the activation states without explicit variations of coupling constants. Correspondingly, we were able to achieve such indirect variations in coupling efficacies in our model by changes in average spike rates (due to different threshold offsets). If the mean of the input level was below the threshold offset (threshold value after complete decline of self-inhibition), spikes could only occur when the random components (GWN) of the input exceeded the threshold. As a result, each output spike caused in our network identical postsynaptic signals at every neuron's coupling input, but these correlated signals only led to correlated output spikes in those neurons that had, at that moment, positive feeding potentials of sufficient amplitude. Hence, lowering the threshold offset of all neurons by the same amount will increase the probability that the linking input is high enough to cause synchronized suprathreshold membrane potentials in a given subgroup of cells. Consequently, increasing the spike rate (by lowering the threshold) in our simulation increased the correlation at the output without any explicit changes in the parameters of the lateral coupling network. A similar enhancement of coupling efficacy was observed by Aertsen et al. (1994) with an increase in the average input activation level.

2.4.3 Input-output correlations

Input-output correlations were stronger with low and weaker with high average spike rates. We controlled the average rates by setting the mean level ("DC") of the feeding input or the threshold offset. At low average spike rates, (< 20/s, typically 5/s) individual spikes were coupled much more strongly to the time course of the GWN at the feeding inputs than with high spike rates (> 40/s, range 45-150/s). States of synchronized oscillations that were generated by the network due to its lateral coupling and increased level of average activation could be suppressed by strong and fast changing input signals. Suppression of oscillations, however, generally increased the strength of input-output correlation. For instance, increasing the GWN standard deviation by a factor of 2 strengthened the input-output correlation by more than that amount. However, the input-output correlation was an order of magnitude lower than with low average activation rates in which the network state was dominated by the time course of the GWN inputs. Similar transitions from synchronized oscillatory network activities to input-locked (non-rhythmic) activities have recently been investigated in detail in visual

cortex (Kruse and Eckhorn 1996). There, stimulus-locked signals were able immediately to suppress ongoing collective oscillations. The latter were generated with the highest amplitudes and stability if a sustained, constant stimulus drive was present and fast changes were avoided.

2.4.4 Other models with related aspects

To our knowledge there have been no simulations explicitly investigating the formation of subassemblies under the influence of different signal correlations at the inputs. One aspect of correlation enhancement has been analyzed by Koch and Schuster (1992). They used a fully connected network with global feedback inhibition and random input signals. In their simulations a brief synchronized activation of the whole network was achieved by activating many inputs simultaneously by synchronous spikes. This mode of activation is rather extreme with respect to biological reality. The separation of groups of neurons on the basis of differences in input correlation has not been investigated.

Many models have been developed with respect to the hypothesis of visual "feature-linking-by-synchronization" in which subassemblies engage in synchronized oscillations (e.g., Eckhorn et al. 1990; Schuster and Wagner 1990; König and Schillen 1991; Sompolinsky et al. 1991; von der Malsburg and Buhmann 1992; Mozer et al. 1992, Grannan et al. 1993, Ritz et al. 1994). In these models spatial "amplitude contrast" at the inputs causes the neurons to segregate into subassemblies by introducing phase correlations among neurons within each subgroup. The formation of subassemblies was not only favored by the amplitudes of input signals but also by special network topographies according to visual retinotopy. In contrast, in this work we have shown that the formation of subassemblies can be induced exclusively by different degrees of correlation in the input signals (see also recent experimental results of Vaadia et al. 1995 on rapid changes in correlation among frontal cortical cells at nearly constant spike rates). No variation in the input spike rates nor special connectivity schemes were necessary for this behavior. However, both surely play important roles in cortical processing.

3 Identical Visual Stimulation Elicited Fast Oscillations in EEG and LFP of Monkey but not in Human EEG

3.0 Abstract

Synchronized oscillatory activity in the gamma range (30-100 Hz), as observed in different brain areas of animals and humans under appropriate stimulation, were proposed to be involved in feature binding and other associative functions. While most investigations on animals worked with intracortical recordings, electroencephalogram (EEG) or magnetoencephalogram was used in human studies. For a comparison of gamma activity in monkeys and humans, we analyzed monkey intracortical local field potentials (LFP), monkey EEG, and human EEG during visual stimulation. In a first experiment, a macaque monkey was stimulated with a smooth fade-in of geometric figures composed of line gratings. The EEG was recorded from dura, recording chamber, and scalp in parallel with multiple-microelectrode LFP recordings from V1. Spectral analysis revealed oscillations in the range of 40-60 Hz in all types of recordings. While the EEG power had a maximum gamma component at about 500 ms after the beginning of stimulus fade-in, the power of intracortically recorded LFP increased with increasing stimulus intensity. This apparent discrepancy was resolved by considering that intracortical coherence of gamma components reached a maximum at the time and frequency of maximum EEG gamma band power (this applies for all analyzed cortical distances of 0.75-4.5 mm), leading to the most constructive superposition of intracortical signals at that moment. In a second experiment, monkey LFP and EEG were directly compared to human EEG during visual stimulation with stationary and moving sinusoidal gratings and comparable recording positions for monkey and human. Gamma components were present at about 40 Hz in both LFP and EEG of monkey but not in human EEG, in contradiction to previous results by others on visually induced gamma oscillations in the human EEG. Some early gamma range components in monkey were found to be phase-locked to stimulus onset during a period of 80-160 ms.

3.1 Introduction

Not only the strength of neural signals but also their synchronization is relevant for brain function. Since the early days of neuroscience it is known that neurons respond with a higher probability to synchronized input signals than to inputs randomly distributed in time (for review see e.g., Abeles 1991), especially in states of weak or medium activation (Bernander et al. 1994; Murthy and Fetz 1994). Based on these cellular features, it was suggested for the visual system that synchronized activity of neurons coding an object might support feature binding and scene segmentation (Milner 1974; Reitboeck 1983; von der Malsburg 1983). In recent publications, evidence for the synchronization of neuronal activity was often associated with oscillations in the range of 30-100 Hz ("gamma range"). These turned out to be present at high amplitudes in the visual cortices of cat (Eckhorn et al. 1988; Gray and Singer 1989) and monkey (Kreiter and Singer 1992; Eckhorn et al. 1993; Frien et al. 1994) and in other sensory and motor cortical areas (Freeman 1975; Murthy and Fetz 1992; Sanes and Donoghue 1993). Gamma band oscillations in the visual cortex were characterized as "stimulus-induced", which means that they depended on stimulation, but had no fixed phase relationship to stimulus onsets (Eckhorn et al. 1988), in contrast to so called "stimulus-locked" oscillations (e.g. Cracco and Cracco 1978). Stimulus dependent synchronization of oscillatory activity in the visual system was particularly strong between cells with overlapping receptive fields, in the same and different cortical areas (Eckhorn et al. 1988; Frien et al. 1994) as well as in different hemispheres (Engel et al. 1991; Eckhorn and Schanze 1991). Synchronization of oscillatory activity depended on the spatial continuity of stimuli (Engel et al. 1991; Brosch et al. 1997; Guettler et al. 1997). The fact, that amplitude and synchronization of gamma oscillations were highly stimulus specific, supported ideas attributing them an important role in cortical function (Eckhorn et al. 1988; Gray et al. 1989). Constraints on these hypotheses were imposed by evidence from cat (Jordan 1989; Brosch et al. 1995) and monkey (Frien et al. 1996; Juergens et al. 1996) visual cortex, that the coupling of stimulus-induced oscillations seems to be restricted to a range of a few millimeters cortical distance and might therefore not be able to bind the representations of larger objects - at least at the level of primary visual cortex where these measurements had been made.

Stimulus-locked oscillations of short latency were observed at frequencies of about 80-160 Hz in recordings from the optic nerve, tract, lateral geniculate body, optic radiation, and visual cortex of animals (for a review see Cracco and Cracco 1978), especially in fast responding cells in monkey striate cortex (Maunsell and Gibson 1992). A comparable phenomenon was also observed in EEG recordings from human subjects during visual (Cracco and Cracco 1978; Whittaker and Siegfried 1983; Tallon-Baudry et al. 1996, 1997a,b) and auditory (Joliot et al. 1994) stimulation. In recent investigations gamma oscillations in cat and monkey visual cortex were generally reported to be stimulus-induced, that is not phase-locked to stimulus onsets and therefore not visible in the averaged stimulus responses (reviews in Eckhorn 1994, Singer and

Gray 1995). However, stimulus-locked gamma range components were not the focus of research.

While stimulus dependent features of oscillatory signals in the visual cortex of higher mammals are well examined, their relevance for behavior has not yet been proved in animal studies, despite some promising recent results (Kottmann et al. 1996a,b; Fries et al. 1996). Studies of human electroencephalogram (EEG) or magnetoencephalogram (MEG) seemed to be promising methods to examine the generality of results on stimulus-induced gamma oscillations as well as their behavioral relevance. Human studies might also allow the investigation of a wider range of experimental paradigms, since instruction and training of human subjects is much easier. In addition, more complex cognitive tasks can be examined than in animals. Most investigations of human brain activity in the gamma range described enhancements of gamma band power during visual stimulation (Sheer 1989; Lutzenberger et al. 1995; Tallon-Baudry et al. 1996, 1997a, b; Müller et al. 1996). On the other hand, reductions of gamma band power during visual stimulation were also reported (Vijn et al. 1991).

Until now, it has not been examined whether gamma oscillations are visible in the EEG of animals, while they can be recorded intracortically. For a comparison of results from animal and human studies such measurements of intra- and extracranial activity are necessary, since in humans measurements are in general restricted to scalp EEG and MEG. Only synchronized activity supplies strong contributions to mass signals (the activity of large neuronal populations), while unsynchronized activity superimposes more destructively. Consequently, the relation between intracortical and scalp EEG measurements cannot be revealed without considering the amount of synchronization of components contributing to the recorded signals.

This study tries to bridge the gap between animal and human studies, as well as between studies of stimulus-induced and stimulus-locked oscillations. Our goal was to answer the following questions concerning the measurability and stimulus relation of oscillatory phenomena in the visual cortices of monkeys and humans:

1. Are gamma oscillations detectable in monkey scalp EEG and how are these signals related to those measured intracortically?
2. Are comparable modulations of gamma band activity detectable in the human EEG during similar stimulation?
3. Are stimulus-locked oscillatory components present in recordings from visual cortices of monkeys and humans and if, how are they related to stimulus-induced components?

We recorded human and monkey scalp EEG during the same type of visual stimulation and additionally measured intracortical local field potentials in the visual cortex of monkeys. The use of multiple electrodes allowed the analysis of distance dependent coupling of intracortically measured signals. The coherence function provided a frequency dependent measure of signal correlation. The present experiments show that stimulus-induced and -locked oscillations were found in the LFP and EEG of monkey but not in the human EEG. A short report on some of the results has been published in abstract form (Juergens et al. 1996, 1997).

3.2 Methods

3.2.1 Visual stimulation

Geometric figures. A monkey (macaca mulatta; age 7 years; weight 7.7 kg) was trained for a delayed match-to-sample task. Visual stimuli were rectangles and triangles of about 18° diameter composed of line gratings with a spatial period of 0.54° (Fig. 3.1 A). Either pairs of identical or different figures were randomly selected as match and sample stimuli.

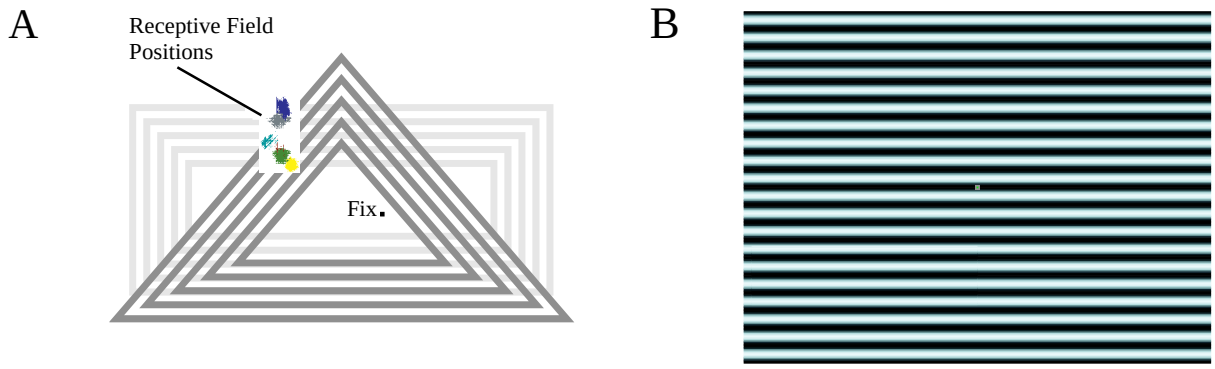

Fig. 3.1A, B. Visual stimuli used in the two types of experiments **A** Geometric figures: Rectangles and triangles composed of line gratings were faded in to avoid strong stimulus-locked effects. Receptive fields of six electrodes are shown (example). **B** Sinusoidal grating: Stationary and moving sinusoidal gratings of different orientations were used as stimuli. The stimuli were instantly switched on, shown stationary, moved perpendicularly to their orientation, and were stationary again. For the exact timing and stimulus features see text (Sect. 3.2.1.2.).

The monkey started a trial by touching a lever. A fixation point appeared on a computer monitor (frame rate 94 Hz, background luminance 2 cd/m^2). 460 ms after fixation of the monkey (controlled by an IR eye position measurement system to be within ±0.5° visual angle) a sample stimulus was faded in for 1000 ms (luminance increase of stimulus figures: 2 cd/m^2 to 48 cd/m^2). Then the figure disappeared and 1000-1300 ms later a match stimulus was faded in for 1276 ms and then remained at the same luminance level (maximum luminance 70 cd/m^2; identical stimulation in the first 1000 ms as for the sample stimulus). The monkey had to decide whether the two figures presented were identical or different by lowering or raising the lever. The fixation point dimmed in an interval of 1000-2500 ms after stimulus onset and the monkey was rewarded for releasing the lever within 650 ms, if the decision was correct. For comparison, the same stimuli were shown with an identical time course of stimulation as the match stimulus but without previous presentation of a sample stimulus. The intertrial interval was 2 s.

Sinusoidal gratings. A point at the center of the screen had to be fixated while sinusoidal gratings were presented (Fig. 3.1 B). Three series of recordings were performed with similar stimulation: EEG recordings from a second monkey (macaca mulatta; age 9 years; weight 9.8 kg), simultaneous EEG and LFP recordings from the same monkey, and EEG recordings from seven male human subjects.

A trial was started by touching a lever. At the beginning of each trial only the fixation point was shown on a dark background (luminance 0.5 cd/m^2 for monkey, 5 cd/m^2 for humans; frame rate 97.8 Hz). After a delay of 409 ms a horizontally orientated sinusoidal grating was presented for 818 ms (18° × 13.5° visual angle; period 0.675°; spatial luminance modulation 0.5-3 cd/m^2 for monkey, 5-15 cd/m^2 for humans). Then, 1227 ms after begin of trial, the grating began to move upwards or downwards with a constant velocity of 0.73°/s (temporal modulation 1.08 Hz). At the same time a patch about 2° wide and 6.8° high centered on average 2° to the left of the fixation point either moved into the opposite direction, remained stationary or moved into the same direction as the background (no patch visible in the last condition). The movement stopped after 1840 ms (3067 ms after begin of trial) at phase lags of 2, 1 or 0 periods between patch and background, so that the patch was not visible at the end of the movement. 1227 ms later the fixation point dimmed and the monkey was rewarded for releasing the lever within 650 ms. The stimuli were presented in pseudo-random sequence, with an intertrial interval of 1-2 s, and in blocks of about 200 trials. In two out of seven recordings with simultaneous measurements of monkey LFP and EEG vertically and horizontally oriented gratings were presented in pseudo-random order. During recordings of monkey EEG diagonally oriented sinusoidal gratings (spatial period 0.93°) were shown instead of horizontally or vertically oriented gratings. The movement phase (velocity 0.79°/s, direction rectangular to the orientation of the grating) was prolonged to 2340 ms during these recordings. Only monkey data from stimulations without grating patch were used for analysis assuring similar stimulation at all microelectrodes. As in the previous experiment, fixation was controlled to be within ±0.5° visual angle.

The experiment was repeated with human subjects, using horizontally oriented sinusoidal gratings and the same timing as during simultaneous EEG and LFP recordings from monkey (200 trials per subject). The grating patches were presented pseudo-randomly on both sides of the fixation point in order to avoid systematic lateralization effects. A second set of stimuli was presented to analyze the influence of stimulus coherence on the interhemispheric coupling of the EEG signals. For that purpose the screen was vertically divided into two subfields of equal size independently moving upwards or downwards yielding one coherently or two incoherently moving sinusoidal gratings. These stimuli were presented in one (4 subjects) or two (3 subjects) blocks of 200 trials. Subjects were instructed to voluntarily produce errors by releasing the lever in case of eye blinks.

3.2.2 Experimental preparation

The heads of both monkeys were fixated with three chronically implanted stainless steel posts to prevent head-movements with minimal force and discomfort. A stainless steel chamber (5 mm o.d.) was inserted into the scull above area V1 in the right hemisphere under deep analgesia (corresponding receptive field positions: 4-5° at the horizontal meridian for the geometric figures experiment and 2° at the horizontal meridian for the sinusoidal grating experiment).

3.2.3 Data recording

Intracortical recordings were performed with a linear array of seven micro fiber-electrodes with shaft diameters of 80 µm and an inter-electrode distance of 750 µm (Eckhorn and Thomas 1993). The electrodes were singly inserted through the intact dura into the upper layers of V1. Local field potentials (LFP) were extracted by bandpass filtering (1-140 Hz during geometric figures experiment, 10-140 Hz during sinusoidal gratings experiment). During the geometric figures experiments, in two out of seven recording sessions EEG-signals were recorded with three different electrodes besides LFP. i) an Ag/AgCl ball electrode (2 mm o.d.) placed on the dura next to the recording array, ii) the steel chamber (6 mm o.d.), and iii) a standard planar Ag/AgCl EEG electrode (4 mm o.d.) on the scalp 1 cm to the right of the chamber. In the sinusoidal grating experiment the scalp EEG was also recorded before chamber implantation with two EEG electrodes (8 mm o.d.) placed 1.5 cm anterior and posterior of the intended chamber location. During intracortical measurements the EEG was recorded from the anterior position. The scalp EEG of human subjects was recorded with Ag/AgCl electrodes (8 mm o.d.) from Iz, Oz, O1, O2, Pz, P3, P4 and Cz according to the international 10-20-system. Impedances of scalp EEG electrodes were below 10 kΩ before and after the recordings. Linked ear lobes, connected by two 5 kΩ resistors, served as reference. EEG signals were bandpass filtered between 1-100 Hz. All signals were digitized with a sampling rate of 500 Hz.

3.2.4 Data analysis

All signals were visually inspected for artifacts, leading to the exclusion of one human subject due to strong muscle activity, confirmed by strongly reduced coherence (see below) between the outer electrodes. A second subject was excluded since further data analysis revealed an EEG anomaly. 2193 of 2400 trials from five subjects (all male, mean age 27) remained for consecutive data processing. Line artifacts were removed by processing the signals off-line by a correlation filter algorithm which subtracted the best fitting 50 Hz sine-wave from the recorded signals of each trial (Eckhorn and Obermueller 1993).

The frequency dependent power and correlation of the measured activity were analyzed by means of power spectra and coherence functions. Power spectra of artifact free trials with correct responses were calculated using Hamming windows of 256 ms length and padding the resulting data by the same number of zeros. The analysis window was shifted over the total recording epochs in steps of 128 ms. The coherence function was used to quantify the frequency dependent correlation between pairs of electrodes:

$$\gamma^2(f) = \left|C_{xy}(f)\right|^2 / \left(C_{xx}(f) \cdot C_{yy}(f)\right),$$

where $C_{xy}(f)$ is the complex cross spectrum of the signals x and y averaged over trials with identical stimulation. This measure is normalized to the range [0, 1]. It reveals the constancy of phase relations over trials and the degree of amplitude covariation. The systematic over-estimation of coherence due to the limited number of contributing time windows was corrected according to Benignus (1969). Averages were calculated after Fischer-Z transform.

Shift predictors of auto spectra $C_{xx}^{sp}(f)$ were calculated to reveal stimulus-locked components (Aertsen 1989). They were subtracted from auto-spectra to exhibit signal components not directly locked to stimulus events. To analyze stimulus-locked oscillatory components with a better temporal resolution than possible with Fourier methods, the measured signals were first averaged time-locked to stimulus onsets. The averaged signals were then bandpass filtered in the frequency domain using cosine taper filters (flank width 5 Hz) with passbands matched to the observed spectral peaks.

3.3 Results

3.3.1 Geometric figures experiment

Interrelations of intra- and extracortically measured activity were first analyzed during the smooth fade-in of geometric figures composed of line gratings. The experiments should show whether synchronized oscillations are observable in the scalp EEG, and if so, how their power depends on the power and coherence of the LFP.

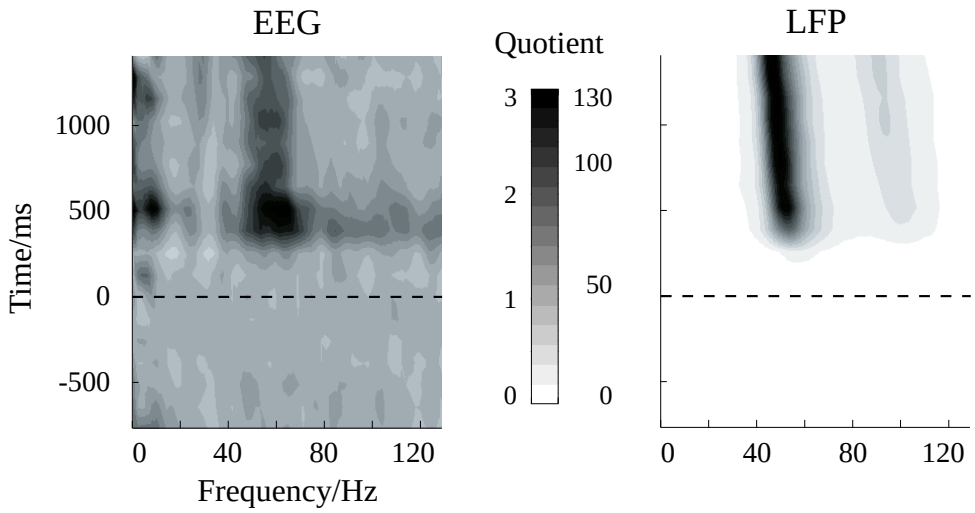

Fig. 3.2. Time course of spectra from monkey LFP and scalp EEG during the presentation of geometric figures, divided by the mean prestimulus activity (fixation task). *Grey level* indicates modulation of activity. The *dashed horizontal line* indicates the onset of stimulus fade-in. Stimulus-induced oscillations of similar time course and frequency were present in both intracortically and extracortically measured signals. EEG: 2 recording sessions (247 trials); LFP: 8 recording sessions (683 trials).

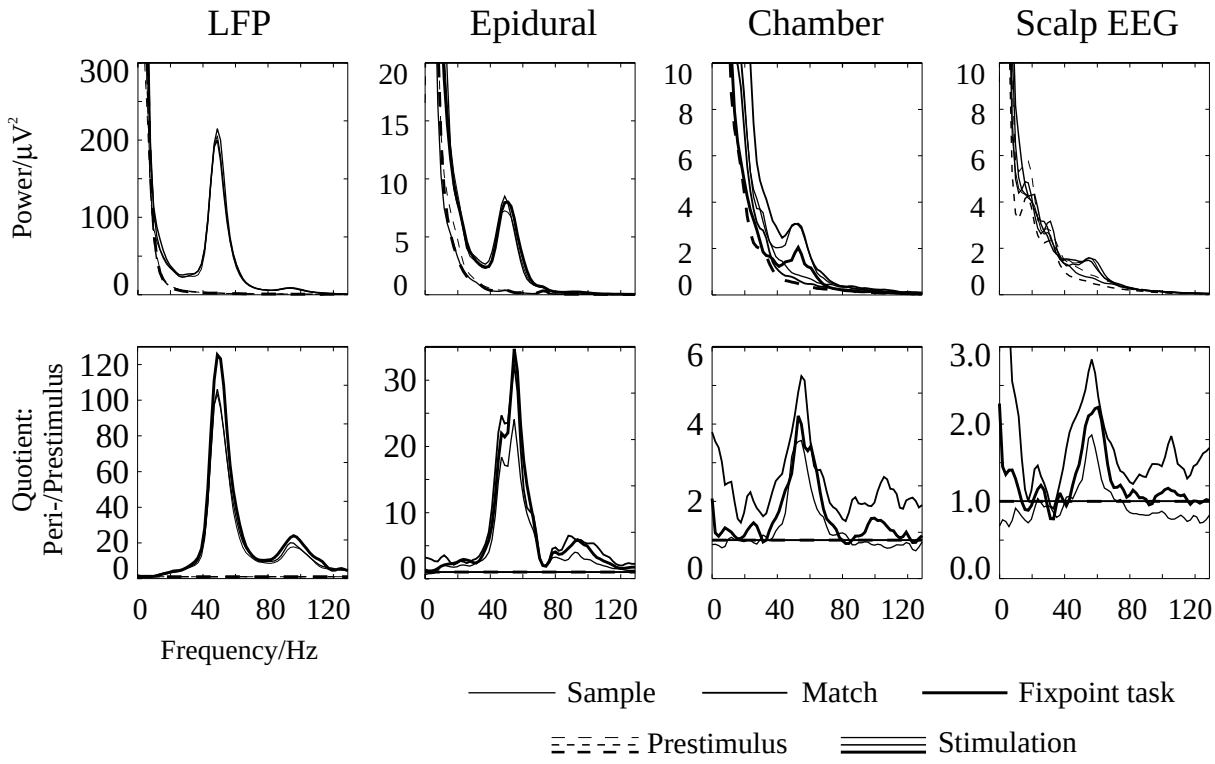

Fig. 3.3. Spectra of stimulus-induced LFP and EEG signals from dura, recording chamber, and scalp during the presentation of geometric figures. Time ranges for spectral analysis: prestimulus: -384 - 0 ms (*dashed lines*), poststimulus: 640 - 896 ms (*continuous lines*). Line thickness indicates different stimulus conditions (*thin lines*: sample stimulus; *medium lines*: match stimulus; *thick lines*: fixation task).

Power spectra. The time courses of LFP and scalp EEG spectra divided by the prestimulus activity are shown in Fig. 3.2 (fixation task). About 300 ms after stimulus onset LFP and EEG gamma activity increased, mainly at a frequency of about 50 Hz (see the discussion of line artifacts in Section 3.4.1), demonstrating that in fact the EEG is able to reveal gamma oscillations in the visual cortex of monkey. EEG gamma oscillations had their maximum power at the onset of the oscillatory response. Contrastingly, the power of the LFP oscillation slightly increased during the trial while the frequency of the dominant oscillation peak decreased. A broad band activation in the EEG accompanied the initial gamma band response at about 500 ms. A second spectral peak was present in the LFP and less pronounced in the EEG at about 100 Hz. It had a comparable time course of spectral power and frequency as the dominant gamma oscillations, representing their first harmonics. Figure 3.3 shows average power spectra and quotients of spectra before and during stimulation for LFP and EEG recordings from dura, recording chamber, and scalp. Spectral peaks in the range of 45-55 Hz were present in all signals during stimulation but not during the prestimulus period. There were no reliable differences between the three behaviorally distinct situations (for a more thorough analysis of this aspect see Frien 1996). The analysis of different EEG recordings shows that peak power and modulation (quotient of post- and prestimulus activity) decreased with increasing distance from the cortical surface. While the LFP gamma amplitude was modulated by a factor of more than 100 the modulation factor was only 1.8-2.8 in the scalp EEG. The first harmonics of the dominant gamma oscillation was visible in the frequency range of 90-110 Hz. Quotients of post- and prestimulus spectra of chamber and scalp EEG showed small additional peaks at about 20-25 Hz, not visible in the LFP.

Coherence functions. The time course of intracortical coherence at different cortical distances is presented in Fig. 3.4. A peak in the gamma range was present, with a comparable time course as in the power spectra of Fig. 3.3. The 50 Hz maximum observed in the EEG 500 ms after stimulus onset (Fig. 3.2) was paralleled by a maximum of coherence in the same time and frequency range. This rather short-time enhancement of gamma range coherence was clearly present at short distances, to a smaller extent also at the largest cortical distances analyzed (4.5 mm). Figure 3.5 shows the pre- and poststimulus coherence of LFP signals. The peak of averaged coherence (640-896 ms) at the prevailing gamma oscillation frequency decreased with increasing cortical distance and nearly vanished for distances exceeding 3 mm. In the range of medium cortical distances peaks existed at about 20 and 30 Hz, less visible at shorter or larger distances (see also Fig. 3.4). Stimulus-induced broad band coherence extended up to 130 Hz for a distance of 1.5 mm, for higher distances coherence was restricted to lower frequencies. The coherence between intracortical and extracortical activity only partly reflects the intracortical coherence at the measured electrodes (Fig. 3.6). Coherence between LFP and epidural EEG had a broad pronounced maximum ($\gamma^2 = 0.4$) in the gamma range while there was less prominent structure for the coherence of LFP with chamber and scalp EEG.

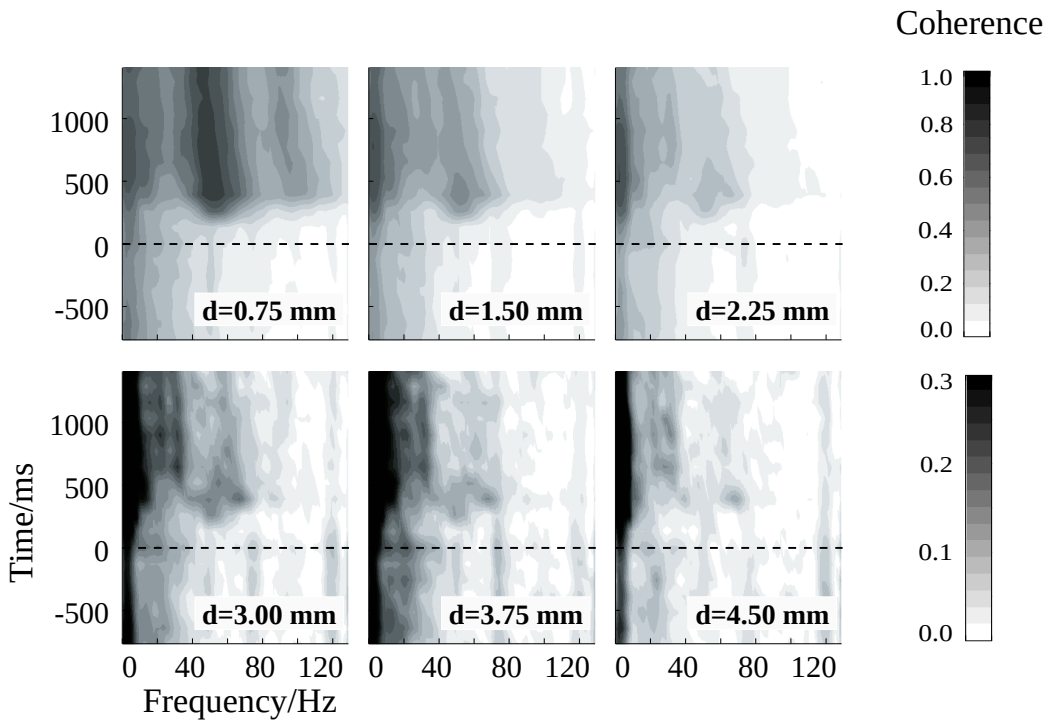

Fig. 3.4. Time course of stimulus-induced LFP coherence for different cortical distances during the presentation of geometric figures, indicated by g*rey level* (fixation task). The *dashed horizontal line* indicates the onset of stimulus fade-in. Coherence had a maximum at about the same time and frequency as the EEG maximum (500 ms, 50 Hz) for all electrode distances analyzed. Note the different scales of coherence values in the upper and lower rows. Number of signal pairs (electrode pairs × trials): 2408, 2015, 1649, 1323, 1031, 628 for cortical distances of 0.75 mm, 1.5 mm, 2.25 mm, 3.0 mm, 3.75 mm, 4.5 mm, respectively.

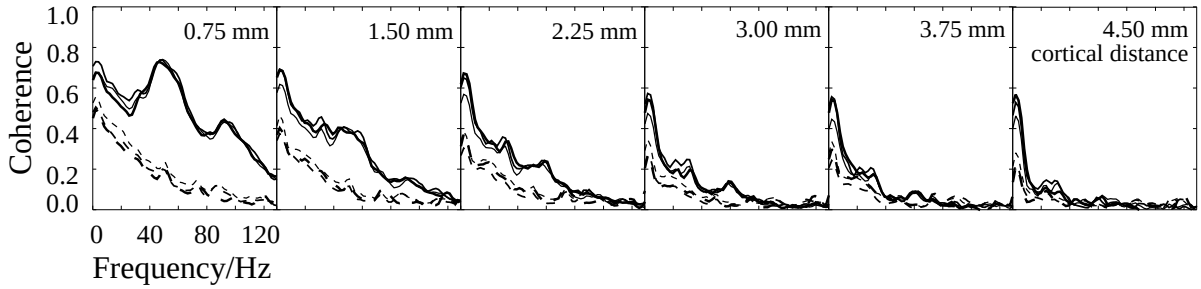

Fig. 3.5. Stimulus-induced LFP coherence for different cortical distances during the presentation of geometric figures. The *dashed horizontal line* indicates the onset of stimulus fade-in. Time ranges for spectral analysis: prestimulus: -384 - 0 ms (*dashed lines*), poststimulus: 640 - 896 ms (*continuous lines*). *Line thickness* indicates different stimulus conditions (*thin*: sample; *medium*: match; *thick*: fixation task).

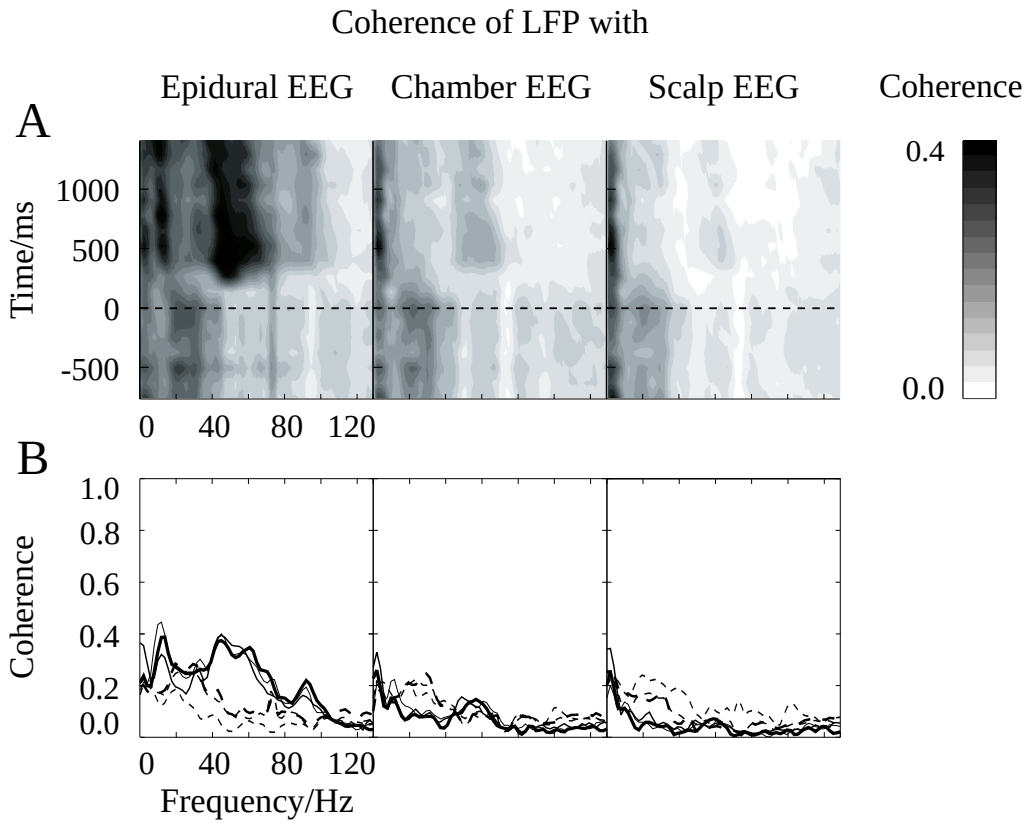

Fig. 3.6A, B. Time course of stimulus-induced LFP-EEG coherence, indicated by g*rey level* (fixation task). EEG signals were recorded from dura, chamber and scalp. The *dashed horizontal line* indicates the onset of stimulus fade-in. **B** LFP-EEG coherence in selected time ranges. Prestimulus: -384 - 0 ms (*dashed lines*), poststimulus: 640 - 896 ms (*continuous lines*). *Line thickness* indicates different stimulus conditions (*thin*: sample; *medium*: match; *thick*: fixation task).

3.3.2 Sinusoidal grating experiment: monkey

The generality of results from the geometric figures experiment described above was examined by this experiment. Main differences to the previous experiment are additional EEG recordings before insertion of the recordings chamber and a larger stimulus with a sharp temporal onset. A whole field sinusoidal grating was instantly switched on and, after a stationary period, began to move, followed by a second stationary period.

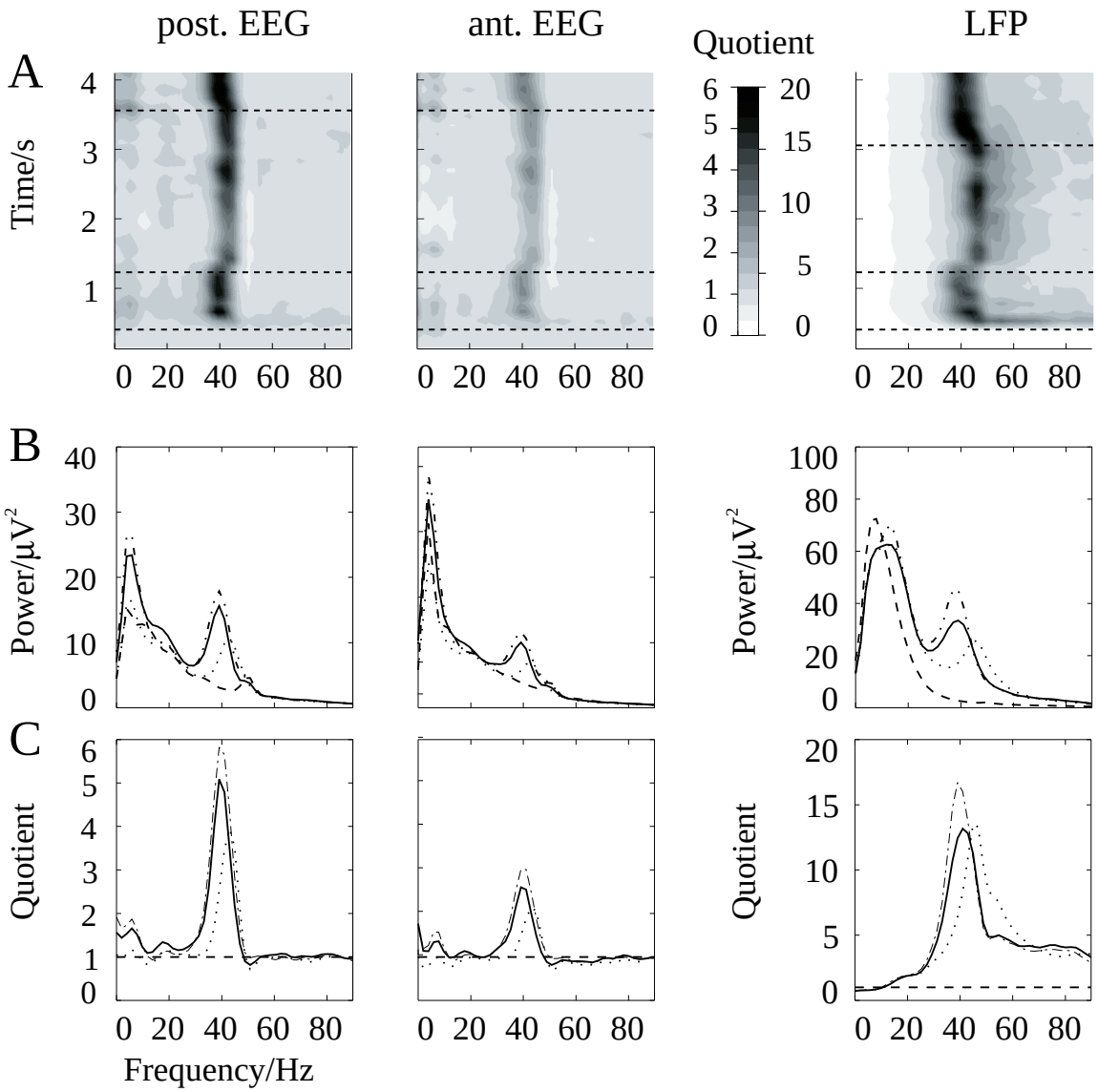

Fig. 3.7A-C. Spectra of stimulus-induced LFP and EEG activity in monkey during stimulation with sinusoidally modulated gratings (EEG was recorded 1.5 cm anterior and posterior of the later chamber location). **A** Time course of stimulus-induced activity in LFP and EEG recordings. All spectra were divided by the mean prestimulus activity. *Dashed horizontal lines* indicate stimulus onset and start and stop of movement. **B** Averaged power spectra, **C** averaged power spectra divided by the mean prestimulus activity. Line style indicates different phases of stimulation. The time course of gamma band activity was similar at EEG and LFP electrodes. Modulation of gamma band activity was stronger for LFP electrodes, matching results from the geometric figures experiment. *Dashed lines*: prestimulus; *continuous lines*: stationary grating (1); *dotted lines*: moving grating; *dash-dotted lines*: stationary grating (2). EEG: 3 recording sessions with two electrodes before implementation of the chamber, 570 trials; LFP: 3 recording sessions with recording from 6 or 7 electrodes simultaneously, 362 trials.

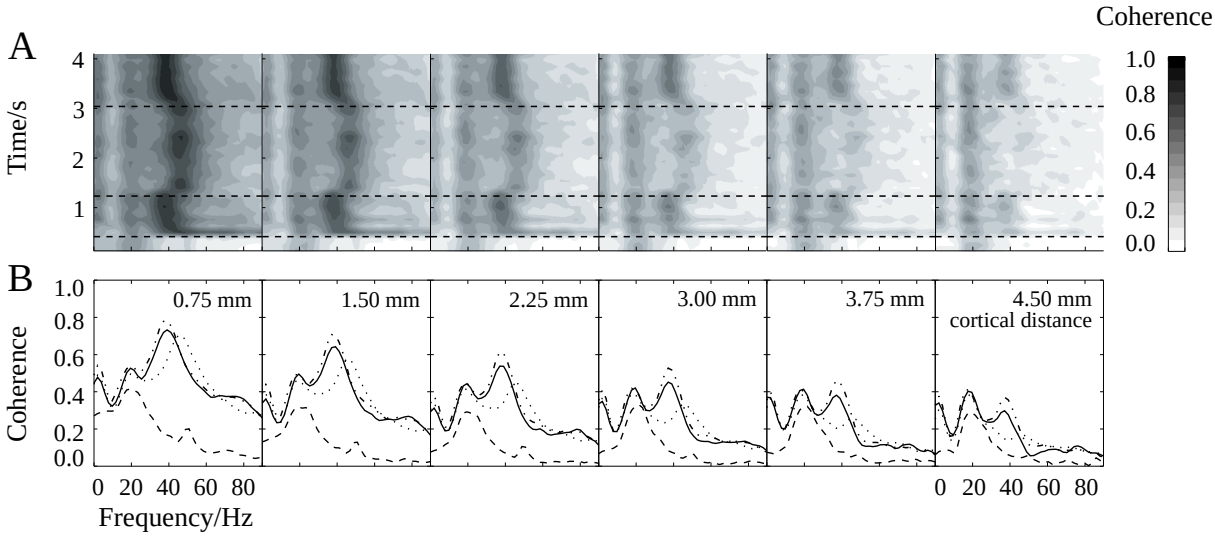

Fig. 3.8A, B. Stimulus-induced LFP coherence for different cortical distances during stimulation with sinusoidally modulated gratings. Intracortical coherence was maximal at low frequencies and in the 20 Hz and 40 Hz ranges. Note the different effects of movement on the frequencies of 20 Hz and 40 Hz components. **A** Time course of stimulus-induced LFP coherence. Dashed horizontal lines indicate stimulus onset and start and stop of movement. **B** Coherence averaged over different phases of stimulation. Line style indicates different phases of stimulation. *Dashed lines*: prestimulus; *continuous lines*: stationary grating (1); *dotted lines*: moving grating; *dash-dotted lines*: stationary grating (2). Number of signal pairs (electrode pairs × trials): 1782, 1485, 1188, 891, 594, 297 for cortical distances of 0.75 mm, 1.5 mm, 2.25 mm, 3.0 mm, 3.75 mm, 4.5 mm, respectively.

Power spectra. As in the geometric figures experiment, the time course of LFP and EEG spectra revealed comparable time courses of intra- and extracortically measured signals (Fig. 3.7). Pronounced oscillation peaks with a frequency of about 40 Hz were present at all electrodes. The frequency of the dominant gamma band component increased by about 4 Hz during movement. A relative maximum of power was present about 250 ms after the middle of the stimulus movement (same stimulus position as during stationary presentation). Broad band enhancement of spectral power was most pronounced in the LFP where power increased above 10 Hz during stimulus presentation, with a maximum at 100 ms after stimulus onset. Figure 3.7B shows average activity during the prestimulus interval and the three phases of stimulation. The prominent gamma band frequency was similar for both presentations of the stationary grating but increased during stimulus movement at all electrodes, while the amplitude decreased. EEG gamma band activity was stronger at the posterior electrode (modulation factor 5.1) compared to the anterior electrode (modulation factor 2.9).

Coherence functions. The time course of intracortical coherence for cortical distances of 0.75 to 4.5 mm is shown in Fig. 3.8A, while averages of the prestimulus interval and the three stimulation phases are presented in Fig. 3.8B. The coherence peak in the gamma range had a similar time course as spectral power: an initial broad band maximum and a persistent gamma peak after the appearance of the stimulus. As for the power spectra, the frequency of the

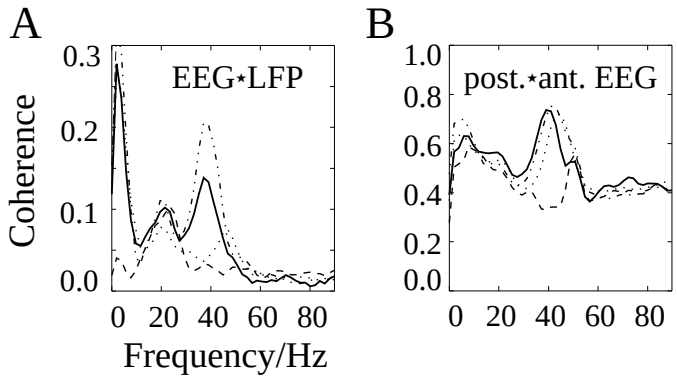

Fig. 3.9A, B. A Coherence between EEG and LFP (362 trials) during stimulation with sinusoidally modulated gratings. **B** Coherence between anterior and posterior EEG recordings (570 trials) averaged over different phases of stimulation indicated by line style. Line style indicates different phases of stimulation. *Dashed lines*: prestimulus; *continuous lines*: stationary grating (1); *dotted lines*: moving grating; *dash-dotted lines*: stationary grating (2).

coherence gamma peak increased during stimulus movement with a maximum about 250 ms after the middle of the movement phase. A coherence peak at about 20 Hz, present already before stimulus onset, increased after the onset of stimulation. The frequency of this peak was nearly constant during stimulus movement while the frequency of the gamma peak increased. These different frequency dependencies exclude a harmonic relation between both phenomena. The fact that the coherence at 40 Hz dropped with increasing cortical distance while the 20 Hz coherence remained rather constant supports this inference. The spatial decrease of coherence with whole field gratings was less pronounced compared to the presentation of geometric figures (except for frequencies below 10 Hz). While during the geometric figures experiment no coherence peak was visible at a cortical distance of 4.5 mm in the upper frequency range ($\gamma^2 < 0.05$), a clear stimulus dependent 40 Hz peak was present at this distance in the sinusoidal grating paradigm (stationary grating: $\gamma^2 = 0.3\text{-}0.4$).

As shown in Fig. 3.9A the coherence between EEG and LFP had a rather stimulus independent peak at about 20 Hz and a stimulus related peak at about 40 Hz. As expected from the far reaching intracortical coherence, the gamma band coherence between intracortically and extracortically measured signals was higher ($\gamma^2 = 0.14\text{-}0.21$ during stationary stimulation) than in the geometric figures experiment ($\gamma^2 < 0.05$). The coherence between the anterior and posterior EEG (Fig. 3.9B) was rather constant apart from a maximum in the range of 30-50 Hz during stimulation. The rather frequency independent coherence, especially in the upper frequency range (> 60 Hz, $\gamma^2 \approx 0.4$), might reflect a large amount of overlap in sources contributing to both electrode signals.

3.3.3 Sinusoidal grating experiment: human subjects

The sinusoidal grating paradigm was repeated with EEG recordings from human subjects to allow a direct comparison with results in monkey.

Power spectra. The spectral time course of stimulus-induced activity at each electrode, averaged over all stimulus conditions, is shown in Fig. 3.10 (all spectra were divided by spectra of prestimulus activity). Stimulus appearance at 409 ms and beginning of movement at 1227 ms were each followed by a decrease of alpha band power. Apart from a very spurious broad band increase of power at the occipital electrodes about 100 ms following stimulus onset no systematic changes in gamma band activity were found. The time averaged power spectra (Fig. 3.11A) for the different stimulus phases and respective quotients of pre- and poststimulus activity (Fig. 3.11B) at the occipital electrodes did not reveal stimulus-induced enhancements but rather small reductions of gamma band activity. In order to get an estimate of random variation during presentation of the stationary grating, partial data sets during identical stimulation were created by selecting data with different subsequent stimulus motions. A comparison of the average activity with results from partial data sets (Fig. 3.11C) showed that the random variation clearly exceeded the amount of variation of the average values. Hence the observed variations of activity were not systematically related to the stimulus but might be explained by random effects.

Activity in selected frequency bands. Broad band effects were examined by averaging the activity in the alpha band (8-12 Hz) and in the lower (30-46 Hz) and upper (56-94 Hz) gamma bands. Frequencies near 50 Hz were excluded from the analysis to avoid misinterpretation of line artifacts. While the alpha activity decreased during stimulus movement and after changes in stimulation, the time courses of the gamma band activities showed only small variation with the phases of stimulation (Fig. 3.12). However, some proportion of the temporal variance of gamma band activity might be explained by short broad band activations after the appearance of the stimulus and movement onset (lower and upper gamma bands) and harmonics of alpha activity (expected to be stronger in the lower than in the upper gamma band).

Interhemispheric coherence. The hypothesis that spatially separate stimulus objects or scene segments might be represented by incoherent activity of the representing neurons was tested by comparing interhemispheric EEG coherence during the presentation of coherently moving whole field gratings and incoherently moving half field gratings. Coherence between occipital and parietal electrodes over the left and right hemispheres showed no systematic differences between both types of stimulation (Fig. 3.13). Small differences during the baseline condition were comparable to those during stimulus movement. Considering all 28 analyzed electrode pairs, a broad band decrease of coherence with electrode distance and a drop of coherence in the frequency range of 15-40 Hz with a minimum at about 20 Hz was revealed (a maximum at 50 Hz is probably caused by line artifacts). However, the coherence between any pairs of electrodes did not show substantial differences between different phases of stimulation.

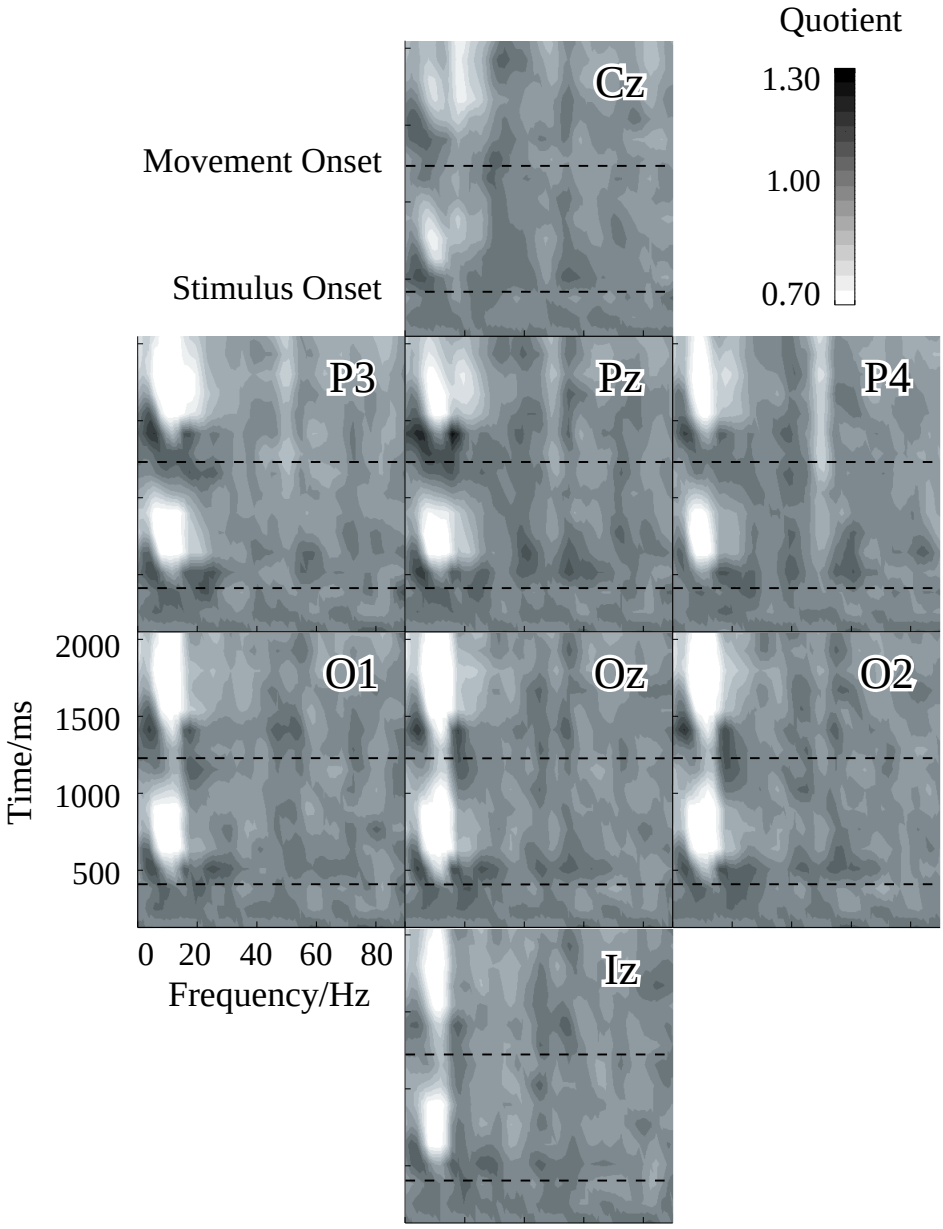

Fig. 3.10. Time course of spectra of stimulus-induced activity in the human EEG at different electrodes. *Grey level* indicates modulation of activity. Power spectra were averaged over subjects and over all stimuli presented (2193 trials from 5 subjects) and divided by the mean prestimulus activity. Appearance of the grating stimulus and movement onset are indicated by *dashed lines*.

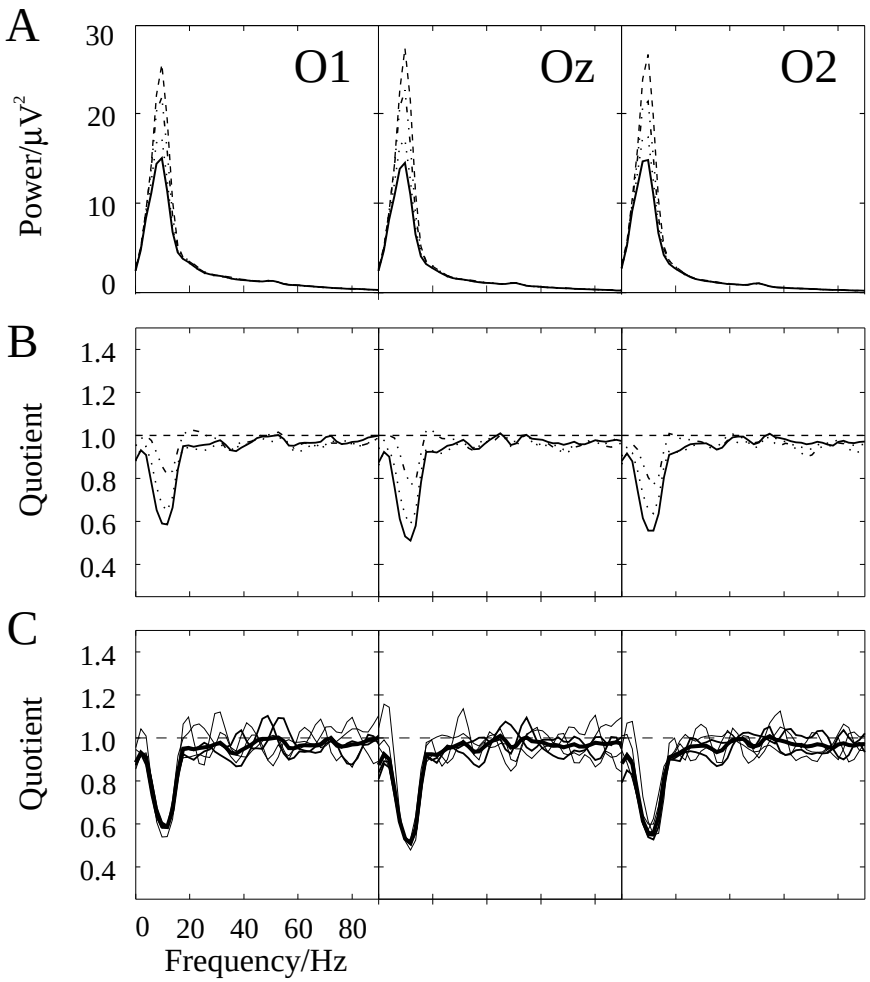

Fig. 3.11A, B. Stimulus-induced activity at occipital electrodes. **A** Time averaged power spectra. Line style indicates different phases of stimulation. *Dashed lines*: prestimulus; *continuous lines*: stationary grating (1); *dotted lines*: moving grating; *dash-dotted lines*: stationary grating (2). **B** Averaged power spectra divided by the mean prestimulus activity. Line styles as in (A). **C** Results from partial data sets during stimulation with stationary grating: averaged power spectra divided by prestimulus activity. The *thick lines* indicates the total average over the partial data sets (same data as indicated by the solid line in **B**). A comparison of data from five partial data sets during identical stimulation with a stationary grating (but different stimulus movements following; *thin lines*: stationary, same or opposite direction of patch movement as background; *medium lines:* coherent or incoherent movement of both hemispheres in the split halves experiment) indicate that variations of the average spectrum are rather small and probably due to random effects

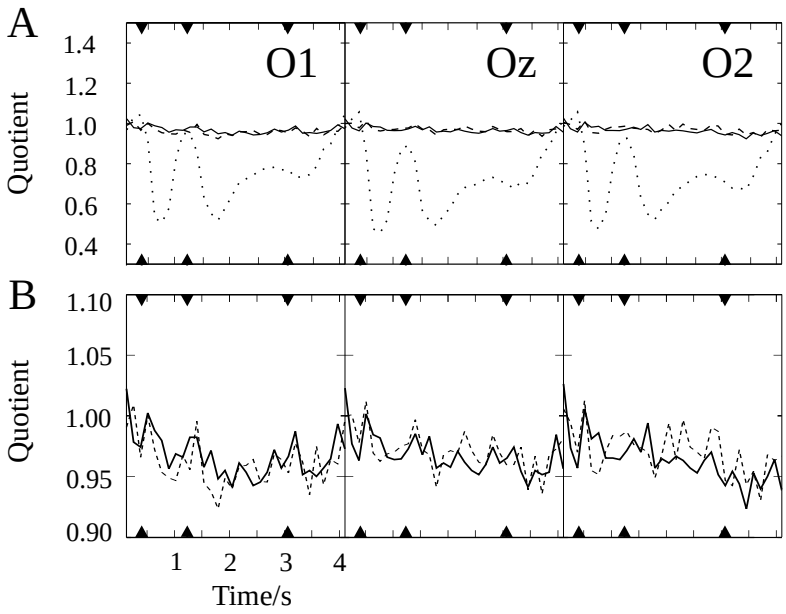

Fig. 3.12. Time courses of band activity at the occipital electrodes in the alpha (8-12 Hz, *dotted lines*) and the lower (30-46 Hz, *dashed lines*) and upper (56-94 Hz, *continuous lines*) gamma ranges. The lower panel shows time courses of gamma band activity with a higher amplitude resolution. *Arrows* indicate stimulus onset, and start and stop of stimulus movement.

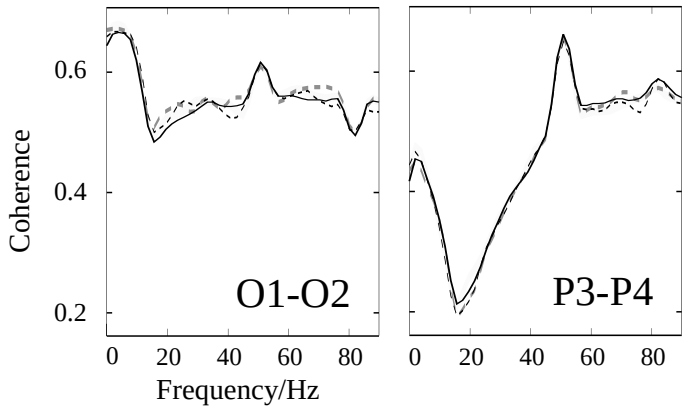

Fig. 3.13. No distinct differences in interhemispheric coherence at occipital and parietal electrodes during the presentation of coherent and incoherent stimuli. Linestyle indicates stationary (dashed lines) or moving (continuous lines) gratings. Line thickness indicates coherently (thin lines) and incoherently (thick lines) moving stimuli. The variance of coherence during stimulation with stationary gratings gives an estimate of random fluctuations.

3.3.4 Stimulus-locked oscillations

Power spectra of stimulus-locked intracortical activity. In the geometric figures experiment no sharp stimulus onset was defined since object contrast increased gradually. Stimulus-locked response components (phase-locked to stimulus onset) were present only at frequencies below 5 Hz starting about 200 ms after stimulus onset. In contrast, after the sudden appearance of the sinusoidal grating stimulus-locked beta and gamma activity in monkey visual cortex was observed in addition to low frequency components. Figure 3.14A shows an increase of stimulus-locked signal power with distinct peaks at about 20 and 40 Hz in the time window centered 103 ms after stimulus onset. In addition, a rather broad band increase of signal power was observed in the range of 50-100 Hz, with maximal modulation by the stimulus at 84 Hz. Stimulus-locked 40 Hz activity had about half the power of the stimulus-induced 40 Hz component (Fig. 3.14B), which increased in the following time window. No comparable stimulus-locked activity was present after the onset and offset of stimulus movement.

Time course of evoked local field potentials in selected frequency bands. The time course of stimulus-locked LFP activity was analyzed with a higher temporal precision by first calculating the averaged evoked potentials (EP) and then filtering in frequency ranges separating the different spectral peaks (10-30 Hz, 30-50 Hz, and 50-100 Hz). Figure 3.15 shows data from three experimental sessions and an average over all. While the activity at 50-100 Hz was strongest at the beginning of the stimulus response, the 30 Hz and 40 Hz activities extended over a time range of about 80-170 ms following the appearance of the stationary grating. Analysis artifacts were excluded by comparing the filter's impulse responses with the filtered EPs. The impulse response of each bandpass filter showed some rhythmicity but had a faster decay than the evoked stimulus responses (see inserts Fig. 3.15). This was most pronounced for the 30-50 Hz components.

Stimulus-locked EEG activity. Stimulus-locked activity was also present in the scalp EEG of monkey. Similar to the LFP, signal power increased with a peak at 40 Hz in the time window centered 103 ms after stimulus onset, while stimulus-induced activity had a stronger 40 Hz peak in the following time window (Fig. 3.16). The 20 Hz stimulus-locked component was superimposed by strong signal components of lower frequency but visible in the neighboring time windows. Activity in the 50-100 Hz range rather continuously decreased with frequency. These results were reflected in the filtered evoked responses (Fig. 3.17). The 40 Hz activity was delayed, shorter and less clearly defined than in the LFP. The durations of the 10-30 Hz and 50-100 Hz responses did not clearly exceed those of the respective impulse responses. No comparable stimulus-locked gamma activity was observed in the EEG of human subjects where spectral analysis showed merely broad-band effects with strong stimulus-locked components in the lower frequency range (1-20 Hz).

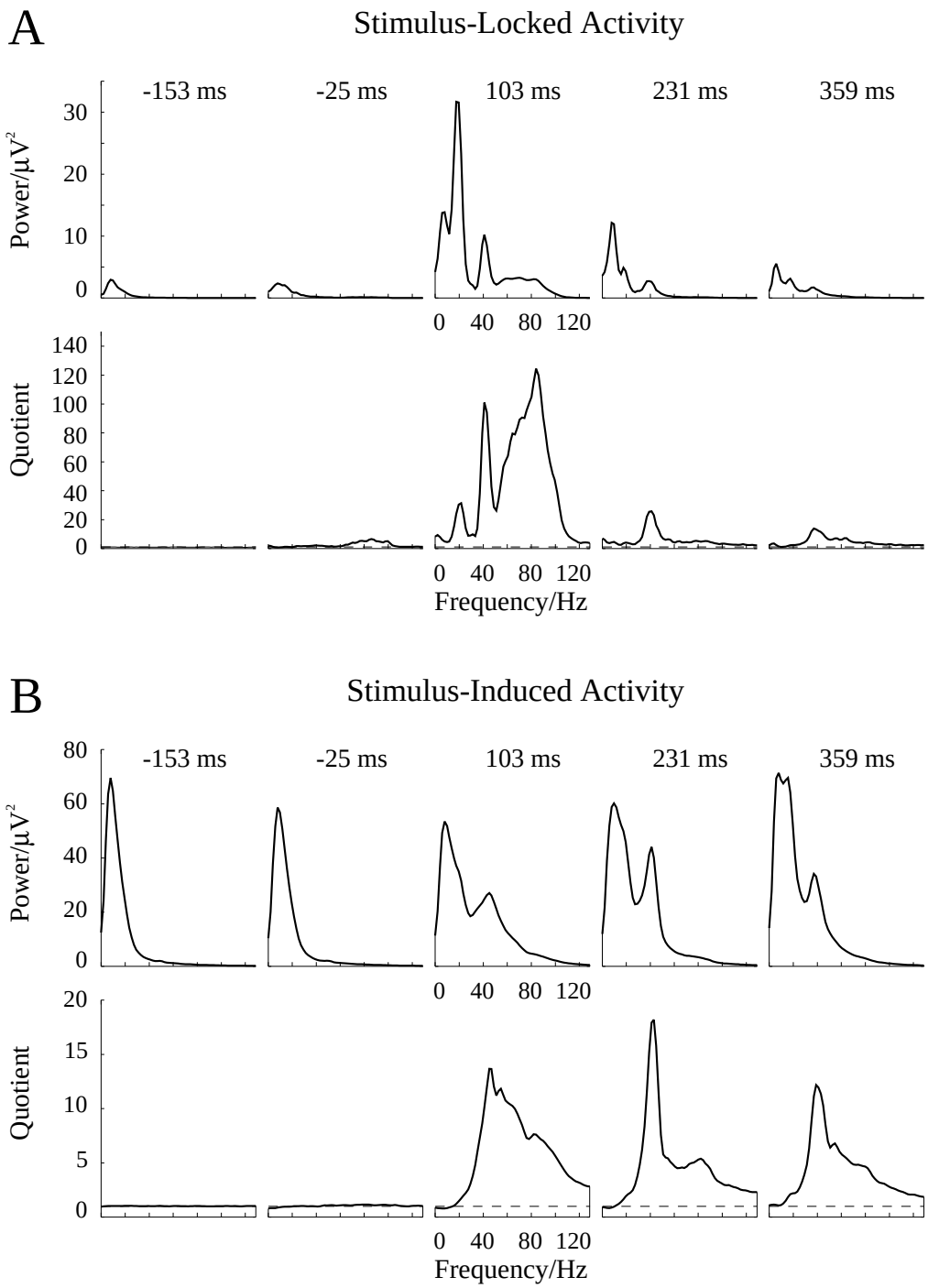

Fig. 3.14A, B. Spectra of stimulus-locked (**A**) and stimulus-induced (**B**) LFP activity in successive time windows during the sinusoidal grating experiment. Stimulus-locked spectra in the time window following stimulus onset at 0 ms show enhancements of power in three distinct frequency ranges: 10-30 Hz, 30-50 Hz, and 50-100 Hz. Spectra in the bottom rows were divided by the mean prestimulus spectra. Data from 3 sessions with recordings from 6 or 7 electrodes simultaneously, total of 895 trials. Note the different scales in (**A**) and (**B**).

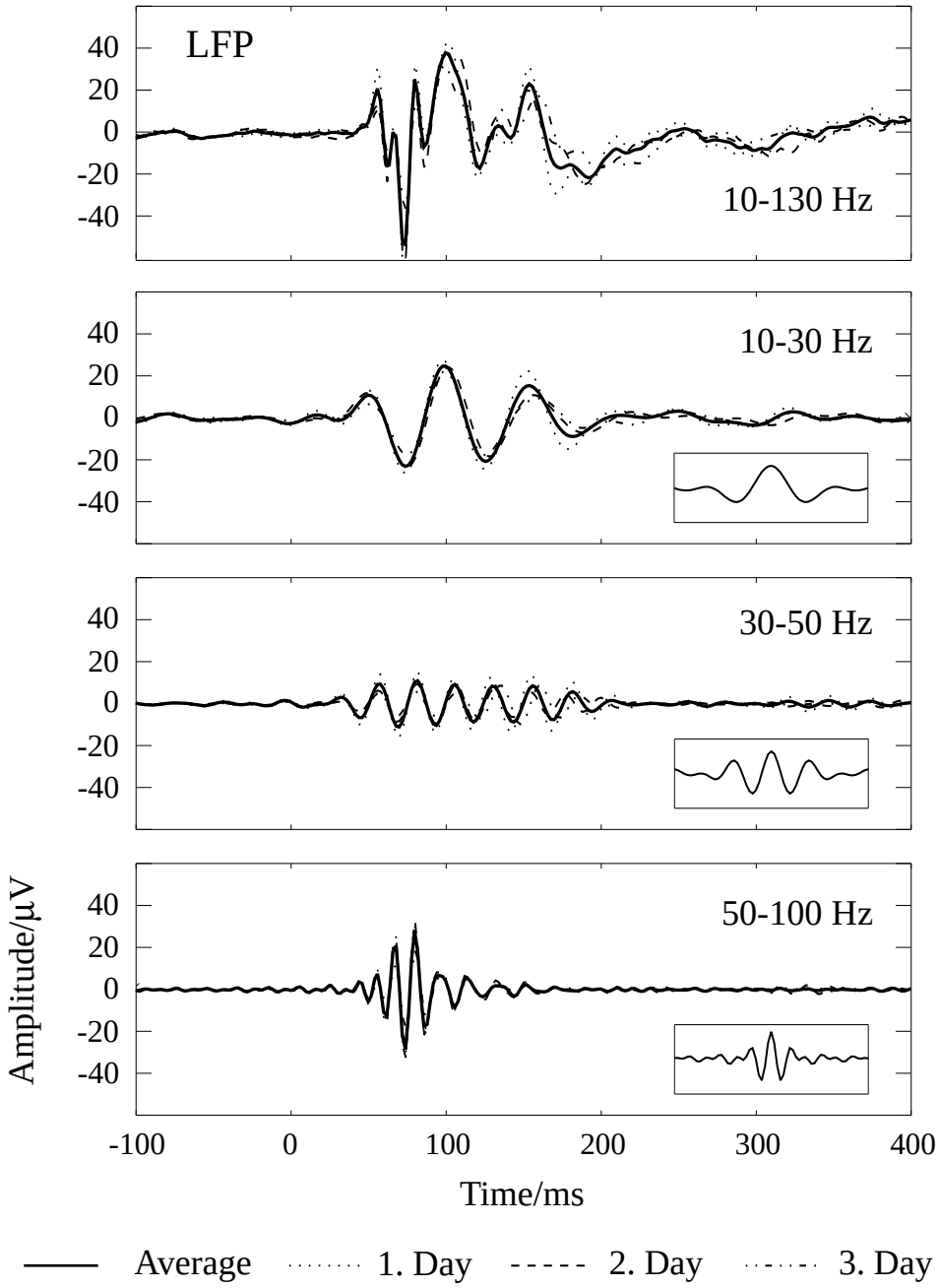

Fig. 3.15. Evoked LFP response and bandpass filtered data in the ranges of 10-30 Hz, 30-50 Hz, and 50-100 Hz. Average data from 3 sessions with recordings from 6 or 7 electrodes simultaneously are shown. In addition, data from each session are presented separately (*dotted*, *dashed*, and *dash-dotted lines*; averages over 423, 218, 254 trials, respectively). The insets show the impulse responses of the respective digital bandpass filters.

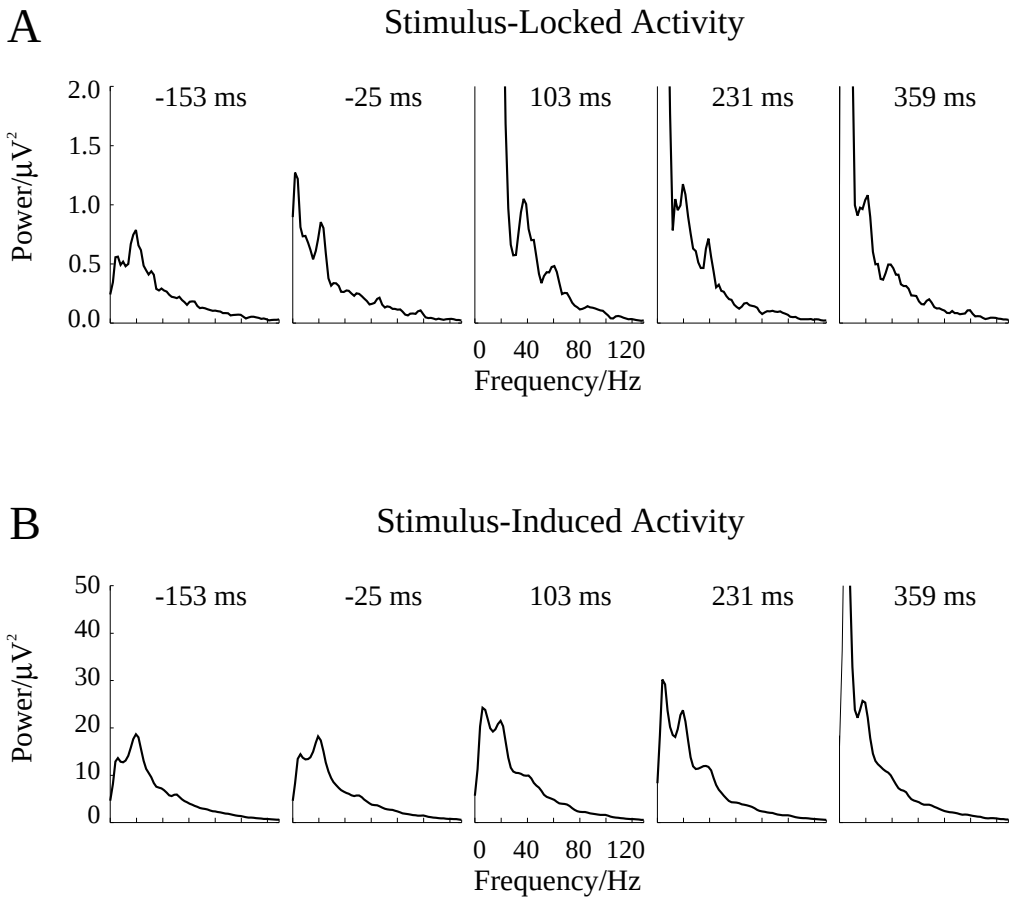

Fig. 3.16A, B. Spectra of stimulus-locked (**A**) and stimulus-induced (**B**) EEG activity in successive time windows. Stimulus-locked gamma oscillations have a similar frequency but reduced amplitude compared to the LFP. Average data from 3 sessions, total of 362 trials. Note the different scales in (**A**) and (**B**).

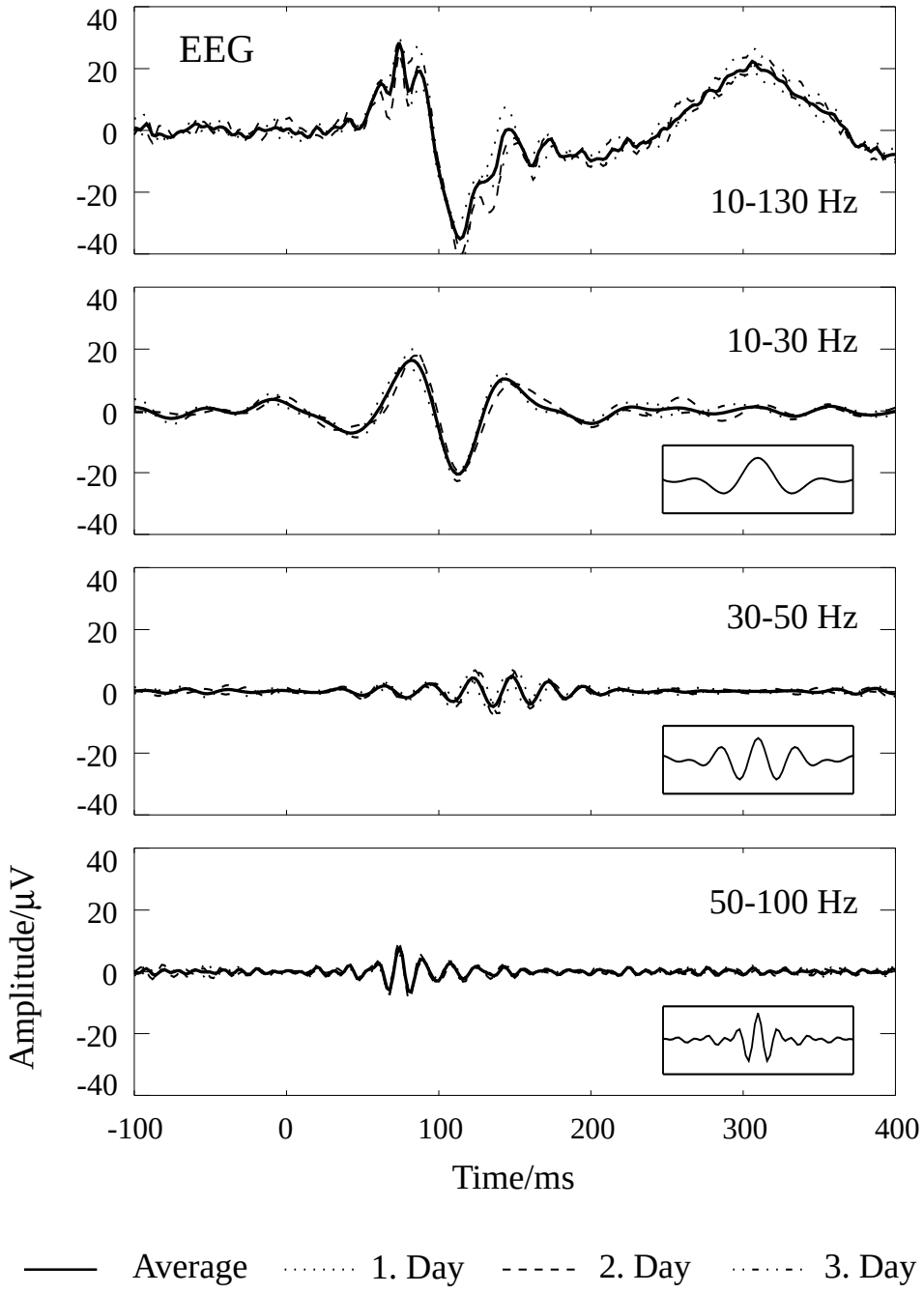

Fig. 3.17. Evoked EEG response and bandpass filtered data in the ranges of 10-30 Hz, 30-50 Hz, and 50-100 Hz. Average data from 3 sessions are shown. In addition, data from each session are presented separately (see Fig. 3.15). The *insets* show impulse responses of the respective bandpass filters.

3.4 Discussion

The present study yielded three major results: (1) Stimulus-induced gamma oscillations were present in monkey scalp EEG, correlated to intracortical oscillations during the visual presentation of geometric figures and sinusoidal gratings, (2) no stimulus-induced gamma oscillations could be observed in the human scalp EEG during a replication of the monkey experiment with sinusoidal gratings, and (3) stimulus-locked gamma oscillations appeared after the onset of a grating stimulus in LFP and EEG of monkey, but not in human EEG.

3.4.1 Stimulus-induced oscillations in monkey LFP and EEG

EEG gamma oscillations. As in previous investigations, stimulus-induced gamma oscillations were observed in intracortical recordings from the primary visual cortex of monkeys. The present results now demonstrate that power and coherence of intracortical high frequency oscillations in the gamma band are sufficient to generate well measurable modulations of gamma band activity in the scalp EEG of monkeys under appropriate stimulation. During visual stimulation with geometric figures or sinusoidal gratings the EEG activity was enhanced by factors of 1.8-5.1 in the range of the gamma band peak, while the relative enhancement of intracortical LFP was more than one order of magnitude stronger (up to 120).
Spatial decay of intracortical coherence. This study confirms and extends previous results of Brosch et al. (1995; 1997), Frien et al. (1996), and Juergens et al. (1996) on the spatial decline of the coherence of gamma oscillations in cat and monkey primary visual cortex. The present results show that the decay of coherence with cortical distance was clearly steeper for geometric figures composed of line gratings with a rectangular profile (down to 0.13 at 3 mm distance) than for sinusoidally modulated gratings (0.4-0.5 at 3 mm). The observed higher coherence between LFP and EEG signals with the second type of stimulation is in accordance with these findings. A possible explanation might be that the sinusoidal grating stimulus produced a more global synchronization of a rather homogeneous and strongly connected population of cells responding to similar spatial frequencies, whereas the gratings constituting the geometric figures activated an inhomogeneous group of contrast coding cells (with receptive fields of different size). It has also been shown that local contrasts may disrupt the synchronization of signals across object contours (Guettler et al. 1997). Another reason for the reduced coherence during the presentation of geometric figures might be that the high local luminance contrast of the geometric figures induced stimulus-locked activity during small eye movements within the fixation frame of 0.5°, enhancing distance-independent coherence at frequencies below 20 Hz and reducing gamma band coherence (Kruse and Eckhorn 1996).
Coherence at high and low frequencies. The coherence of LFP signals increased during stimulation in a rather broad frequency range. The maximum frequency of such stimulus-induced synchronization decreased with cortical distance. This means that LFP synchroniza-

tion at high frequencies was present exclusively at short distances, while low frequencies were coupled also over larger distances. The coherence at frequencies below 8 Hz increased strongly after stimulation, while the coherence at slightly higher frequencies (12 Hz) was substantially weaker and less stimulus dependent (see Figs. 3.5, 3.8). Low frequency coherence showed a weak spatial decay and was not stimulus-locked, i.e. not directly caused by the stimulus. A possible reason for the strong and far reaching coherence at low frequencies might be threshold control processes, caused by unspecific activation from subcortical structures which was still increased during stimulation.

Influence of intracortical coherence on EEG amplitude. As expected, the scalp EEG amplitude was determined not only by the amplitude of the intracortically measured components, but also by their spatial coherence. This was particularly evident during the smooth fade-in of geometric figures, where the LFP gamma band activity increased during stimulation while the EEG activation was maximal at the beginning of the stimulus response. The apparent discrepancy between results from intra- and extracortical measurements is resolved by taking into account that the spatial extent of gamma band coherence was maximal at the beginning of the stimulus response. Such initial stimulus-induced coherence was strongest at the gamma oscillation frequencies and present also at distant electrodes. This presumably led to a more constructive superposition of activities from different cortical locations and thus to higher EEG amplitudes during this phase of stimulation.

Why is the gamma band EEG less modulated by the stimulus than the LFP? According to the present results, stimulus related modulation of the scalp EEG gamma peak was reduced compared to the LFP. In the following it is argued, that this reduction contradicts simple models of EEG generation which are based exclusively on cortical spectral power and coherence. Standard models try to understand the EEG as a weighted superposition of sources from several cm^2 cortical tissue, transmitted to the scalp with a rather constant frequency characteristic in the upper bands relevant for the present study (Nunez 1981). In such a superposition it is of essential importance whether contributions from different locations add up constructively or rather cancel out. From its definition, a high coherence value requires that the phase difference between two signals is rather constant over trials. Previous experiments have shown that, although phase jitter increased with cortical distance, the average phase seldomly deviated significantly from zero (Frien et al. 1994). Consequently, highly coherent signals will add up more constructively than less coherent signals. As a gedankenexperiment, we assume at first that coherence is constant over frequencies, so that the amount of constructive superposition is identical for all frequency components. Consequently, the shape of the EEG spectrum should be identical to that of intracortical activity. If, however, intracortical coherence was increased at a spectral maximum of the LFP, this maximum should be even more pronounced in the EEG. In a word, both high intracortical power and coherence support high EEG amplitudes at a certain frequency. The present results show that both LFP power and coherence at gamma peak frequencies were increased during stimulation. Reasonable models

of EEG generation, confined to the influence of cortical sources, would therefore predict a more pronounced EEG gamma peak and a stronger modulation of EEG amplitudes at the gamma oscillation peaks compared to the LFP. One possible explanation of the observed small EEG modulation might be the contribution of neuronal activity that is unrelated to the stimulus and does not exhibit spectral peaks. The inclusion of more distributed (e.g. subcortical) sources producing a broad band "noise" level might thus account for the low gamma range modulation of the EEG and might contribute to a more realistic model of EEG generation. However, a more exact implementation of such a model would require simultaneous measurements of data from many brain regions with high spatial and temporal sampling, hardly available with the current recording technology.

20 Hz activity. The coherence function had a maximum at about 20 Hz being more pronounced for sinusoidal gratings than for geometric figures. This beta activity differed from the gamma activity in its weaker stimulus dependence and less spatial decline. Beta activity might be functionally relevant since in experiments with bar stimuli 20 Hz monkey LFP was shown to depend on stimulus orientation, in a similar way as the broad band response (see Fig. 3 in Eckhorn et al. 1993). It can be excluded that beta and gamma components were harmonically related since the gamma range peak frequency increased during stimulus movement while the frequency of the beta peak did not shift.

Functional implications of spatially declining coherence. The observed steep decline of coherence with cortical distance as found especially during the presentation of geometric figures seems to impose restrictions on functional hypotheses based on synchronized gamma oscillations and related computer models of scene segmentation. While many previous models assume a strong synchronization at zero average delay of all representational neuronal elements constituting an object (for a short review see Juergens and Eckhorn 1997 - chapter 1) the present results confirm earlier work of our group implying that the binding of object features may rather rely on the synchronization of neighboring neurons (Eckhorn et al. 1990; Eckhorn and Frien 1995). This local synchronization might be used at higher levels of cortical representation as a basis for the binding of more extended objects (Schanze and Eckhorn 1997).

Validity of spectral peaks: line artifacts. The frequencies of the observed gamma oscillations were in some cases quite close to the 50 Hz of the line signal. We used a correlation method to reduce line artifacts which, as all comparable methods, has its limitations. However, for both experiments analyzed here, there are strong arguments against suspected misinterpretations of line artifacts. During the presentation of the stationary sinusoidal grating rather narrow band maxima at 40 Hz were present in the spectra of EEG and LFP, clearly distinguishable from the 50 Hz line artifact. In addition, the oscillation frequency increased during stimulation, not explainable by line interference. During the geometric figures experiment the peak was rather close to 50 Hz. However, the oscillation frequency decreased during the time course of stimulation, showing that it cannot be explained by line artifacts, either.

Another argument against suspected line interference is the spatial decrease of intracortical coherence at the frequency of the gamma oscillation.

Reliability of gamma band effects. While gamma oscillations in the monkey LFP were found to be very strong (increase by factors of 13-120 with respect to the prestimulus condition), the effects in the scalp EEG were comparably weaker (modulation factors 1.8-5.1). However, EEG effects were demonstrated to be reliable in showing that gamma band peaks were present in scalp EEG spectra (i) at the same frequency as in the LFP (ii) in both monkeys, (iii) under two different types of visual stimulation, (iv) in different partial data sets for each type of stimulation, and (v) with similar amplitude in successive time windows during comparable stimulation. Similar arguments hold for the observed effects in stimulus-induced coherence. A statistical demonstration of the reliabilty of monkey EEG gamma band effects seems to be not necessarily required considering this strong and converging evidence.

Miscellaneous methodological aspects. The pronounced frequency dependence of neuronal synchronization confirms the use of the coherence function, which provides a frequency dependent measure, in contrast to commonly used cross-correlation techniques. The strong stimulus dependence of coherence excludes a major influence of volume conduction on the coherence of LFP signals. The finding that gamma oscillations are well measurable in the monkey EEG seems to open a perspective for a more global analysis of this phenomenon (at least in this species) with noninvasive techniques and low experimental effort. Simultaneous measurements of monkey LFP and EEG might help to reveal the role of local activity within extended synchronized assemblies.

3.4.2 Absence of fast oscillations in the human EEG

No gamma band effects comparable to those in monkey EEG were found in human EEG during a replication of the sinusoidal grating paradigm. Power spectra of signals from occipital and parietal cortex displayed no gamma oscillations during the presentation of sinusoidal gratings. It was demonstrated that the modulation of gamma band power in humans was at least two orders of magnitude lower than in the monkey EEG.

Possible reasons for the observed differences between results in monkey and human. First, there might be a total lack of oscillatory activity in human visual cortex, which would cast serious doubts on their proposed role in brain function. Nevertheless, this can *not* be concluded from our results, since very small modulations of activity are not detectable in noisy signals as the EEG within a limited time of observation. On the contrary, the fact that gamma oscillations of strong amplitude have been observed both in cats and monkeys might be an argument that gamma oscillations are a more general phenomenon which is not restricted to a certain species. Second, it is possible that only few cells in human visual cortex take part in gamma range oscillations. In this case random variations of activity, unrelated to the experimental manipulation, might lead to a small but non-measurable effect. For basic

reasons this cannot be excluded in case of negative results. Third, the coherence of generators of oscillatory signals may be restricted to a smaller spatial range in human visual cortex compared to monkey. In that case the resulting EEG amplitude would be reduced due to a stronger mutual cancellation of counterphase signals. Fourth, the different cortical, cranial, and scalp anatomy of humans might be responsible for the lack of stimulus-induced gamma signals in the EEG. In humans, visual area 17 is to a larger extent buried inside the gyrus occitemporalis medialis (especially the foveal and parafoveal parts). This causes rather tangential dipole orientations and a large distance between the locations of signal generation and EEG measurement, resulting in diffuse EEG activity of reduced amplitude. In addition, the human scull is thicker than that of macaque monkey, enhancing the spatial smearing of cortical activity. Fifth, it cannot be excluded a priori that gamma oscillations occur under different mental conditions in different species. However, the strong resemblance between results in lightly anesthetized cat and awake monkey under different types of stimulation makes this hypothesis somewhat implausible. Obviously, a combination of different factors might be responsible for a low EEG gamma amplitude. The sometimes discussed mutual cancellation of opponent dipoles in the gyrus occitemporalis medialis during stimulation of the whole visual field should not be very strong. Cancellation of signals from opponent dipoles was possible only if signals in the right and left hemispheres were highly coherent and if both hemispheres were highly symmetric with respect to the recording position (i.e., mutual dipole orientation 180° and similar distance) which both is not supported by experimental results (Eckhorn and Schanze 1991).

Previous results on gamma oscillations in the human EEG and ECoG. In contrast to the present results some recent publications reported on gamma band effects in the human EEG during visual stimulation. Sheer (1989) found increased 40 Hz EEG during a visual search task requiring focused arousal. Enhanced activity in the 35-45 Hz range during the initial phase of stimulation with moving line gratings was reported by Lutzenberger et al. (1994). Müller et al. (1996) found a broad band increase of activity in the range of 40-96 Hz during a period of 400-900 ms after the start of movement with a single bar but no gamma band response at all in case of two incoherently moving bars. Tallon-Baudry et al. (1996) reported on short episodes of early stimulus-locked (100 ms after stimulus onset) and late stimulus-induced (300 ms after stimulus onset) activity with maxima at 30-40 Hz during the presentation of real and illusory triangles and non-triangle stimuli as well as during the detection of Dalmatian dog pictures (Tallon-Baudry et al. 1997a). The existence of the stimulus-induced component was confirmed in a second EEG experiment but not in corresponding MEG recordings (Tallon-Baudry et al. 1997b). Vijn et al. (1991) found a broad band reduction of activity in the parieto-occipital region with a rotating checkerboard compared to the stationary stimulus. In a study of the human gamma band electrocorticogram (ECoG) during somatosensory stimulation no gamma band oscillations were observed (Menon et al. 1996), in contrast to results from intracortical recordings in monkeys (Murthy and Fetz 1992; Sanes

and Donoghue 1993). The temporal and parietal ECoG of epileptic patients (Bruns 1997) did not reveal gamma band oscillations during visual stimulation, in contrast to respective results in the awake monkey (Freeman and van Dijk 1987). The negative result of the present study is further substantiated by several unpublished investigations of the human scalp EEG during visual and auditory stimulation and during memory tasks in the laboratory of F. Rösler (Dept. Psychology, Univ. Marburg). These investigations did not yield any stimulus related gamma band effects, apart from harmonics of alpha activity in the gamma band (Jürgens et al. 1995; Juergens and Roesler 1995), which may be considered as merely epiphenomena.

Possible reasons for differences between the present and related results on gamma oscillations in the human EEG. The visual stimuli used in investigations of other groups were not identical to those used in the present investigation. However, it remains difficult to explain why the results are so contradictory. Our stimuli generated strong oscillatory activity in monkey experiments and were therefore expected to elicit comparable signals in humans. Methods of data analysis differed somewhat between the cited investigations but should have produced results principally comparable to ours. However, we have serious doubts concerning the validity of results reported in the literature since it is very difficult to exclude that either (i) harmonics of low frequency activity (Jürgens et al. 1995, Juergens and Roesler 1995), (ii) muscle activity, (iii) misinterpretation of filtered data, or (iv) spurious significances were responsible for at least some of the effects communicated.

In principle, some of these effects could also be the reason for our negative results. However, as explicated in the following, this seems rather implausible for the present study or can even be completely excluded. (i) Harmonics of alpha activity were present to a small extent at the occipital and parietal electrodes, leading to a stimulus related slight reduction of activity in the gamma range (see Figs. 3.12, 3.10). Nevertheless, in order to fully cancel out stimulus related gamma band activity, these harmonics must have had identical frequencies and time courses as genuine gamma brain activity with inverse modulation, which seems rather improbable. (ii) A similar argument holds for muscle artifacts. It also seems rather improbable that they had a similar but inverted time course as truly existing effects. Muscle activity, having a maximum of power in the gamma range, is difficult to exclude from EEG-data. We used one of the most common and powerful methods to cope with this problem which is the visual inspection of the recorded data and manual exclusion of outliers. However, this method works only for rather strong nonstationarities and, as all other methods known to us, neglects muscle activity of low amplitude. Analysis of coherence lead to the exclusion of one subject due to extremely low coherence values of signals measured at the outer electrodes (close to the neck muscles). This decision was confirmed by the topography of gamma band activity, showing a broad gamma band maximum at these electrodes. (iii) Filtered evoked potentials were compared to the filters' impulse responses, showing that oscillations in evoked potentials had a much longer duration and therefore could not be explained as simple filter artifacts. Moreover, power spectra of evoked potentials showed clear peaks at the relevant frequencies (20 and 40

Hz), further excluding the possibility of artificially generated oscillations. (iv) For principle reasons, there is no statistical method to determine the probability of finding an existing effect which is covered by noise, unless its magnitude is already known (which is not the case here).

In addition to these more technical aspects it might be considered that the chance of publication is much higher for positive than for negative results. So it is imaginable that other negative findings, supporting the present results, did not get into common knowledge. A replication of positive results on visually induced gamma oscillations in humans by independent groups and data analysis procedures seems advisable but has not been published until now. An experiment performed by Tallon-Baudry and coworkers (1996) was repeated by colleagues in the group of F. Rösler (Dept. Psychology, Univ. Marburg). However, preliminary results could not verify any of the reported effects (Gölz and Rösler, in preparation). As detailed above, a replication of results from Tallon-Baudry and coworkers (1997a) was attempted (Tallon-Baudry et al. 1997b), yielding diverging results in EEG and MEG data.

3.4.3 Stimulus-locked oscillations

Three different stimulus-locked components were distinguished in monkey LFP recordings after the temporally sharp onset of a sinusoidal grating stimulus: an early component in the range of 50-100 Hz with maximum amplitude 80 ms after stimulus onset and two narrow band processes with frequencies of 20 and 40 Hz during a period of 80-160 ms after stimulus onset. The 40 Hz component was also observable in monkey EEG while the 20 Hz and the 50-100 Hz components were not clearly visible.

Stimulus-locked high frequency component. The early high frequency component probably reveals a well known phenomenon called "wavelets", which appear in retinal structures after visual stimulation (Cracco and Cracco 1978; Ariel et al. 1983). Phase-locked periodic single unit activity in the visual cortex of monkey was described by Maunsell and Gibson (1992). They found oscillatory activity in all analyzed neurons with very short stimulus-response latencies with a maximum of oscillatory activity about 50 ms after the onset of stationary square wave gratings. Responses of different neurons had the same period and phase within animals. A comparable phenomenon was found in multi unit activity in layer IV of awake monkey (see Fig. 1 in Kraut et al. 1990). Human EEG response to light flashes (Whittaker and Siegfried 1983), sometimes called "wavelets", had frequencies around 100 Hz (80-140 Hz). Their amplitudes reached a maximum 70-100 ms after stimulus onset, with shorter delays for higher stimulus intensities.

Stimulus-locked components at 20 Hz and 40 Hz. LFP oscillations at 20 Hz and 40 Hz, were found to be phase-locked to the onset of the visual stimulus. Common to both phenomena was a concentration of signal power in a temporal range of 80-160 ms. Most important for an interpretation seems to be the fact that both the 20 Hz and the 40 Hz component corresponded to stimulus-induced activity at about the same frequencies. This stimulus-induced

activity increased during the decline of stimulus-locked activity. Such a concurrent decrease of stimulus-locked and increase of stimulus-induced activity might be explained by temporal jitter between oscillatory activity during different stimulus repetitions, since temporal jitter should be stronger with increasing time interval to stimulus onset. Both the identity of frequencies and temporal contiguity suggest that stimulus-locked and stimulus-induced components were produced by related processes. If this is true, a simple harmonic interrelation among 20 and 40 Hz stimulus-locked components can be ruled out considering the dissimilar features of 20 and 40 Hz stimulus-induced activities (see section 3.4.1). In addition, stimulus-locked oscillatory responses might be interpreted as "resonance phenomena" of the underlying neuronal structures (Basar et al. 1995).

Validity and reliability of stimulus-locked oscillations. Short phases of oscillatory activity may be confounded with filter resonance phenomena, if the data are analyzed with narrow bandpass filters. However, this can be excluded for the present data, since the filter's impulse responses were clearly shorter than the observed oscillations and the spectra of stimulus-locked activity showed distinct peaks at the oscillation frequencies (matching those of stimulus-induced components). The reliability of stimulus-locked oscillations was tested by comparing data from three different recording sessions. Stimulus-locked components in all three data sets showed very similar effects. The oscillation phase varied mainly at the end of the stimulus response, as expected from plausible models (see "Related computer models"**)**.

Previous results on stimulus-locked oscillations in the lower gamma range. Recent reports on oscillatory gamma band activity in the visual cortex concentrated on stimulus-induced activity, having a phase relation to stimulus onsets which varied between trials (reviews in Eckhorn 1994, Singer and Gray 1995). Lacking previous evidence on stimulus-locked activity at the dominating frequencies of the stimulus-induced components might be explained by (i) the choice of stimuli which slowly approached the receptive fields (e.g. light bars) or were faded in to prevent intermixture of stimulus-locked and stimulus-induced components, (ii) analysis intervals restricted to rather stationary phases excluding stimulus onsets, or (iii) the explicit subtraction of stimulus-locked components. Recently, stimulus-locked oscillatory components in the frequency range of 30-90 Hz were described in the human EEG during visual tasks by Tallon et al. (1995) and Tallon-Baudry et al. (1996, 1997a,b). These stimulus-locked components had a maximum about 100 ms after stimulus onsets. They depended on physical stimulus parameters but not on the tasks performed by the subjects. These results could not be verified in the present experiments on human subjects where only spurious broad band effects were found.

Related computer models. Computer models on stimulus-induced gamma oscillations, aimed at the explanation of the respective experimental results, were mostly analyzed in states without strong transients. However, most of these models, especially those with neuron-like elements, should reveal stimulus-locked components when activated with suddenly changing input. The "step" response of such a model neuron network to the onset of a stimulus

(Eckhorn et al. 1990, 1991) started with a synchronized initial response caused by common activation. It was followed by stimulus-locked and subsequently stimulus-induced oscillatory components with vanishing phase-lock due to the increasing influence of noise. These simulation results might help to explain the present experimental results and should be typical for the dynamics of physiologically plausible models of gamma oscillations.

3.4.4 Conclusion

The present results show that gamma oscillations in local field potentials of *monkey* primary visual cortex were reflected by well measurable effects in the scalp EEG, covarying with the power and coherence of activity at different intracortical locations. The scalp EEG might therefore be a suitable method, also together with intra- or extracortical measurements from other areas, to reveal oscillatory gamma range signals in different parts of the monkey brain. In contrast to the results in monkey, the analysis of *human* EEG data exhibited no enhancement of gamma band power during similar stimulation. Due to the contradictory results in the literature concerning if and how visual stimulation affects the gamma band scalp EEG in humans, it seems valuable to replicate some of these experiments. In addition to stimulus-induced components, stimulus-locked gamma oscillations with a latency of less than 100 ms were found. Such phenomena are a consequence of common model assumptions aimed at the explanation of induced gamma oscillations and might be the basis of fast sensory processing after saccades or following suddenly appearing stimuli.

4 Stimulus Induced Gamma Oscillations: Harmonics of Alpha Activity?

4.0 Abstract

Event-related changes of spectral power of the EEG were studied for each integer frequency between 5 and 100 Hz in three subjects during memory storage and retrieval. Spectra were calculated for successive, overlapping time epochs in seven channels. In one subject a stimulus-locked increase of power was observed at 12 Hz, while in the other two alpha power decreased at the individual peak frequencies of 9 and 11 Hz, respectively. In all subjects corresponding changes of power appeared at frequencies which were integer multiples of the individual dominant alpha frequencies. An analysis of the cross covariance of the alpha, beta and gamma activity revealed high coefficients for harmonic frequencies only while all other covariances were negligibly small. It is argued that event-related gamma activity may be an epiphenomenon of event-related changes within the alpha band.

4.1 Introduction

It is a well known fact that sensory, cognitive and motor activity has an influence on the power and the duration of alpha oscillations in the EEG (Michael 1994; Pfurtscheller and Klimesch 1991). The most common finding reported in the literature is that alpha-power decreases after stimulus onset or during cognitive load ('event-related desynchronization'). In some psychophysiological experiments in which the quality and the difficulty of tasks are varied systematically, an increase of alpha-power has been found. Moreover, other studies in which alpha activity was not analyzed as a whole (i.e. as total power between 7 and 13 Hz) but separately for narrow frequency bands revealed that alpha is by no means a functionally homogenous phenomenon: different frequencies within the alpha band may respond differently to changes of arousal. For example, when a subject with closed eyes attends to the environment, slow alpha activity (8-10 Hz) may decrease while fast alpha activity (11-13 Hz) may increase in power at the same time (Gale et al. 1977; Rösler 1975). In identical experimental settings pronounced interindividual differences of spontaneous and of task-related changes of alpha activity can also be observed (Deakin and Exley 1979; Gale 1973).

In more recent studies, gamma activity (frequency range > 30 Hz) was picked up from the cortex of cats and monkeys with intracranial recordings. These measurements revealed stimulus induced gamma oscillations in sensory (Eckhorn et al. 1988, 1993; Engel et al. 1992) and motor areas (Murthy and Fetz 1992; Sanes and Donoghue 1993). Moreover, it was claimed that activity in the range of 30-80 Hz can also be observed in EEG recordings in human subjects and that this activity is related to specific functional states of the brain (Banquet 1973; Sheer 1989; Llinas and Ribary 1993; Desmend and Tomberg 1994; Kristeva-Feige et al. 1993; Tiltinen et al. 1993; Lutzenberger et al. 1994, 1995).

In some studies the relationship between alpha and gamma activity in the EEG was examined (Pfurtscheller et al. 1993; Pfurtscheller and Neuper 1992). Before and during voluntary movements, for example, activity between 34 - 40 Hz increased while at the same time 10 Hz activity decreased. Both phenomena appeared to be time-locked to movement onset, but the time course and the topography were somewhat different.

In the present study we examined whether similar changes of alpha and gamma activity could be observed while the subjects were engaged in a more difficult cognitive task, i.e. during storage and retrieval of verbal and non-verbal memory contents. In contrast to previous studies the power of the EEG was not only analyzed for selected frequency bands but for the full spectrum between 5 and 100 Hz. Power maxima were found at 12 Hz as well as at the first and second harmonics of this frequency (24, 36 Hz). The power of these frequencies showed a pronounced temporal correlation and a similar topography, suggesting that some phenomena of gamma activity may just be the result of changes in the alpha frequency range.

4.2 Materials and Methods

4.2.1 Subjects and task

Three right handed subjects (two female, mean age 25 years) participated in a memory experiment which comprised a learning and a retrieval phase (Heil et al. 1994). In the first part of the experiment the subjects had to learn associations between so called target-items and mediators. Target-items were line-drawings showing concrete objects, e.g. different exemplars of fish, plants, airplanes etc. Mediators were either positions in a checkerboard grid with three rows and three columns (spatial task) or nouns which were not associated *a priori* with the objects depicted as line drawings (semantic task). In a trial at the beginning of the training session one of 54 possible line drawings was presented in the center of a computer screen, and 6.5 s later either one or two of nine possible positions (spatial task) or one or two of nine possible words (semantic task) appeared for another 4 s above the drawing. The total set of the target-mediator pairs was presented three times in this manner. After this

the drawings were shown together with the complete set of positions or words and the subject had to select by a mouse-click the associated position(s) or word(s), respectively. Upon mistakes, the computer indicated the correct associations. Subjects were trained until they could anticipate the mediators correctly in 94% of all trials.

The retrieval experiment took place on the following day. In the trial two of the 54 line drawings were shown side by side in the center of the screen for 6 s while none of the mediators was visible. The subjects´ task was to decide, whether the two drawings were associated via a common mediator or not. Positive and negative decisions had to be indicated by briefly lifting either the index or the middle finger of the right hand. This movement was detected by a light gate. To come up with a decision in this situation the respective mediators (positions or words) must be activated in memory. Subjects have no other option to solve the task. Thus, memory search can be studied with different types of representations while all other aspects of the retrieval situation (the target stimuli, the associative structure, the response etc.) are kept constant (Heil et al. 1994).

4.2.2 EEG recording and analysis

The EEG was recorded with Ag-AgCl electrodes from the positions F3, Fz, F4, P3, Pz, P4 and Oz. Linked ear lobes, connected via two 5 kW resistors, served as reference. The EEG was recorded for 13 s in the trials of the first learning phase and for 9 s in the trials of the retrieval test, respectively. In the learning trials the recording epoch began with a prestimulus baseline of 2.5 s during which a fixation frame was presented on the monitor. This epoch was followed by the presentation of a line drawing for 6.5 s. Then the mediator(s) were added to the display above the line-drawing and the whole ensemble was presented for another 4 s. The corresponding event times in the test trials were: 3 s prestimulus baseline with presentation of the fixation frame and 6 s presentation of the pair of line-drawings. All signals were analogue-filtered with a pass-band of 5-100 Hz and digitized with a rate of 512 Hz. The vertical EOG was recorded for artifact control. Trials with blink artifacts, eye movements or excessive EMG activity were removed on visual inspection.

Power spectra were calculated using a Hanning window of one second length and a FFT-algorithm. In each channel the window was shifted over the total recording epoch in steps of 500 ms which provided 25 consecutive spectra in a learning trial and 17 in a test trial. The power spectra obtained for one electrode with the same lag were averaged over all artifact-free trials. For each subject this average comprised about 100 replications in the learning and 350 replications in the test phase, respectively.

4.3 Results

All calculated spectra showed a very a similar pattern of power coefficients. In each case the maximum appeared in the alpha range and the power decreased towards higher frequencies. The absolute power ranged from 15 μV^2 for the dominant alpha frequency to less than 0.1 μV^2 for the highest frequencies in the upper gamma band. One subject had her maximum power in the lower alpha range, at 9 Hz, while in the other two subjects the maximum peak appeared in the upper alpha range, at 11 and 12 Hz, respectively. The power spectra of the subject with the 12 Hz peak showed two additional peaks at 24 and 36 Hz, i.e. at integer multiples of the alpha peak frequency. These additional maxima were very pronounced at electrode P4, less prominent but still visible at electrodes F3, Pz and Oz, and not present at P3, Fz and F4. Fig. 1 shows for electrode P4 the time course of the spectral power of the three peak frequencies and of adjacent frequencies during the learning and the retrieval phase (b, c, d). Power of three frequencies of the lower alpha range is also shown (a).

While the activity in the lower alpha range revealed no event-related changes in this subject, the activity in the dominant alpha frequency (12 Hz) increased significantly after each stimulus presentation. A corresponding increase of power was present in the harmonic frequencies of 24 and 36 Hz. During learning the power of these frequencies showed a phasic peak between 0.5 to 2.0 s after each stimulus with a maximum at about 1.0 s after stimulus onset. During retrieval the event-related peak was broader, extending from 0.5 to 3.0 after the stimulus onset with a maximum at about 2.0 s. The spectral power of frequencies adjacent to the 12 Hz peak (10, 14 Hz) or adjacent to one of the harmonics (22, 26 and 34, 36) was significantly smaller than the power of the center frequencies (12, 24, 36 Hz). Moreover, power coefficients of these adjacent frequencies did not change systematically over time nor were they in any way related to the stimulus presentations.

The similarity of the time course of the spectral power in the alpha and in the gamma range was quantified by calculating the covariances of the time series. The covariances obtained for electrode P4 are summarized in Table 1, separately for the learning and the recall phase. This analysis reveals high coefficients of covariance between frequencies of the gamma band in the 35-38 Hz range on one side and of the alpha band between 11 and 13 Hz on the other. The covariances of the same gamma frequencies with frequencies of the adjacent low alpha (8 - 10 Hz) or low beta band (14 - 15 Hz) was negligibly small. Likewise, the covariance of the 12 Hz activity with the activity of lower or higher gamma frequencies, 33, 34 Hz and 39, 40 Hz, respectively, was also small or even negative. A similar pattern is revealed if the covariances are calculated between the time series of the activity in the alpha and lower beta range (8-15 Hz) on one side and the time series of the activity in the higher beta range (21-28 Hz) on the other. Again the maximum covariance is found between frequencies 11-13 Hz on one side and 23-25 Hz on the other. Equivalent effects of a temporal covariance between the 12 Hz band and its harmonic frequencies could be observed at the other electrodes where the power of the harmonics was less pronounced, e.g. at F3.

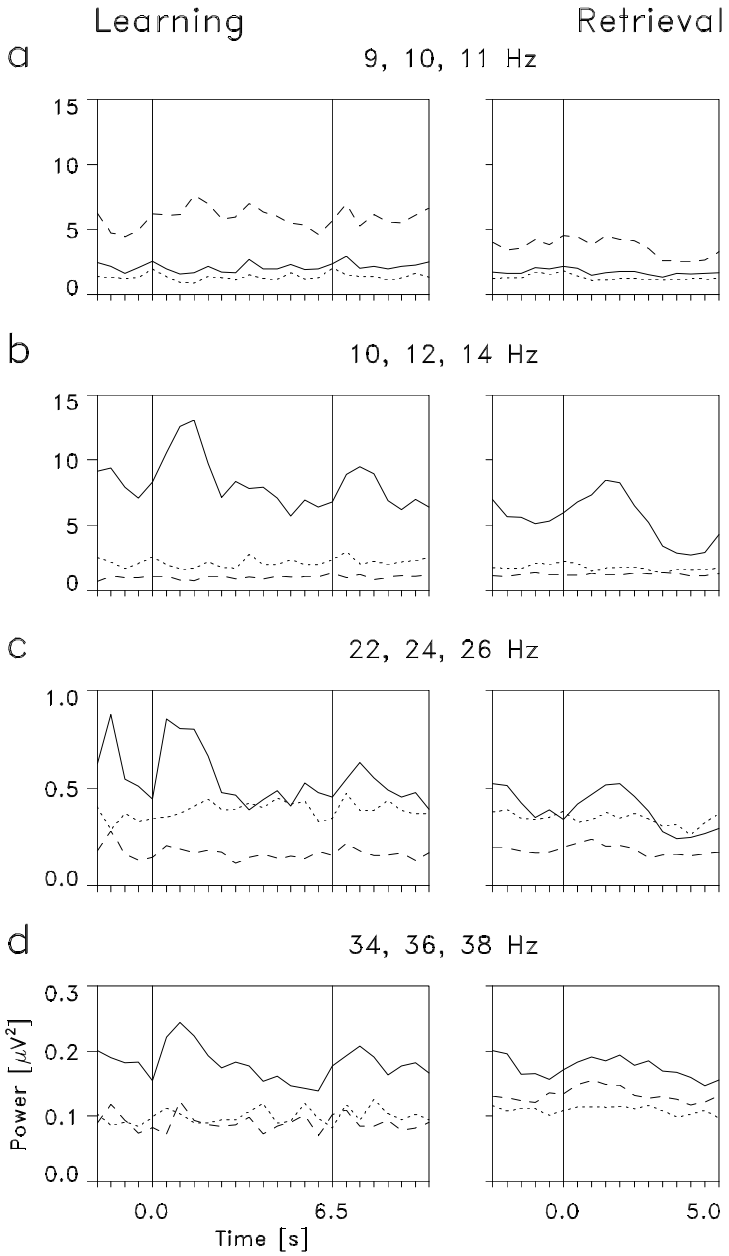

Fig. 4.1. Time course of the activity of one subject in the alpha band and in the higher harmonics at electrode P4. **Left**: Learning phase (average over 90 trials); *vertical lines* indicate the onset of the line-drawing at time 0 s and of the mediators at time 6.5 s. **Right**: Retrieval phase (average over 353 trials); the *vertical line* indicates the onset of the two line-drawings. From **top to bottom**: Time course of the activity in four distinct frequency bands with center frequencies of 10, 12, 24, and 36 Hz. In each plot the center frequency is shown as continuous line, the frequency below the center as dotted and the frequency above the center as dashed line, respectively. Notice the different scaling of the ordinates in the four rows. Activity in the lower alpha band (9, 10, 11 Hz) shows no systematic trend over time **(a)**. Activity of 12 Hz and of integer multiples of 12, 24 and 36 Hz, however, shows clear event-related changes over time **(b, c, d)**. This effect is very selective. The activity in each of the adjacent frequencies ± 2 Hz (10, 14, 22, 26, and 34, 38) is not related to the event sequence nor does it show any other systematic changes over time.

Table 4.1. Coefficients of covariance between the activity in the alpha and gamma bands at electrode P4 (multiplied by 1000).

Frequency [Hz]	33	34	35	36	37	38	39	40
Learning phase								
8	0.471	-0.111	-0.603	-1.906	-1.535	-0.942	-0.440	0.378
9	0.560	-0.211	-0.387	-1.988	-1.284	-0.225	-0.083	0.068
10	1.188	0.805	-0.710	-1.836	-0.037	-0.426	0.373	0.169
11	-0.154	2.536	2.517	6.465	7.989	0.894	-0.489	-0.389
12	-7.938	2.135	16.039	39.374	27.162	8.174	5.077	-2.202
13	-3.330	0.109	5.871	16.376	11.478	4.225	3.604	-0.501
14	0.220	-0.637	-0.553	-1.427	-1.253	-0.207	0.007	0.188
15	0.030	-0.730	-0.555	-1-392	-1.123	-0.174	-0.247	0.140
Retrieval phase								
8	-0.045	-0.196	-0.734	-1.014	-1.013	-0.534	-0.303	-0.213
9	0.065	-0.102	-0.577	-0.702	-0.760	-0.296	-0.203	-0.179
10	0.133	0.055	-0.501	-0.250	0.074	0.203	-0.069	-0.098
11	2.334	2.264	3.777	5.246	5.528	4.234	1.509	0.618
12	6.848	6.961	15.319	20.113	19.982	14.413	6.104	2.350
13	2.957	3.059	6.902	8.918	9.070	7.220	3.531	1.418
14	0.017	-0.028	-0.043	-0.234	0.020	0.042	0.013	0.178
15	-0.063	-0.170	-0.343	-0.484	-0.592	-0.527	-0.295	-0.101

In the other two subjects, who had their alpha peak at 9 and 11 Hz, respectively, a substantial decrease of alpha power could be observed after each stimulus presentation. In temporal correspondence to this event-related desynchronization in the alpha range a reduction of power appeared in the harmonic beta and gamma frequencies. Cross covariances showed again a pattern of high and low covariances between neighboring harmonic and non-harmonic frequency bins, respectively. For example, in the subject with the 11 Hz peak the average covariance at P4 between the 10-11 Hz bin and the harmonic 20-22 Hz bin was 39.12, while the respective covariance with the neighboring non-harmonic bins at 17-19 Hz and 23-25 Hz, respectively, were 30.12 and 23.96. The corresponding covariances between the 10-11 Hz bin and bins of the gamma range amounted to 5.25, 10.13, and 3.47 for bins 27-29, 30-32 Hz and 33-35 Hz, respectively. For the subject with the 9 Hz peak a similar pattern holds for the beta range. At P4 the respective covariances between the 9-10 Hz bin and the 14-16 Hz, 18-20 Hz, and 22-24 Hz bins were 127.35, 384.24, and 49.97, respectively. For this subject no systematic relationships were found between the alpha and the gamma range. In both subjects equivalent effects were also found at other electrodes, e.g. Oz.

4.4 Discussion and conclusions

In the present study event-related changes of the power of selected frequencies could be observed in the EEG while subjects were engaged in the difficult cognitive task of storing and retrieving memory representations. The most pronounced and systematic changes were found in one subject at electrode P4 for a very narrow frequency band in the upper alpha range with a center frequency of 12 Hz. Corresponding changes also appeared in the power of integer multiples of this frequency band, i.e. around 24 and 36 Hz. The power of all three frequencies - 12, 24, and 36 Hz - increased phasically after each stimulus presentation. Power in adjacent frequency bands was significantly smaller and not related to any of the events. This holds in particular for the lower alpha band (8-10 Hz), the lower beta band (14-15) Hz, and other gamma frequencies, e.g. 33-34 Hz or 38-40 Hz.

The systematic and event-related change of the power in the upper alpha band is in line with previous work in which also an increase of fast alpha was observed in states of activation for some subjects (Gale 1973; Rösler 1975; Herrmann 1982). New is the finding that these changes in the alpha band may covary with corresponding changes at higher, harmonic frequencies in the beta and gamma range. A straightforward explanation is provided by the fact that rhythmic activity in the EEG with a dominant center frequency and clearly visible oscillations has not the shape and the time course of a pure sinus wave. In a spectral analysis these deviations from an ideal sinus wave will cause significant power coefficients in frequencies which are harmonic to the base frequency, i.e. multiple integers of it (Brigham 1975).

Event-related changes of alpha power can be observed in almost all experimental paradigms in which stimuli are presented and in which cognitive and motivational states of the subjects are manipulated systematically. Considering this and the findings of the present study, it is very likely that in most experiments systematic changes of power are also present in higher frequency bands. Moreover, as the dominant alpha frequency usually shows pronounced inter-individual differences, and because different alpha frequencies may respond differently to the very same experimental manipulation, the "alpha harmonics" will not be restricted to narrow frequency ranges, e.g. multiples of 10 Hz only. This possibility has to be taken into account by researchers whose primary interest are state-related changes of beta and gamma activity. In order to claim that a change in one of the upper frequency bands is genuine and restricted to either beta or gamma activity it has to be shown that it is not simply an effect of harmonic alpha activity.

Pfurtscheller et al. (1992, 1993), for example, examined the activity in the alpha range (pass-band 10-12 Hz) and in the gamma range (pass-bands for different subjects 34-36, 36-38, 38-40, and 40-42 Hz). They did not analyze the power of the higher alpha range (e.g. with pass-bands 11-13 and 12-14 Hz) and of the beta ranges ($14 < f < 30$ Hz). Therefore, it cannot be excluded that stimulus-coupled activity changes in the gamma range, as found in these studies, are caused by corresponding stimulus-related changes of selected frequencies within

the alpha range. Llinás and Ribary (1993) found increased oscillations in the range of 35 to 45 Hz during REM sleep. Again, the influence of harmonics of alpha activity is a possible explanation of these results. The same caveat applies also to recently published studies of Lutzenberger et al. (1994, 1995). In these studies only the power in the higher frequency bands was analyzed without considering possible changes in the alpha range. Moreover, in these studies each of the analyzed gamma bands extended over a broad frequency range of 10 Hz width (25-35, 35-45, 55-65 Hz). Thus, it is not unlikely that activity which is harmonic to one or the other of the alpha frequencies was the primary cause of the very subtle power changes being observed by Lutzenberger et al. in the higher frequency bands.

The present data suggest that event-related changes of beta and gamma activity, may be, at least in part, an epiphenomen of equivalent changes in the alpha band. Therefore, for any study in which the higher frequency bands are of primary interest it is a prerequisite that also activity changes at integer fractions of these frequencies are examined. To detect such dependencies the full power spectrum must be evaluated - not just the activity in selected bands - and further, the power of single frequencies and their harmonics have to be analyzed separately. If only the average activity within broad bands is analyzed, the influence of harmonic alpha may be obscured. Alpha peak frequencies and alpha power changes can show substantial inter- and intraindividual variability, and therefore, increases and decreases of power at particular frequencies may cancel each other. Another method to study interrelations between different frequency components is given by bispectral analysis (Dumermuth and Gasser 1978). This method uncovers in a more systematic manner than the present approach interrelations between different frequency components which are either due to phase locking as an inherent feature of a stationary signal or due to nonstationarities.

5 Gamma Oscillations in Human Reaction Time Distributions: a Reliable Phenomenon?

5.0 Abstract

Recently Dehaene (1993) published an investigation of human reaction time distributions during the discrimination of simple or composed features of visual or auditory stimuli. It was reported that significant gamma oscillations were present in most reaction time distributions analyzed. We tried to replicate the results from the auditory experiments with identical experimental setup and data analysis procedures. Our data analysis revealed only one significant frequency peak in the spectra of all RT distributions analyzed (four subjects performing two different tasks). Moreover, this peak existed in only one of three spectra from the different experiment days. Coefficients of correlation between pairs of spectra from the six different experimental sessions were very small for all subjects and for both feature and conjunction tasks. Regarding the present results and the fact that the oscillations observed by Dehaene were neither consistent over subjects nor over stimulus conditions we conclude that gamma oscillations in human reaction time distributions are at least a highly unreliable phenomenon.

5.1 Introduction

Recently Dehaene (1993) published an investigation on the hypothesis that cognitive processing might be discrete in time, especially an oscillating process. It was carefully controlled for artifacts in data acquisition and provided a convincing method for data analysis. An experimental paradigm was used where subjects had to discriminate simple or composed features of visual or auditory stimuli. Significant reaction time (RT) oscillations in the 20-100 Hz range were found in most of the RT histograms analyzed. The peak frequencies were higher for simple feature tasks compared to the more complex conjunction tasks. Because of the far reaching consequences of these findings we tried to replicate the experiments. We concentrated on the auditory tasks in order to get a high number of reaction times for subsequent analysis.

5.2 Methods

5.2.1 Design and Stimuli

Four right handed subjects (2 female, mean age 23 years) served as subjects in an experiment comprising two auditory tasks of different difficulty. The experimental procedure was very similar to that described by Dehaene (1993). Subjects had to make two choice decisions either about simple tones (feature task) or about sequences of two tones (conjunction task). The time interval between stimuli was 3000 ± 250 ms. During the feature task subjects had to distinguish between computer generated square-wave sounds with a pitch of 440 Hz (A) or 1245 Hz (D#), respectively. The durations of these tones were 100 ms. They were generated by the sound chip of an Atari ST and presented by the loudspeaker of a computer monitor. During the conjunction task two-part sequences of the same tones (A - D# or D# - A), each shortened to 50 ms duration, were presented. At the beginning of each trial a fixation point appeared on a computer screen. One second later the acoustic stimulus was presented. Subjects had to react by either lifting their right index or middle fingers thereby interrupting a light barrier. The assignment of finger to stimulus was varied systematically between subjects. The photo diode voltage was converted into a TTL signal. We performed two simultaneous and independent RT measurements. The first measurement was carried out by the computer which generated the auditory stimuli and was used for further data analysis. The timer chip of this computer was programmed to send a hardware interrupt every 1/1024 s. This interrupt was used to increment a counter which had been set to zero at the onset of the acoustic stimulus. The counter was stored when the light barrier signal at the parallel port changed from -5 to 5 V. Interrupting the light barrier by means of a magnetic shutter in known time intervals revealed an accuracy of this measurement of better than 1 ms. As a further control the light barrier signal was recorded using an analog to digital converter with a sampling rate of 512 Hz. A comparison of the results of both measurements revealed no unexpected differences. At the first day of each series of RT measurements, subjects performed a training that consisted of two sessions of 800 trials each. Feature and conjunction stimuli were presented alternately in groups of 200 trials. This experiment was repeated three times within the following week, yielding a total number of 2400 RTs for each of both tasks (without training). Two possible sequences of feature and conjunction task groups (FCFC vs. CFCF) were pseudo-randomized over sessions and subjects.

5.2.2 Analysis of RT distributions

Each subject's distributions of all correct RTs during the three regular experimental days were calculated separately for feature and conjunction tasks. In order to detect periodicities, a frequency analysis was performed in a similar way as described by Dehaene (1993).

Spectra of the RT distributions were calculated using a FFT in a window of 256 time bins (250 ms) centered around the median RT, yielding 20 spectral values between 20 and 96 Hz. The significance of a deviation of these spectra from randomness was determined by comparing them with spectra from simulated RT distributions which were very similar but contained no oscillations. A total of 10,000 such control sets were calculated by means of the following procedure. First, each original RT histogram was digitally low-pass filtered with a cut-off frequency of 20 Hz. The resulting non-oscillatory distribution was used to generate an identical number of RTs in the time window used for the FFT as analyzed from the original data. The resulting RT distributions were then transformed into the frequency domain.

In each of the 20 frequency bins between 20 and 96 Hz the value of the original spectrum was compared with all the respective values from the 10,000 simulated data sets. The statistical significance of the departure of each frequency bin from the hypothesis of non-oscillating RT distributions was determined by the rank of the original spectral value with regard to the simulated data. For example, a rank of 500 corresponds to a significance level of 0.05. All significance levels were Bonferroni corrected for the 20 frequencies tested in the range from 20 - 96 Hz. Low significance levels were nearly constant over frequencies, reflecting the lack of non stochastic components in the Monte-Carlo spectra above the low pass frequency of 20 Hz. Strong deviations from this constancy could be observed only at higher significance levels and were caused by the small number of random spectral values used for their determination (e.g. 5 random spectral values for a significance level of 0.01 after Bonferroni's correction).

5.3 Results

The amplitude spectra of the RT distributions for each of the four subjects are shown in Fig. 1. Only one frequency peak was statistically significant: The spectrum of the second subject revealed a significant peak ($p < 0.02$ after Bonferroni's correction) at 72 Hz during the conjunction task.

In order to test the reliability of this peak, spectra and significance levels were calculated separately for each of the three days. As shown in Fig. 2, a significant frequency peak at 72 Hz existed only in the data of the first day ($p > 0.01$). At the second day, there was a peak at 44 Hz ($p > 0.05$), while at the third day there was no significant peak at all. Again splitting the data sets revealed that the most significant frequency differed between both sessions of each

day (1. day: 32, 72 Hz; 2. day: 56, 44 Hz; 3. day: 72, 60 Hz). None of these peaks was significant.

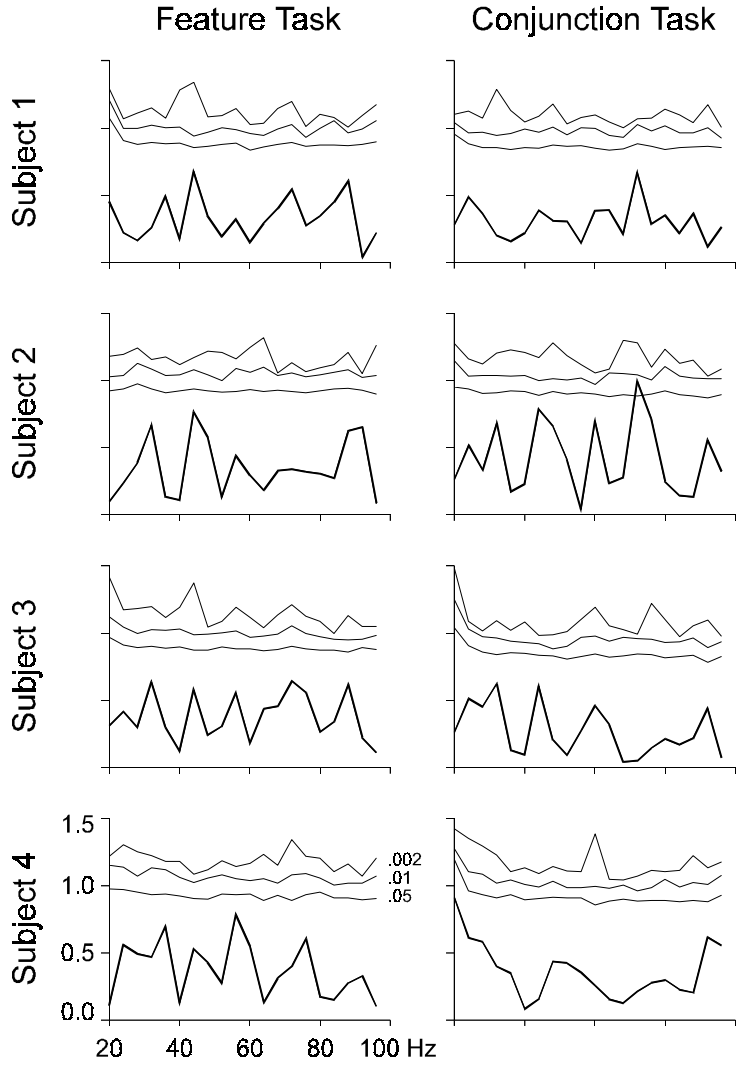

Fig. 5.1. Spectra of RT distributions from 4 subjects during the auditory feature and conjunction tasks. The *thin lines* above the original spectra indicate significance levels after Bonferroni's correction, from bottom to top: $p < 0.05$, 0.01, 0.002. Only one significant frequency peak was detected (subject 2, conjunction task, $p < 0.02$)

To quantify the degree of similarity between spectra of the six different sessions the Pearson correlation coefficients of all possible pairs of spectra were calculated and averaged after application of Fischer's-Z-transform. Table 1 shows the results for the eight analyzed data sets. Very small correlation coefficients (absolute values less than 0.1) show high dissimilarities between spectra of different subsets of data. The small degree of correlation (0.059) between the spectra of the second subject performing the conjunction task shows that the peak at 72 Hz was no consistent feature.

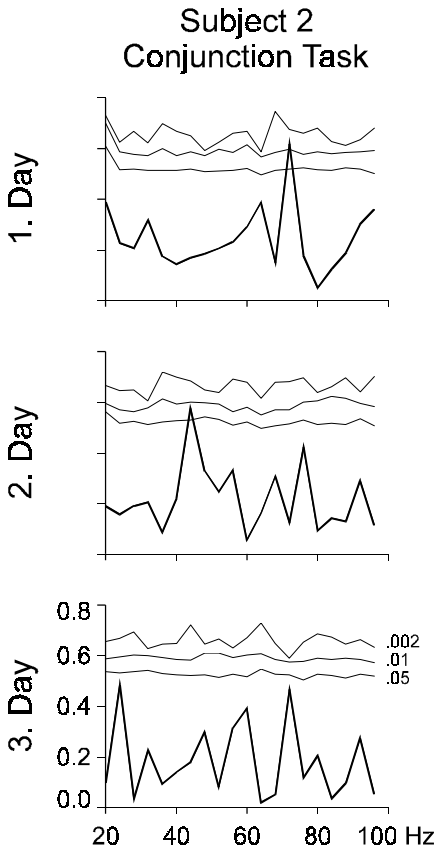

Fig. 5.2. Spectra of RT distributions from the second subject during the auditory conjunction task, calculated separately for each of the three days of the experiment. The peak at 72 Hz, which was visible in the summation of the daily RT distributions, was observed in only one of these partial data sets.

Table 1. Mean coefficients of correlation between spectra of RT distributions from six experimental sessions. Each coefficient was determined from 15 pairs of spectra. The mean RT was calculated as the arithmetic mean of median RTs from the four subjects (± standard deviation between subjects). Wrong reactions and reactions before 150 ms or after 999 ms were counted as errors.

Subject	Feature task	Conjunction task
1	-0.057	0.035
2	-0.047	0.059
3	0.057	0.036
4	-0.075	0.009
Mean Correlation	-0.031	0.035
Mean RT (ms)	336 ± 23	402 ± 65
Errors (%)	0.8	2.0

5.4 Discussion

Our data analysis procedures, which were equivalent to those of Dehaene (1993), revealed only one significant frequency peak in the spectra of all RT distributions analyzed (four subjects performing two different tasks). Moreover, this peak existed in only one of three spectra from the different experiment days. Coefficients of correlation between pairs of spectra from the six different experimental sessions were very small for all subjects and for both feature and conjunction tasks. These results clearly demonstrate the low reliability of rhythmic structure in the analyzed reaction time distributions.

Differences in experimental settings and errors in data acquisition and analysis were carefully examined as potential reasons for the inconsistency between Dehaene's and our results. (i) The acoustic stimuli were identical to those used in the investigation of Dehaene. (ii) Subjects were specially trained for this task and highly motivated. (iii) The number of about 2400 analyzed RTs was higher than in the investigation of Dehaene (1600 RTs) and should have led to even more significant results. (iv) As described above, the light barrier RT measurement was tested with a mechanical device that interrupted the light beam in known time intervals and was validated with a second independent registration method. (v) Spectra of RT distributions were checked for consistent periodicities with two independent methods: the Monte-Carlo method used by Dehaene and the analysis of correlations between spectra from split data sets. Both methods showed that spectral peaks above 20 Hz were not consistent during the course of the experiment. (vi) A comparison of spectra from RT distributions of each of the three days or six session revealed no systematic variation of peak frequencies during the course of the experiment as discussed by Dehaene. (vii) Simulated oscillatory and non-oscillatory RT distributions were used to exclude programming errors in Fourier analysis and in the implementation of the Monte Carlo method.

Doubts concerning the reliability of gamma oscillations in human reaction times do not only result from the present evidence, but also from Dehaene's results. The significance values in Table 1 of Dehaene (1993) show that for each of the five subject there was at least one of four stimulus conditions without a significant gamma band peak. In addition, in three of four stimulus conditions, results were non-significant for two of five subjects.

Regarding the literature concerning oscillations in RT distributions, the work of Dehaene (1993) is the first which used convincing statistical methods that should lead to correct estimations of statistical significances. The experimental conditions in our experiments were equivalent to those of Dehaene and our data analysis should have revealed periodicities in the measured RT distributions if there were any. Regarding the present results and the fact that the oscillations observed by Dehaene were neither consistent over subjects nor over stimulus conditions we conclude that gamma oscillations in human reaction time distributions are at least a highly unreliable phenomenon.

6 Summarizing Discussion

Each chapter of this thesis represents an independent investigation, including a discussion of the respective results. Therefore this chapter will concentrate on more general aspects. It will give a short summary of each investigation, show relations between results given in the different chapters, and make proposals for future work.

6.1 Summary of the results

As worked out in the previous chapters, a multi-methodological approach revealed new aspects of oscillatory and nonoscillatory neuronal activity at different spatial and temporal scales.

Chapter 2: "Parallel processing by a homogeneous group of coupled model neurons can enhance, reduce, and generate signal correlations"

The generation and transmission of correlated signals in neuronal networks were examined in computer simulations. A previously disregarded problem of correlation theories of brain function was pointed out: When differently correlated inputs were presented to a simulated group of neurons in a state of low activation, the correlation of the output signals was diminished compared to the input. This means that the "correlation contrast" was reduced, leading to a weaker separability of both groups by "correlation detectors" (a basic property of neurons). However, it was shown that lateral coupling between the neurons enhanced the correlation contrast. Multiplicative lateral coupling proved to yield a stronger separation between differently correlated groups than coupling of additive type as used in most of the other models. The input-output correlation, providing a measure for the information transmission of the network, decreased with lateral coupling strength and increased more than proportionally with input amplitude. In states of high discharge rates, input-output correlations were comparably weak. Here uncorrelated input signals were used to allow undisturbed self-organization of the network activity. States characterized by synchronized oscillations, stochastic activity, and rhythmic bursting were produced with increasing strength of lateral coupling. These simulations may help to explain the generation of synchronized high frequency oscillations as described in the following chapters.

Chapter 3: "Identical visual stimulation elicited fast oscillations in EEG and LFP of monkey but not in human EEG"

It was shown that stimulus-induced oscillations at 40-60 Hz, as found in our intracortical recordings, were also present in the monkey electroencephalogram (EEG). The amplitude of these EEG components was related both to the amplitude and coherence of intracortically measured local field potentials (LFP). The apparent inconsistency of different time courses of intra- and extracortically measured oscillation amplitudes could be explained by showing that the time course of intracortical coherence had a maximum at the time and frequency of the EEG maximum. A replication of one of the experiments with human subjects did not reveal any comparable modulation of gamma activity in the scalp EEG. Stimulus-locked oscillations were found in the LFP and EEG of monkey, in an interval of about 80 ms to 160 ms after stimulus onset. The frequencies of these stimulus-locked oscillations matched those of stimulus-induced oscillations, suggesting that both phenomena are closely related.

Chapter 4: "Stimulus-induced gamma oscillations: harmonics of alpha activity?"

In a memory storage and retrieval experiment with human subjects stimulus-related changes of alpha activity covaried with changes of activity at integer multiples of the dominant alpha frequencies. Variations of activity in the upper frequency range were probably not a product of genuine brain processes at these frequencies, but merely harmonics of activity at lower frequencies. No other modulation of gamma activity was found. Our demonstration of the effect of alpha harmonics on the gamma band requires a critical evaluation of some recent findings concerning gamma oscillations in the human EEG and MEG.

Chapter 5: "No oscillations in human reaction time distributions?"

Human reaction time distributions were analyzed with respect to gamma band oscillations during an auditory choice task. A replication of the experimental paradigm and data analysis procedures described by Dehaene (1993) could not verify any of the reported results. One significant spectral peak in the analyzed reaction time distributions was not observed in partial data sets and is therefore regarded as a chance event.

6.2 Common aspects of different chapters

The main topic of this thesis, common to all four investigations, is the synchronization of neuronal activity. Synchronization of activity with an oscillatory time course played a prominent role in all these investigations. Major differences between these investigations are the spatial scales on which synchronization was analyzed, according to the methods used, and the system or species under investigation: computer models, humans, and macaca mulatta.

6.2.1 Generation of gamma oscillations

A model for the generation of synchronized oscillatory gamma band activity was given in Chapter 2. Main elements of this model were neurons, which produced oscillatory output signals with strong and rather constant input (the same model as used for the analysis of nonoscillatory components, see Section 6.2.5), and lateral coupling connections between these neurons, synchronizing their activities. LFP oscillations (Chapter 3) mainly reflect synchronized components of postsynaptic potentials, averaged in a volume of about one millimeter diameter, and might in part be explained by that model. Although not explicitly simulated, it can be predicted that stronger activation will increase the frequency of neuronal firing. Exactly this was found in the present investigations for stimulus movements (Chapter 3). However, the reduction of gamma amplitude during stimulus movement and the decrease of oscillation frequency during slowly increasing stimulus intensity cannot be deduced from this model and require further explanation. The stimulus-lock of gamma oscillations (see Section 6.2.4) is a feature of integrate-and-fire neurons as used for the present simulations. Stimulus-locked oscillations in monkey LFP and EEG are predicted by this class of models, explaining the present results. However, these experimental findings may also be elucidated by other models with "resonating" behavior.

6.2.2 No gamma oscillations in the human EEG

The absence of stimulus-induced oscillations in the human gamma band EEG (Chapters 3 and 4) was a rather unexpected result. Recent publications claimed to have detected such oscillations under visual (Lutzenberger et al. 1995; Tallon-Baudry et al. 1996; Müller et al. 1996) stimulation. This inconsistency may have different causes. First, it is possible that our experimental paradigms failed to produce gamma oscillations of sufficient amplitude. However, one type of stimuli used (sinusoidal grating) has been shown to evoke strong gamma oscillations in monkey. The other stimuli (line drawings in the memory experiment) induced intensive cognitive processing and yielded strong effects in slow EEG components (Heil et al. 1994), suggesting that gamma oscillations should be strong if they played a major role in memory storage or retrieval. A comparison with stimuli used in previous investigations shows that even rather simple stimuli as single moving bars (Müller et al. 1996) and line gratings (Lutzenberger et al. 1995), which are not very different from the sinusoidal gratings used in one of the present experiments, were reported to evoke gamma band responses in the EEG. So our stimuli should in principle yield comparable results. However, possible reasons for findings of gamma oscillations as described in the literature include artifacts as harmonics of activity in the lower frequency ranges (see Chapter 4), muscle activity, or misinterpretation of narrow band filter responses. Another problem might be the occurrence of spurious significances of statistical tests due to chance events, especially if multiple tests were applied to

results from different data analysis procedures. A meta analysis of results on gamma oscillations in the human EEG or MEG is even more complicated by the fact that the publication of results supporting the zero hypothesis of nonexistent gamma band effects is rather difficult compared to the publication of positive results. Thus, it is thinkable that negative evidence on human gamma oscillations, supporting the present results, did not get into common knowledge.

6.2.3 Harmonics of alpha activity

An analysis of the human EEG during a memory and retrieval task revealed the presence of harmonics of stimulus related alpha activity in the beta and gamma ranges (Chapter 4), possibly causing misinterpretation of analysis results in the upper frequency bands. Such harmonics were less pronounced during the presentation of sinusoidal gratings (Chapter 3), where only a small point in the middle of the screen had to be fixated. In principle, harmonics of low frequency oscillations may not only produce spurious gamma band effects but, inversely, might also occlude genuine gamma oscillations, if the harmonics had identical frequency and inverse modulation. However, it seems to be at least very improbable that enhancements and reductions of gamma band activity exactly canceled each other during the whole time course of stimulation.

While we believe that harmonics of low frequency activity may cause misinterpretations of gamma band results in the human EEG, they should not be very significant for the interpretation of gamma band effects in the monkey experiments. Activity in the low frequency range had no prominent frequency peaks but was rather broadly tuned, excluding narrow band harmonics in the gamma band. Another argument against suspected artifacts is the fact that the observed gamma oscillations were more strongly modulated by the stimulus than the activity at lower frequencies. For a more thorough analysis of harmonics higher order spectral analysis might be used (Schanze and Eckhorn 1997).

6.2.4 Stimulus-locked gamma oscillations

The phase-lock of gamma oscillations to stimulus onsets was examined in Chapters 3 and 5. While such a phenomenon was present in the LFP and EEG of monkey after the sudden appearance of visual stimuli, no comparable effect was observed in the human EEG during identical stimulation (Chapter 3). The latter result disagrees with other investigations of the human EEG during visual tasks (e.g., Tallon-Baudry et al. 1996). Stimulus-locked gamma oscillations are in principle detectable in reaction time distributions. While in a recent investigation stimulus-locked oscillations were reported in human reaction time distributions during visual and auditory discrimination tasks (Dehaene 1993), a replication of the auditory tasks did not confirm the results of the previous study (Chapter 5).

6.2.5 Nonoscillatory components

The processing of nonoscillatory synchronized components by a local group of neurons was examined in Chapter 2. It was shown that the synchronization between signals was reduced by the processing in unconnected model neurons, but selectively enhanced by lateral connections. Such nonoscillatory broad band synchronization was shown to be induced in the intracortical local field potentials in monkey visual cortex by stimulation yielding synchronization in extended groups of neurons of several millimeters diameter (Chapter 3). Nevertheless, signal components of higher frequencies were not synchronized over larger distances but only in a more local range. This observation might serve as a constraint for computer simulations of more extended circuits with considerable signal transmission delays.

6.2.6 Functional aspects

Synchronization of neuronal activity, the main topic of this thesis, is commonly assumed to be relevant for brain function. While the previous discussion emphasized empirical and methodological aspects, the relevance of the present results for the investigation of brain function will be discussed in the following section.

A necessary prerequisite of correlation theories of brain function, claiming that the brain codes a coherent object by a group of neurons with correlated activity, is the preservation of "correlation contrast" in neuronal processing. The present simulation study shows that differently correlated signals can be processed by a neuronal network without loss of correlation contrast if, and only if, lateral connections are present.

We did not find any signs of synchronized gamma oscillations in the human EEG. This result, together with known methodological problems (the problem of "alpha harmonics" was elucidated in this thesis), leads to doubts concerning previous reports on gamma oscillations. However, this does not prove that gamma oscillations cannot be measured in the human EEG, or even that gamma oscillations are not present in humans. It seems to require new investigations to prove the existence of gamma oscillations in human visual cortex, necessary for a claim that they play a general role in brain function.

While experimental paradigms and data analysis methods in investigations on gamma oscillations in the human EEG varied between different groups, our experiment on gamma oscillations in human reaction times was an exact replication of a previous experiment. Our result of non-oscillatory reaction time distributions contradicts the previous result. Nevertheless, similar to the outcome of the experiments on the human EEG described above, this does not prove the non-existence of stimulus-locked gamma oscillations in the human brain. On the contrary, such stimulus-locked gamma oscillations were found in monkey visual cortex at frequencies matching those of stimulus-induced oscillations, giving a hint that they might be found in humans, too.

Our findings of stimulus-locked oscillations in the EEG and LFP of monkeys suggest to intensify research on this field of research. The early appearance of these oscillations less than 100 ms after stimulus onset is a necessary condition for a role in fast scene segmentation.

All in all, the results of this thesis give rise to as many new questions as they answer old ones. Future experiments will most probably show the validity and reliability of our and of contradicting results.

6.3 Outlook

We conclude with suggestions for future work, emerging from the present results and the current state of research.

- The present results on harmonics of alpha activity require a replication of some previous investigations on gamma oscillations in the human EEG.
- In such replications a thorough control for artifacts seem to be of main importance.
- The negative outcome in our replication of an experiment on gamma oscillations in human reaction time distributions contradict the previously published results and require clarification, as well.
- Our demonstration of gamma oscillations in the monkey EEG show that simultaneous recordings of EEG and intracortical signals may be a promising approach for an investigation of gamma activity in monkeys.
- The analysis of stimulus-locked oscillations after saccades may provide insights into mechanisms of pattern recognition under the conditions of natural vision.
- Simulations of neuronal networks, possibly similar to those presented in Chapter 2, may help to explain mechanisms involved in the generation of stimulus-locked oscillations.

7 References[1]

Abeles M (1991) Corticonics: neural circuits of the cerebral cortex. Cambridge University Press, Cambridge [2, 3]

Aertsen AMHJ, Arndt M (1993) Response synchronization in the visual cortex. Curr Opin Neurobiol 3:586-594 [1, 2]

Aertsen AMHJ, Gerstein GL, Habib MK, Palm G (1989) Dynamics of neuronal firing correlation: modulation of "effective connectivity". J Neurophysiol 61:900-917 [2, 3]

Aertsen AMHJ, Erb M, Palm G (1994) Dynamics of functional coupling in the cerebral cortex: an attempt at a model-based interpretation. Physica D 75:103-128 [2]

Banquet J P (1973) Spectral analysis of the EEG in meditation. Electroencephalogr Clin Neurophysiol 35, 143-151 [4]

Basar E, Basar-Eroglu C, Demiralp T, Schürmann M (1995) Time and frequency analysis of the brain's distributed gamma-band system. IEEE Eng Med Biol 14, 400-410. [3]

Bauer H-U, Pawelzik K (1993) Alternating oscillatory and stochastic dynamics in an model for a neuronal assembly. Physica D 69:380-393 [2]

Bedenbaugh P, Gerstein GL (1994) Rectification of correlation by a sigmoid nonlinearity. Biol Cybern 70:219-225 [2]

Benignus VA (1969) Estimation of the coherence spectrum and its confidence intervals using the fast fourier transform. IEEE Trans Audio Electroacoust 17:145-150 [3]

Bernander O, Koch C, Usher M (1994) The effect of synchronized inputs at the single neuron level. Neural Comput 6:622-641 [3]

Bibbig A, Wennekers T, Palm G (1995) A neural network model of the cortico-hippocampal interplay and the representation of contexts. Behav Brain Res 66:169-175 [2]

Braitenberg V, Schüz A (1991) Anatomy of the cortex: statistics and geometry. Springer, Berlin [2]

Brigham EO (1975) The fast fourier transform. Prentice Hall, Englewood Cliffs NJ [4]

Bringuier V, Fregnac Y, Debanne D, Shulz D, Daranyi A (1992) Synaptic origin of rhythmic visually evoked activity in kitten area 17 neurons. Neuroreport 3:1065-1068 [2]

Brosch M, Bauer R, Eckhorn R (1995) Synchronous high-frequency oscillations in cat area 18. Europ J Neurosci 7:86-95. [3]

Brosch M, Bauer R, Eckhorn R (1997) Stimulus-dependent modulations of correlated high-frequency oscillations in cat visual cortex. Cerebral Cortex 7:70-76 [3]

Bruns (1997) Untersuchung der raum-zeitlichen Dynamik subdural registrierter Kortexpotentiale beim Menschen. Unpublished diploma thesis, Philipps-University Marburg. [3]

Cracco RQ, Cracco JB (1978) Visual evoked potential in man: early oscillatory potentials. Electroenceph Clin Neurophysiol 45:731-739 [1, 3]

[1] The numbers in brackets refer to the chapters in which the respective item is quoted.

Crick F, Koch C (1990) Towards a neurobiological theory of consciousness. Semin Neurosci 2:263-275 [1, 2]

Deakin JFW, Exley KA (1979) Personality and male-female influences on the EEG alpha rhythm. Biol Psychol 8:285-290 [4]

Dehaene S (1993) Temporal oscillations in human perception. Psych Sci 4:264-270 [1, 5, 6]

Desmedt JE, Tomberg C (1994) Transient phase-locking of 40 Hz electrical oscillations in prefrontal and parietal human cortex reflects the process of conscious somatic perception. Neurosci Lett 168:126-129 [1, 4]

Deppisch J, Bauer H-U, Schillen T, König P, Pawelzik K, Geisel T (1993) Alternating oscillatory and stochastic states in a network of spiking neurons. Network 4:243-257 [2]

Douglas R, Martin K (1991) A functional microcircuit for cat visual cortex. J Physiol 440:735-769 [2]

Dumermuth G, Gasser T (1978) The Computation of EEG Bispectra. Computer Methods and Programs in Biomedicine 8:235-242 [4]

Eckhorn R (1994) Oscillatory and non-oscillatory synchronizations in the visual cortex of cat and monkey. In: Pantev C (ed) Oscillatory event-related brain dynamics. Plenum Press, New York, pp 115-134 [1, 3]

Eckhorn R, Bauer R, Jordan W, Brosch M, Kruse W, Munk M, Reitboeck HJ (1988) Coherent oscillations: a mechanism of feature linking in the visual cortex? Multiple electrode and correlation analyses in the cat. Biol Cybern 60:121-130 [1, 2, 3, 4]

Eckhorn R, Frien A (1995) Neural signals as indicators of spatial and temporal segmentation coding in the visual system. In: Moreno-Diaz R, Mira-Mira J (eds) Brain processes, theories and models. MIT Press, Cambridge, Mass, pp 381-390 [2]

Eckhorn R, Frien A, Bauer R, Woelbern T, Kehr H (1993) High frequency (60-90 Hz) oscillations in primary visual cortex of awake monkey. Neuroreport 4:243-246 [1, 3, 4]

Eckhorn R, Obermueller A (1993) Single neurons are differently involved in stimulus-specific oscillations in cat visual cortex. Exp Brain Res 95:177-182 [3]

Eckhorn R, Reitboeck HJ, Arndt M, Dicke P (1990) Feature linking via synchronization among distributed assemblies: simulations and results from cat visual cortex. Neural Comput 2:293-307 [2, 3]

Eckhorn E, Schanze, T (1991) Possible neural mechanisms of feature linking in the visual system: stimulus-locked and stimulus-induced synchronizations. In: Babloyanz (ed) Self-organization, emerging properties, and learning. Plenum Press, New York, pp 63-80 [3]

Eckhorn R, Thomas U (1993) A new method for the insertion of multiple microprobes into neural and muscular tissue, including fiber electrodes, fine wires, needles and microsensors. J Neurosci Methods 49:175-179 [3]

Engel AK, König P, Kreiter AK, Schillen TB, Singer W (1992) Temporal coding in the visual cortex: New vistas on integration in the nervous system. TINS 15:218-226 [4]

Engel AK, König P, Kreiter AK, Singer W (1991) Interhemispheric synchronization of oscillatory neuronal responses in cat visual cortex. Science 252:1177-1179 [3]

Engel AK, König P, Singer W (1991) Direct physiological evidence for scene segmentation by temporal coding. Proc Natl Acad Sci USA 88:9136-9140 [3]

Freeman WJ (1975) Mass action in the nervous system. Academic Press, New York [1, 3]

Freeman WJ, van Dijk BW (1987) Spatial patterns of visual cortical fast EEG during conditioned reflex in a rhesus monkey. Brain Res 422:267-276 [1, 3]

French AS, Stein RB (1970) A flexible neural analog using integrated circuits. IEEE Biomed Engin 17:248-253 [2]

Frien A (1996) Oszillationen und Synchronisation neuronaler Gruppensignale in visuellen Kortex des wachen Affen. Unpublished doctoral dissertation, Philipps-University Marburg. [3]

Frien A, Eckhorn R, Bauer R, Woelbern T, Kehr H (1994) Stimulus-specific fast oscillations at zero phase between visual areas V1 and V2 of awake monkey. NeuroReport 5:2273-2277 [3]

Fries P, Engel AK, Roelfsema PR, König P, Singer W (1996) Conditions of dominance and suppression in squinting cats: a psychophysical study of binocular rivalry. In: Elsner N, Schnitzler H-U (eds) Göttingen Neurobiology Report. Thieme, Stuttgart, p 409 [3]

Gale A (1973) The psychophysiology of individual differences: Studies of extraversion and the EEG. In Kline P (ed) New Approaches in Psychological Measurement. John Wiley & Sons, London New York Sydney Toronto, pp 211-256 [4]

Gale A, Davies R, Smallbone A (1977) EEG correlates of signal rate, time on task and individual differences in reaction time during a five-stage sustained attention task. Ergonomics 20:363-376 [4]

Gerstein GL, Aertsen A, Bloom M, Espinosa I, Evenczuk S, Turner M (1986) Multi-neuron experiments: observation of state in neural nets. Proc Symposium Synergetics. Springer, Berlin [2]

Gerstein GL, Bedenbaugh P, Aertsen AMHJ (1989) Neuronal assemblies. IEEE Biomed Eng 36:4-14 [1, 2]

Gerstein GL, Perkel DH (1969) Simultaneously recorded trains of action potentials: analysis and functional interpretation. Science 164:828-830 [2]

Gerstner W, Ritz R, van Hemmen JL (1993) A biologically motivated and analytically soluble model of collective oscillations in the cortex. I. Theory of weak locking. Biol Cybern 68:363-374 [2]

Grannan ER, Kleinfeld D, Sompolinsky H (1993) Stimulus-dependent synchronization of neuronal assemblies. Neural Comput 5:550-569 [2]

Gray CM (1994) Synchronous oscillations in neuronal systems: mechanisms and functions. J Comput Neurosci 1:11-38 [2]

Gray CM, König P, Engel AK, Singer W (1989) Oscillatory responses in cat visual cortex exhibit inter-columnar synchronization which reflects global stimulus parameters. Nature 338:334-337 [2]

Gray CM, Singer W (1989) Stimulus-specific neuronal oscillations in orientation columns of cat visual cortex. Proc Natl Acad Sci USA 86:1698-1702 [1, 3]

Guettler A, Eckhorn R, Juergens E, Frien A (1997) Neural correlation contrast in visual cortex of monkey changes with stimulus contrast across an object-background-border. In: Elsner N, Wässle H (eds) Göttingen Neurobiology Report. Thieme, Stuttgart, p 551 [3]

Hansel D, Mato G, Meunier C (1995) Synchrony in excitatory neural networks. Neural Comput 7:307-337 [2]

Heil M, Rösler F, Hennighausen E (1994) Dynamics of activation in long-term memory: The retrieval of verbal, pictorial, spatial, and color information. J Exp Psychol: Learning, Memory and Cognition 20:185-200 [4, 6]

Lutzenberger W, Pulvermüller F, Elbert T, Birbaumer N (1995) Visual stimulation alters local 40-Hz Responses in Humans: An EEG-Study. Neuroscience Letters 183:39-42 [4, 6]

Herrmann WM (1982) Electroencephalography in drug research. Gustav Fischer, Stuttgart New York

Hirsch JA, Gilbert CD (1991) Synaptic physiology of horizontal connections in the cat's visual cortex. J Neurosci 11:1800-1809 [2]

Joliot M, Ribary U, Llinas R (1994) Human oscillatory brain activity near 40 Hz coexists with cognitive temporal binding. Proc Natl Acad Sci USA 91:11748-11751 [1, 3]

Jordan (1989) Ein Modell zur globalen Kodierung von Musterzusammenhängen in visuellen Cortex. Unpublished doctoral dissertation, Philipps-University Marburg. [3]

Juergens E, Eckhorn R, Frien A, Woelbern T (1996) Restricted coupling range of fast oscillations in striate cortex of awake monkey. In: Elsner N and Schnitzler H-U (eds) Göttingen Neurobiology Report. Thieme, Stuttgart, p 418 [3]

Juergens E, Eckhorn R, Guettler A, Frien A, Woelbern T (1997) Stimulus-locked and -induced gamma oscillations as present in visual cortex of awake monkeys were not detected in human EEG. In: Elsner N, Wässle H (eds) Göttingen Neurobiology Report. Thieme, Stuttgart, p 552 [3]

Jürgens E, Eckhorn R (1993) Transmission and generation of correlated signals by a simulated neural network. In: Elsner N, Penzlin H (eds) Gene - Brain - Behaviour. Thieme, Stuttgart, p 869 [2]

Juergens E, Eckhorn R (1997) Parallel processing by a homogeneous group of coupled model neurons can enhance, reduce and generate signal correlations. Biol Cybern 76:217-227 [1]

Jürgens E, Rösler F (1995) How do alpha oscillations influence gamma band activity? Psycoloquy 6(9) brain-rhythms.10.juergens [3]

Jürgens E, Rösler F, Hennighausen E, Heil M (1995) Stimulus-induced gamma oscillations: harmonics of alpha activity? Neuroreport 6:813-816 [1, 3]

Kraut MA, Arezzo JC, Vaughan HG Jr (1990) Inhibitory processes in the flash evoked potential of the monkey. Electroencephalogr Clin Neurophysiol 76:440-452 [3]

Kreiter A, Singer W (1992) Oscillatory neuronal responses in the visual cortex of the awake macaque monkey. Europ J Neurosci 4:369-375 [1]

Kristeva-Feige R, Feige B, Makeig S, Ross B, Elbert T (1993) Oscillatory brain activity during a motor task. Neuroreport 4:1291-1294 [4]

Koch C, Schuster H (1992) A simple network showing burst synchronization without frequency locking. Neural Comput 4:211-223 [2]

König P, Engel A, Singer W (1995) Relation between oscillatory activity and long-range synchronization in cat visual cortex. Proc Natl Acad Sci USA 92:290-294 [2]

König P, Schillen B (1991) Stimulus-dependent assembly formation of oscillatory responses: I. synchronization. Neural Comput 3:155-166 [2]

Kottmann M, Eckhorn R (1996a) Perception related synchronized oscillations in monkey striate cortex in a binocular rivalry task. Soc Neurosci Abstr 22:644 [3]

Kottmann M, Eckhorn R, Woelbern T, Frien A, Bauer R (1996b) Synchronized fast oscillation in striate cortex correlate with perception of grating orientation in a binocular rivalry task in monkey. In: Elsner N and Schnitzler H-U (eds) Göttingen Neurobiology Report. Thieme, Stuttgart, p 419 [3]

Kreiter AK, Singer W (1992) Oscillatory neuronal responses in the visual cortex of the awake macaque monkey. Eur J Neurosci 4:369-375 [2, 3]

Krüger J (1983) Simultaneous individual recordings from many cerebral neurons: techniques and results. Rev Physiol Biochem Pharmacol 98:177-233 [2]

Kruse W, Eckhorn R (1996) Inhibition of sustained gamma oscillations (35-80 Hz) by fast transient responses in cat visual cortex. Proc Natl Acad Sci USA 93:6112-6117 [2, 3]

Lankheet MJM, Molenaar J, van de Grind WA (1989) The spike generating mechanism of cat retinal ganglion cells. Vision Res 29:505-517 [2]

Llinás R, Ribary U (1993) Coherent 40-Hz oscillation characterizes dream state in humans. Proc Natl Acad Sci USA 90:2078-2081 [4]

Lutzenberger W, Pulvermüller F, Elbert T, Birbaumer N (1995) Visual stimulation alters local 40-Hz response in humans: an EEG study. Neurosci Lett 183:1-4 [3, 4]

Maunsell JHR, Gibson JR (1992) Visual response latencies in striate cortex of the macaque monkey. J Neurophysiol 68 (4):1332-1344 [3]

Melssen WJ, Epping WJM (1987) Detection and estimation of neural connectivity based on crosscorrelation analysis. Biol Cybern 57:403-414 [2]

Menon V, Freeman WJ, Cutillo BA, Desmond JE, Ward MF, Bressler SL, Laxer KD, Barbaro N, Gevins AS (1996) Spatio-temporal correlations in human gamma band electrocorticograms. Electroencephalogr Clin Neurophysiol 98:89-102 [3]

Michel CM, Kaufman L, Williamson SJ (1994). Duration of EEG and EMG alpha suppression increases with angle in a mental rotation task. J Cog Neurosci 6:139-150 [4]

Milner PM (1974) A model for visual shape recognition. Psychol Rev 81:521-535 [1, 3]

Mitzdorf U (1985) Current source-density method and application in cat cerebral cortex: investigation of evoked potentials and EEG phenomena. Physiol Rev 65:37-100. [3]

Mountcastle VB (1992) Preface. In: Basar E, Bullock TH (eds) Induced rhythms in the brain. Birkhäuser Boston, p xviii [1]

Mozer MC, Zemel RS, Behrmann M, Williams CK (1992) Learning to segment images using dynamic feature binding, Neural Comput 4:650-665 [2]

Müller MM, Bosch J, Elbert T, Kreiter A, Valdes Sosa M, Valdes Sosa P, Rockstroh B (1996) Visually induced gamma band responses in human EEG - a link to animal studies? Exp Brain Res 112:96-102 [3, 6]

Murthy VN, Fetz EE (1992) Coherent 25- to 35-Hz oscillations in the sensorimotor cortex of awake behaving monkeys. Proc Natl Acad Sci USA 89:5670-5674 [3, 4]

Murthy VN, Fetz EE (1994) Effects of input synchrony on the firing rate of a three-conductance cortical neuron model. Neural Comput 6:1111-1126 [1, 3]

Nelson JI, Salin PA, Munk MHJ, Arzi M, Bullier J (1992) Spatial and temporal coherence in cortico-cortical connections: a cross-correlation study in areas 17 and 18 in the cat. Vis Neurosci 9:21-37 [2]

Nischwitz A, Glünder H (1995) Local lateral inhibition: a key to spike synchronization. Biol Cybern 73:389-400 [2]

Nunez PL (1981) Electric fields of the brain. Oxford University Press, New York Oxford [3]

Palm G (1993) On the internal structure of cell assemblies. In: Aertsen (ed) Brain theory. Elsevier, Amsterdam [2]

Pantev C, Makeig S, Hoke M, Galambos R, Hampson S, Gallen C (1991) Human auditory evoked gamma-band magnetic fields. Proc Natl Acad Sci USA 88:8996-9000 [1]

Perkel DH, Gerstein GL, Moore GP (1967) Neuronal spike trains and stochastic point processes. II. Simultaneous spike trains. Biophys J 7:419-440 [1]

Pfurtscheller G, Klimesch W (1991) Event-related desynchronization during motor behavior and visual information processing. In: Brunia CHM, Mulder G, Verbaten MN (eds) EEG Suppl: 42. Event-related brain research. Elsevier, Amsterdam, pp 58-65 [4]

Pfurtscheller G, Neuper C (1992) Simultaneous EEG 10 Hz desynchronization and 40 Hz synchronization during finger movements. Neuroreport 3:1057-1060 [4]

Pfurtscheller G, Neuper C, Kalcher J (1993) 40-Hz oscillations during motor behavior in man. Neurosci Lett 24:179-182 [4, 6]

Reitboeck HJ (1983) A multi electrode matrix for studies of temporal signal correlations within neural assemblies. In: Basar E, Flor H, Haken H, Mandell AJ (eds) Synergetics of the brain. Springer-Verlag, Berlin, pp 174-182 [1, 2, 3]

Ritz R, Gerstner W, Fuentes U, van Hemmen JL (1994) A biologically motivated and analytically soluble model of collective oscillations in the cortex. II. Application to binding and pattern segmentation. Biol Cybern 71:349-358 [2]

Rösler F (1975) Die Abhängigkeit des Elektroenzephalogramms von den Persönlichkeitsdimensionen E und N sensu Eysenck und unterschiedlich aktivierenden Situationen. Zeitschrift für experimentelle und angewandte Psychologie 22:630-667 [4]

Sanes JN, Donoghue JP (1993) Oscillations in local field potentials of the primate motor cortex during voluntary movement. Proc Natl Acad Sci USA 90, 4470-4474 [1, 3, 4]

Schanze T (1996) Struktur und Kopplung reizabhängiger rhythmischer Aktivität der Sehrinde. Doctoral dissertation. Philipps-University Marburg. ISBN 3-922906-92-3 [3]

Schanze T, Eckhorn R (1997) Phase correlation among rhythms present at different frequencies: spectral methods, application to microelectrode recordings from visual cortex and functional implications. Int J Psychophysiol 26:171-189 [3, 6]

Schuster HG, Wagner P (1990) A model for neuronal oscillations in the visual cortex. Biol Cybern 64:72-82 [2]

Sheer DE (1989) Sensory and cognitive 40-Hz event-related potentials: behavioral correlates, brain function, and clinical application. In Basar E, Bullock TH (eds) Springer Series in Brain Dynamics: 2. Springer Series in Brain Dynamics. Springer, Berlin, pp 339-374 [4]

Sheer DE (1989) Sensory and cognitive 40-Hz event-related potentials: behavioral correlates, brain function, and clinical application. In: Basar E, Bullock TH (eds) Springer series in brain dynamics, Vol 2. Springer, Berlin, pp 339-374 [1, 2, 3]

Singer W, Gray CM (1995) Visual feature integration and the temporal correlation hypothesis. Annual Rev Neurosci 18:555-586 [1, 3]

Sompolinsky H, Golomb D, Kleinfeld D (1991) Cooperative dynamics in visual processing. Phys Rev A 43:6990-7011 [2]

Steriade M, Contreras D, Amzica F, Timofeev I (1996) Synchronization of fast (30 - 40 Hz) spontaneous oscillations in intrathalamic and thalamocortical networks. J Neurosci 16:2788-2808 [1]

Steriade M, Gloor P, Llinas RR, Lopes da Silva FH, Mesulam MM (1990) Basic mechanisms of cerebral rhythmic activities. Electroencephalogr Clin Neurophysiol 76:481-508 [2]

Tallon C, Bertrand O, Bouchet P, Pernier J (1995) Gamma-range activity evoked by coherent visual stimuli in humans. Europ J Neurosci 7:1285-1291 [3]

Tallon-Baudry C, Bertrand O, Delpuech C, Pernier J (1996) Stimulus specificity of phase-locked and non-phase-locked 40 Hz visual responses in human. J Neurosci 16:4240-4249 [1, 3, 6]

Tallon-Baudry C, Bertrand O, Delpuech C, Pernier J (1997a) Oscillatory γ-Band (30-70 Hz) activity induced by a visual search task in humans. J Neurosci 17:722-734 [3]

Tallon-Baudry C, Bertrand O, Wienbruch C, Ross B, Pantev C (1997b) Combined EEG and MEG recordings of visual 40 Hz responses to illusory triangles in human. Neuroreport 8:1103-1107 [3]

Tiltinen H, Sinkkonen J, Renikainen K, Alho K, Lavikainen J, Näätänen R (1993) Selective attention enhances the auditory 40 Hz transient response in man. Nature 364:59-60 [4]

Usher M, Schuster HG, Niebur E (1993) Dynamics of populations of integrate-and-fire neurons, partial synchronization and memory. Neural Comput 5:570-586 [2]

Vaadia E, Haalman I, Abeles M, Bergman H, Prut Y, Slovin H, Aertsen A (1995) Dynamics of neuronal interactions in monkey cortex in relation to behavioural events. Nature 373:515-518 [2]

Vijn PCM, van Dijk BW, Spekreijse H (1991) Visual stimulation reduces EEG activity in man. Brain Res 550:49-53 [3]

von der Malsburg C (1983) How are nervous structures organized? In: Basar E, Flor H, Haken H, Mandell AJ (eds) Synergetics of the brain. Springer, Berlin, pp 238-249 [1, 3]

von der Malsburg C, Buhmann J (1992) Sensory segmentation with coupled neural oscillators. Biol Cybern 67:233-242 [2]

von der Malsburg C, Schneider (1986) A neural cocktail-party processor. Biol Cybern 54:29-40 [2]

Wennekers T, Sommer FT, Palm G (1995) Iterative retrieval in associative memories by threshold control of different neural models. In: Herrmann HJ, Wolf DE, Pöppel EP (eds) Supercomputing in brain research: from tomography to neural networks. World Scientific Publishing, Singapore, pp 301-319 [2]

Whittaker SG, Siegfried JB (1983) Origin of wavelets in the visual evoked potential. Electroenceph Clin Neurophysiol 55:91-101 [3]

Danksagung

Viele Menschen hatten Anteil am Zustandekommen dieser Arbeit, ich freue mich, ihnen hier danken zu können.

Durch Prof. Dr. Reinhard Eckhorn bin ich zur Neurowissenschaft gekommen und dabei geblieben. Ich danke ihm für wichtige Anregungen, die Förderung meiner Ideen und seine mitreißende Begeisterungsfähigkeit und Kreativität.

Die Arbeit mit Prof. Dr. Frank Rösler gab mir interessante Einblicke in die Kognitive Psychophysiologie. Ich danke ihm für seine hilfreichen Anregungen zur Konzentration auf das Wesentliche und seine kritische Skepsis, die mir wichtige Impulse gegeben haben.

Prof. Dr. Dr. Heribert J. Reitböck danke ich für die Möglichkeit, Teile der Dissertation in seiner Arbeitsgruppe anzufertigen.

Für seinen besonderen Beitrag am Gelingen dieser Arbeit danke ich Dr. Thomas Schanze. Er sorgte dafür, daß ich öfters was zu lachen hatte, und hat mich mit fachmännischem Rat und ansteckender Dynamik über eine lange Zeit am Nachbarschreibtisch begleitet.

Prof. Dr. Roman Bauer, Dr. Axel Frien, Andreas Güttler und Thomas Wölbern aus der Arbeitsgruppe Neurophysik danke ich für die freundliche Überlassung mühsam gewonnener Daten, ihre Unterstützung bei der Vorbereitung und Durchführung von EEG-Ableitungen, sowie ihre fördernde Anteilnahme an der Auswertung und Interpretation der Messungen. Außerdem möchte ich allen Versuchspersonen danken, die sich für EEG-Experimente zur Verfügung gestellt haben.

Sigrid Thomas danke ich die professionelle Führung des Sekretatiats und ihr Interesse an meinem Weiterkommen. Vielen Dank auch an Uwe Thomas für gelegentliche Überraschungsbesuche und das gekonnte Löten meiner Brille.

Während meiner Zeit in der Arbeitsgruppe Kognitive Psychophysiologie waren viele der dort Tätigen an der Entstehung dieser Dissertation beteiligt. Besonders danke ich Jasmin Bajric, Markus Funke, Hansjerg Gölz, Dr. Martin Heil, Erwin Hennighausen und Jascha Rüsseler für ihre Unterstützung bei den Experimenten und der Auswertung der Daten.

Vielen genannten und nicht genannten Mitgliedern der beiden Arbeitsgruppen danke ich für ein offenes und herzliches Arbeitsklima, das viel zum Gelingen dieser Arbeit beigetragen hat. Besonders erwähnen möchte ich Andreas Bruns, Alexander Gail, Dr. Klaus Kopecz, Jan Lindemann, Karim Mohraz, Peter Pütz, Dr. Brigitte Röder und Judith Streb, sowie die alte Garde (vielen Dank für die Frage nach der Frage), die mich bei meinen ersten wissenschaftlichen Gehversuchen begleitet hat.

Auch angehende und gestandene Wissenschaftler außerhalb Marburgs haben mir durch Fragen, Anregungen, Kritik und Bestätigung geholfen. Dafür danke ich beispielhaft Prof. Dr. Ad Aertsen, Andrea Bibbig, Dr. Sonja Grün, Prof. Dr. Günther Palm und Thomas Wennekers.

Für das Korrekturlesen englischer Texte danke ich Nicole Dusör und Schirin Mohraz.

Die Arbeit an dieser Dissertation hatte natürlich Auswirkungen auf das „wahre" Leben außerhalb der Universität und wurde ebenso davon beeinflußt. Daher danke ich ganz besonders denen, die mit der Arbeit zwar nichts direkt zu tun, aber dennoch einen besonderen Anteil an ihrem Gelingen hatten, vor allem Petra Herzog, meinen Eltern und Geschwistern, vielen Freunden und dem Montagslehrer.